

NASA CONTRACTOR REPORT



NASA CR-846

NASA CR-846

LAUNCH VEHICLE WIND AND TURBULENCE RESPONSE BY NONSTATIONARY STATISTICAL METHODS

by James E. Bailey, John L. Palmer, and Ruric E. Wheeler

Prepared by
HAYES INTERNATIONAL CORPORATION
Huntsville, Ala.

for George C. Marshall Space Flight Center

N67-34401

(ACCESSION NUMBER)

130

(PAGES)

(NASA CR OR TMX OR AD NUMBER)

(THRU)

1

(CODE)

31

(CATEGORY)

**LAUNCH VEHICLE WIND AND TURBULENCE RESPONSE
BY NONSTATIONARY STATISTICAL METHODS**

By James E. Bailey, John L. Palmer, and Ruric E. Wheeler

Distribution of this report is provided in the interest of information exchange. Responsibility for the contents resides in the author or organization that prepared it.

Issued by Originator as Report No. 1340

Prepared under Contract No. NAS 8-20344 by
HAYES INTERNATIONAL CORPORATION
Huntsville, Ala.

for George C. Marshall Space Flight Center

NATIONAL AERONAUTICS AND SPACE ADMINISTRATION

PRECEDING PAGE BLANK NOT FILMED.

SUMMARY

This report presents the development of a Nonstationary Adjoint Statistical Algorithm for use in determining wind loading on a launch vehicle during ascent through the atmosphere. The evolution of this algorithm included the development of a wind model shaping filter which reproduces the statistics of the winds as determined from Jimsphere soundings over Cape Kennedy. The wind model includes the nonstationarity of the winds and turbulence and the technique presented represents an excellent method for performing response and load alleviation studies which is based on a sound theoretical foundation.

This work was performed at Hayes International Corporation from April 1966 to April 1977 under Contract NAS8-20344, "Statistical Analysis of Wind Profile Data and Application to Large Booster Control," for the Aero-Astrodynamics Laboratory of the George C. Marshall Space Flight Center. Mr. M. H. Rheinfurth of the Control Theory Branch of the Dynamics and Flight Mechanics Division was the primary NASA Technical Supervisor and he was assisted by Mr. J. R. Scoggins of the Environment Applications Branch of the Aerospace Environment Division.

TABLE OF CONTENTS

SECTION	TITLE	PAGE
	SUMMARY	iii
	TABLE OF CONTENTS	v
	LIST OF FIGURES	vii
	LIST OF SYMBOLS	x
I	INTRODUCTION	1
II	THE SYSTEM MODEL	3
1	MODEL CONCEPT	3
2	SYSTEM EQUATIONS OF MOTION	9
3	WIND AND TURBULENCE MODEL	12
4	COMBINED SYSTEM MODEL	15
III	THE WIND MODEL	19
1	SHAPING FILTER CONCEPT AND THEORY	25
2	SHAPING FILTER SYNTHESIS	26
IV	EXTENSION TO THE FREQUENCY DOMAIN	40
1	POWER SPECTRA AND ZADEH SYSTEM FUNCTION	40
2	USE OF THE SYSTEM FUNCTION	43
3	COMBINED SYSTEM FUNCTION USING	45
	SHAPING FILTER	
4	OBTAINING THE SYSTEM FUNCTION	47
5	SAMPLE CALCULATIONS	49
6	COMPUTER SOLUTION TO OBTAIN SYSTEM FUNCTION	51

TABLE OF CONTENTS (Continued)

SECTION	TITLE	PAGE
IV (Continued)		
7	APPROXIMATE METHODS FOR OBTAINING THE SYSTEM FUNCTION	54
8	HIGHER DEGREES OF FREEDOM SYSTEM	56
9	THE WIND MODEL FUNCTION SIMULATION	57
10	RESULTS OF SIMULATION	62
V	APPLICATION	76
VI	CONCLUSIONS AND RECOMMENDATIONS	84
1	CONCLUSIONS	84
2	RECOMMENDATIONS	84
VII	LIST OF REFERENCES	86
	APPENDIX I	89
	DESCRIPTION OF LINEAR SYSTEM	
	APPENDIX II	92
	DEVELOPMENT OF COVARIANCE DIFFERENTIAL EQUATION	
	APPENDIX III	94
	WEIGHTING FILTER SYNTHESIS	
	APPENDIX IV	120
	OPTIMAL CONTROL FORMULATION OF WEIGHTING FILTER	

LIST OF FIGURES

FIGURE	TITLE	PAGE
1	LAUNCH VEHICLE MODEL GEOMETRY	10
2	$W_1(t_1, t_2)$ WEIGHTING FUNCTION	11
3	TYPICAL ENSEMBLE OF WIND SOUNDINGS	13
4	MEAN WIND VELOCITY FOR NASA JIMSPHERE	21
	WIND SOUNDINGS	
5	VARIANCE FOR NASA JIMSPHERE WIND SOUNDINGS	22
6	COVARIANCE FOR NASA JIMSPHERE WIND	23
	SOUNDINGS	
7	SMOOTHED COVARIANCE - 10 KM	24
8	NASA WIND MODEL COEFFICIENT $a_0(h)$	32
9	NASA WIND MODEL COEFFICIENT $a_1(h)$	33
10	NASA WIND MODEL COEFFICIENT $b_1(t)$	34
11	NASA WIND MODEL COEFFICIENT $b_0(t)$	35
12	WIND MODEL COEFFICIENT $b_0(t)$ DERIVED	36
	FROM ANALOG	
13	NASA WIND MODEL VARIANCE $C(t, t)$	38
14	VERIFICATION OF SHAPING FILTER OUTPUT COVARIANCE BY	39
	ANALOG SIMULATION	
15	WIND MODEL FROZEN TIME SPECTRA COMPARED WITH NASA	42
	SPECTRA OBTAINED BY ANALYZING INDIVIDUAL PROFILES	

LIST OF FIGURES (Continued)

FIGURE	TITLE	PAGE
16	SYSTEM BLOCK DIAGRAM	45
17	SHAPING FILTER SYSTEM BLOCK DIAGRAM	45
18	COMBINED SYSTEM BLOCK DIAGRAM	46
19	BODE DIAGRAM, AMPLITUDE RATIO AND PHASE FOR EULER EQUATION SYSTEM FUNCTION, $G(s, t)$	52
20	THREE-DIMENSIONAL REPRESENTATION OF THE EULER EQUATION SYSTEM FUNCTION	53
21	a_0 COEFFICIENTS FOR INTERIM WIND MODEL	58
22	a_1 COEFFICIENTS FOR INTERIM WIND MODEL	59
23	b_0 COEFFICIENTS FOR INTERIM WIND MODEL	60
24	b_1 COEFFICIENTS FOR INTERIM WIND MODEL	61
25	COMPUTER DIAGRAM FOR WIND MODEL SYSTEM FUNCTION $\omega = .01$	63
26	COMPUTER DIAGRAM FOR WIND MODEL SYSTEM FUNCTION $\omega = .01$	64
27a	FROZEN SYSTEM FUNCTIONS COMPUTER CALCULATIONS	67
27b	FROZEN SYSTEM FUNCTIONS COMPUTER CALCULATIONS	68
27c	FROZEN SYSTEM FUNCTIONS COMPUTER CALCULATIONS	69

LIST OF FIGURES (Continued)

FIGURE	TITLE	PAGE
27d	FROZEN SYSTEM FUNCTIONS	70
	COMPUTER CALCULATIONS	
28	REAL AND IMAGINARY PARTS OF SYSTEM FUNCTIONS VS. ALTITUDE $\omega = 0.1$	71
29	REAL AND IMAGINARY PARTS OF SYSTEM FUNCTIONS VS. ALTITUDE $\omega = 0.01$	72
30	REAL PART OF THE SYSTEM FUNCTION VS. ALTITUDE WITH VARIOUS INITIAL CONDITIONS, $\omega = 0.01$	73
31	JIMSPHERE, MEAN WINDS AND DETERMINISTIC WIND PROFILES	78
32	VEHICLE BENDING MOMENT RESPONSE VS. TIME	82

LIST OF SYMBOLS

A_i	Indicated lateral acceleration
$a_o(t)$	Wind model coefficients
$a_1(t)$	Wind model coefficients
a_o^*	Attitude loop gain of attitude control system
a_1	Rate loop gain of attitude control system
B_E	Elastic bending moment
BM	Total bending moment
B_R	Rigid body bending moment
$b_o(t)$	Wind model coefficients
$b_1(t)$	Wind model coefficients
$C(h_r, h_s)$	Covariance of wind velocity altitudes h_r, h_s
D_1, D_2	Flexible vehicle aerodynamic coefficients
F_o, F_1	Rigid vehicle aerodynamic coefficients
F-X	Thrust
F_s	Swivel engine thrust
$G_{xx}(\omega)$	Input spectral density function
$G_{yy}(\omega)$	Output spectral density function
g	Longitudinal acceleration of the vehicle
g_2	Gain of accelerometer control loop
I	Effective moment of inertia of the vehicle about its c.g.
m	Vehicle mass
$m(h)$	White noise

LIST OF SYMBOLS (Cont'd.)

M_α	Aerodynamic bending moment coefficient
M_β	Bending moment coefficient for engine deflection
Q	Dynamic pressure
R_{yy}	System output correlation function
R_{vw}^v	System input correlation function
t	Time
V_w	Lateral wind velocity
$\bar{V}_w(h_i)$	Mean wind velocity, altitude (h_i)
v	Vehicle velocity
$W^*(t, \tau)$	Combined system weighting function
	Unit impulse at $t = 0$
$g_i(t, \tau)$,	System weighting function
$W_i(t, \tau)$	
X_E	Coordinate of gimbal point (measured positive from center of gravity towards the tail of the vehicle)
\dot{Y}	Translation displacement of rigid vehicle
$Y(j\omega)$	System transfer function
Y	Lateral drift velocity
$\langle Y^2(t) \rangle$	Mean squared system output
$\langle \quad \rangle$	Denotes ensemble average
α	Rigid body angle of attack

LIST OF SYMBOLS (Cont'd.)

α_G	Angle of attack due to a gust input
β	Swivel angle (angle of the engine gimbal relative to the center line of the vehicle at the gimbal point)
σ	Standard deviation
$\phi(j\omega, t)$	Zadeh system function
ϕ	Pitch angle of rigid vehicle relative to inertial space

I. INTRODUCTION

The purpose of this report is to discuss the application of nonstationary statistical methods to computation of launch vehicle flight loads due to winds and turbulence, and the synthesis of the necessary statistical wind model.

The theory, computational methods, and results of this study which define the statistical wind model are presented.

During the past decade, several approaches to the problem of flight load computation for large booster launch and exit from the atmosphere have been tried. Deterministic wind profiles have been constructed from atmospheric wind soundings, which when used as the input to the flight vehicle model are supposed to cause loads which are representative of 99% vehicle loads. The ensemble of vehicle load outputs directly generated from the wind soundings have been used to give estimates of vehicle output statistics. Also, nonstationary statistical methods have been used, via matrix techniques, to compute nonstationary vehicle output statistics. All of these methods have particular advantages. However, in some cases the lack of a theoretical foundation prevents an accurate interpretation of the results whereas others proved extremely unwieldy when used in practical system design.

This report will present a flight load computational method and a combined vehicle-wind model which offers a firm theoretical foundation for output process statistics computation. In addition, it affords accuracy, a physical feel for the problem, minimal computational difficulties, and direct application to the problem at hand. The mean and variance of the response of a vehicle mathematical

model can be computed directly. No assumptions of input or output process stationarity are made. The only assumption which governs the statistics of the process is that the process (i. e., ensemble of wind-versus-altitude plots) be normally distributed at each altitude for all times. More generally, if the winds at fixed altitudes are considered as variables, the whole distribution of winds would be a multivariate normal distribution.

An investigation of the possibility for the use of the system function for the combined nonstationary system to define a time-varying output spectrum for the vehicle is presented. The system function for the wind model may be used to define the time-varying spectrum for the winds. This system function and corresponding output spectrum for the winds is asymptotic at high frequencies to piece-wise stationary properties of the atmosphere at various altitudes (in the short wavelength turbulence range).

Use of a high-speed analog computer facility will permit direct implementation of the computations for system output variance and covariance. Proper implementation of the adjoint equation relationships and relations for correlation functions presented in this report offers an order of magnitude increase in the presentation and display of major system design features which can be determined from system output statistical properties.

II. THE SYSTEM MODEL

The system model will consist primarily of two parts: (1) the launch vehicle equations of motion which are a set of time-varying, linear, differential equations which represent the dynamic motions of the vehicle during launch and in the atmosphere, and (2) the wind model, which is a linear differential equation with variable coefficients. For a white noise input the output of the wind model differential equations has the same variance and covariance as the winds. Altitude is the independent variable for the wind model (shaping filter) equation.

1. MODEL CONCEPT

The concept upon which this report is based is that complete system output statistical properties can be defined by knowledge of a combined wind model - - vehicle weighting function. System design can be performed by shaping of the combined system weighting function so as to minimize the variance and the covariance of the vehicle outputs at all altitudes.

The method proposed and implemented in this report is a computer solution of the combined vehicle-wind model adjoint equations. The idea that the adjoint system equations could be used directly to solve for the output variance of a physical system was proposed by Lanning and Battin, Reference (4). The basic ideas presented in Reference (4) have since been extended by Solodovnikov to the form used in this report, Reference (1).

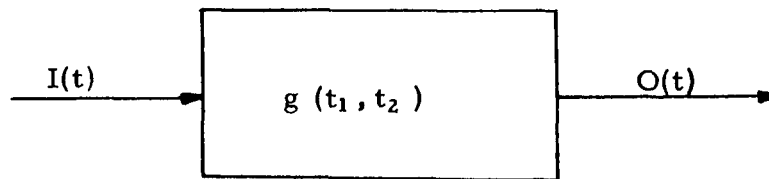
In their simplest form, the computational techniques used in this report are as follows: Consider a system with input $I(t)$, output $O(t)$ defined by an n th

order linear, variable coefficient differential equation:

$$\begin{aligned}
 & a_n(t) \frac{d^n O(t)}{dt^n} + a_{n-1}(t) \frac{d^{n-1} O(t)}{dt^{n-1}} + \dots + a_1(t) \frac{dO(t)}{dt} \\
 & + a_0(t) O(t) = b_m(t) \frac{d^m I(t)}{dt^m} + b_{m-1}(t) \frac{d^{m-1} I(t)}{dt^{m-1}} \\
 & + \dots + b_1(t) \frac{dI(t)}{dt} + b_0(t) I(t).
 \end{aligned}$$

The output of the system may be expressed in terms of the impulse response or weighting function of the system $g(t_1, t_2)$ as

$$O(t_1) = \int_{-\infty}^{t_1} I(t_2) g(t_1, t_2) dt_2$$



For $I(t)$ equal a stationary, random, Gaussian (normal) process with correlation function $R(\tau) = \delta(\tau)$, i. e., a white noise process, the system output correlation function may be expressed as (Reference (1)):

$$\begin{aligned}
 R(t_1, t_2) &= \int_{-\infty}^{t_1} g(t_1, \lambda) g(t_2, \lambda) d\lambda, \quad t_1 < t_2 \\
 &= \int_{-\infty}^{t_2} g(t_1, \lambda) g(t_2, \lambda) d\lambda, \quad t_1 > t_2.
 \end{aligned}$$

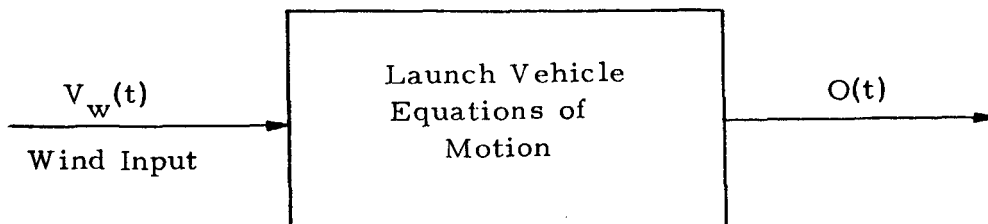
Also, the mean of the output process, $\overline{O(t)}$ for different times t can be computed by using the mean of the input process $\overline{I(t)}$ as a deterministic input. (See Appendix I). Also, in Appendix I it is shown that, if a normal process $I(t)$ is applied to a linear system, the output $O(t)$ is likewise normal.

Thus, if the input to a system is Gaussian, white noise, the mean output $\overline{O(t)}$ at different times t may be computed from the differential equation of the system or from the weighting function. With the correlation function of the output, $R(t_1, t_2)$, computed from the integrals given above, the covariance $C(t_1, t_2)$ of the output may be obtained from $C(t_1, t_2) = R(t_1, t_2) - \overline{O(t_1)} \overline{O(t_2)}$. It should be noted that the mean and covariance of the normal distribution completely define the output process. That is, these two statistics completely define the system output statistical characteristics.

The launch vehicle mathematical model can be made to fit the formula

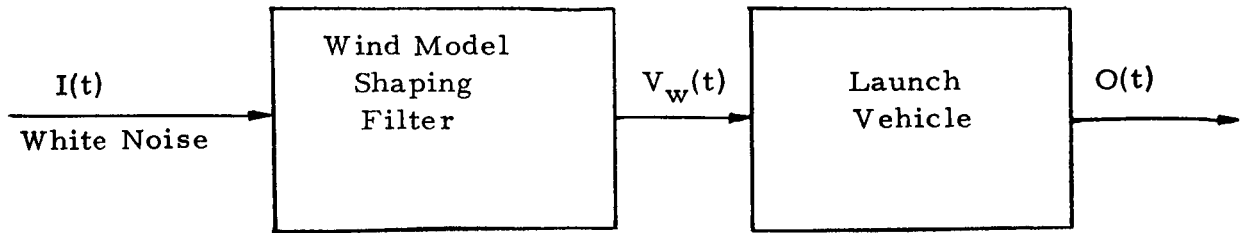
$$R(t_1, t_2) = \int_{-\infty}^{t_1} g(t_1, \lambda) g(t_2, \lambda) d\lambda$$

if the problem is implemented in the following manner. The system (launch vehicle) can be represented by

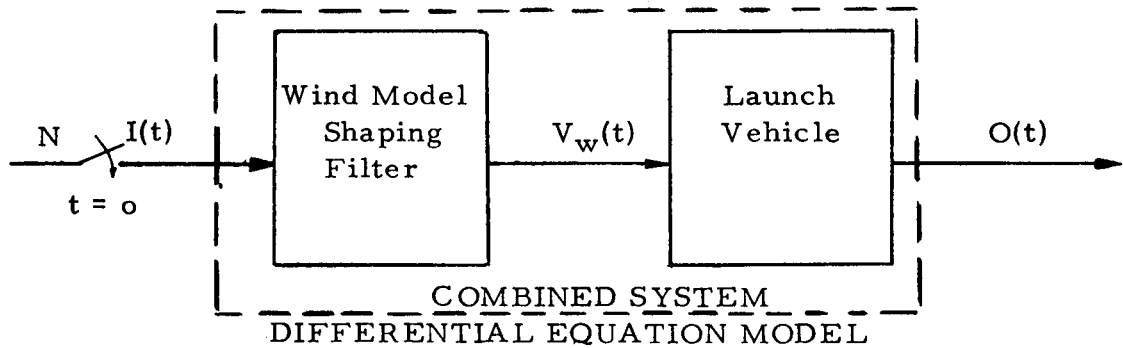


Obviously $V_w(t)$ does not possess the desired properties of white noise. It is known, in this case, to be a highly nonstationary process. By adding a shaping

filter to the system above, we can define a combined system which does have white noise as an input.



The wind inputs to the launch vehicle are now generated by a shaping filter. White noise is the input to the combined system model.



If $g_c(t_1, t_2)$ is the combined system weighting function, then the correlation of the output is given by

$$R(t_1, t_2) = \int_{-\infty}^{t_1} g_c(t_1, \lambda) g_c(t_2, \lambda) d\lambda \quad t_1 < t_2$$

Thus, the combined system weighting function (impulsive response) can be squared and integrated to give the second moment or multiplied $(g(t_1, \lambda) \cdot g(t_2, \lambda))$, and integrated to define the correlation function. The shaping filter gives a simple method for computation of output process statistics.

The conversion of the system to accept a white noise input is a mere artifice which is necessary to get a simple expression for the output statistics in terms of the weighting function. The white noise input is never really generated or used in practice except perhaps for experimental verification of the shaping filter.

The steps in formulating the combined system model are as follows:

- (1) Determine the launch vehicle equations of motion;
- (2) Synthesize a shaping filter differential equation such that for a white noise input the output variance and covariance are identical to the wind variance and covariance;
- (3) Combine the shaping filter and vehicle differential equations and determine the combined system weighting function.

The combined system equations can now be implemented so that the following information is easily obtained:

- (1) From the system equation response to the mean wind input the mean value of vehicle output can be obtained;
- (2) From the adjoint combined system equations, in the independent variable t_2 , the combined system weighting functions can be computed;
- (3) If these weighting functions are squared and integrated with respect to the second argument, the variance is obtained for each t_1 taken;
- (4) If the product $g_c(t_1, t_2) \Big|_{t_1=k} \times g_c(t_1, t_2) \Big|_{t_1=l}$ is taken and integrated, $R(k, l)$ is evaluated;

It can be seen that system design can now be performed by shaping the weighting function for the system such as to minimize system output mean, variance, and covariance.

Now that the shaping filter weighting function and the combined system weighting function have been defined, another concept, the spectral implication which can be associated with Fourier transforms of both weighting functions, follows immediately. Also, an output spectra of the wind model and the combined system model may be defined even though it is time-variant.

System function theory was first introduced in the late 1940's by L. Zadeh, and others. The system function of a system which is defined by a set of linear time-varying differential equations, is by definition the Fourier transform of the weighting function for the system; i. e., $\phi(j\omega, t) = \int_{-\infty}^t g(t, \tau) e^{-j\omega(t-\tau)} d\tau$. Also, the frozen time system equations can be transformed to give the so-called frozen time transfer function for the system which is asymptotically related to the system function.

A major portion of this report is relegated to the task of synthesizing a shaping filter for the Cape Kennedy winds aloft data which is presently available. The task of shaping filter synthesis has been theoretically defined by Lanning and Battin, Solodovnikov and others, but little practical and applied work is available in literature for the nonstationary case. The shaping filter synthesis problem has been extensively studied during this investigation, and several practical implementation schemes have been developed and used.

2. SYSTEM EQUATIONS OF MOTION

The equations of motion for the launch vehicle are assumed to be a set of linear differential equations with time-varying coefficients. These equations are not restricted as to complexity except by the physical capacity of the computing equipment used. The sole disturbance input to the vehicle system for this initial study was assumed to be the horizontal wind as depicted in Figure 1. A typical set of equations are: (Reference (6)).

$$[A] \{Y\} = \{B\} [V_w] \quad (1)$$

$$\text{or } \begin{bmatrix} (a_{11}(t)\frac{d^2}{dt^2} + b_{11}(t)\frac{d}{dt} + c_{11}(t)) & A_{12} & \dots & A_{1n} \\ A_{21} & \dots & \dots & \cdot \\ \cdot & \dots & \dots & \cdot \\ \cdot & \dots & \dots & \cdot \\ \cdot & \dots & \dots & \cdot \\ A_{n1} & \dots & \dots & A_{nn} \end{bmatrix} \begin{bmatrix} Y_1 \\ \cdot \\ \cdot \\ \cdot \\ \cdot \\ Y_n \end{bmatrix} = \begin{bmatrix} B_1 \\ \cdot \\ \cdot \\ \cdot \\ \cdot \\ B_n \end{bmatrix} [V_w(t)]$$

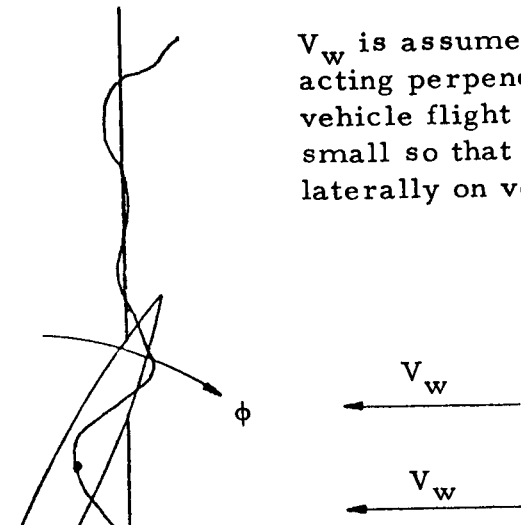
The solution of these equations can be simply written by the convolution integral as

$$Y_i(t_1) = \int_{-\infty}^{t_1} W_i(t_1, t_2) V_w(t_2) dt_2$$

Altitude - h

Vertical

V_w is assumed always acting perpendicular to vehicle flight path. ϕ is small so that V_w acts laterally on vehicle.



V_w = east-west wind

Vehicle Trajectory

LAUNCH VEHICLE MODEL GEOMETRY

FIGURE 1

where $W_i(t_1, t_2)$ is defined as the general weighting function for the system of equations. It represents the i th output at time t_1 obtained in the system response to a unit impulse at time t_2 , with all other inputs identically zero.

If the Y_i 's are defined as follows:

$$Y_1 = \phi = \text{pitch angle}$$

$$Y_2 = Y = \text{lateral deviation}$$

$$Y_3 = \beta = \text{engine gimbal angle}$$

$$Y_4 = \text{BM}(x) = \text{bending moment at station } x, \text{ etc.}$$

then, the $W_i(t_1, t_2)$'s are:

$$W_1(t_1, t_2) = W_\phi(t_1, t_2)$$

$$W_2(t_1, t_2) = W_Y(t_1, t_2)$$

$$W_3(t_1, t_2) = W_\beta(t_1, t_2)$$

etc.

The $W_i(t_1, t_2)$ weighting function is illustrated in Figure 2.

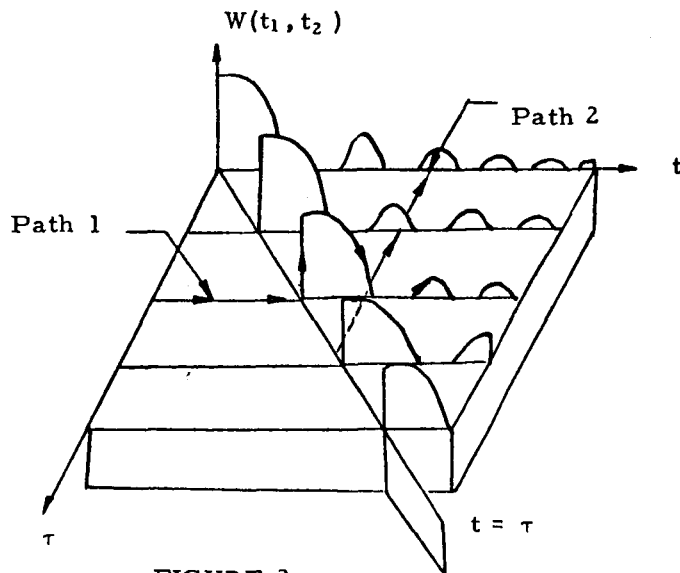


FIGURE 2

The time variability of the system response to a unit impulse at various times should be noted. Solution of equation (1) gives $W_i(t_1, t_2)$ as a function of the independent variable, t_1 . If the equations (1) are rewritten in state vector form, we have

$$\{\dot{Y}\} = [A] \{Y\} + \{B\} [V_w]$$

The adjoint equations for this system are: (Reference (6)).

$$\{\dot{Y}^*\} = -[A]^T \{Y^*\}$$

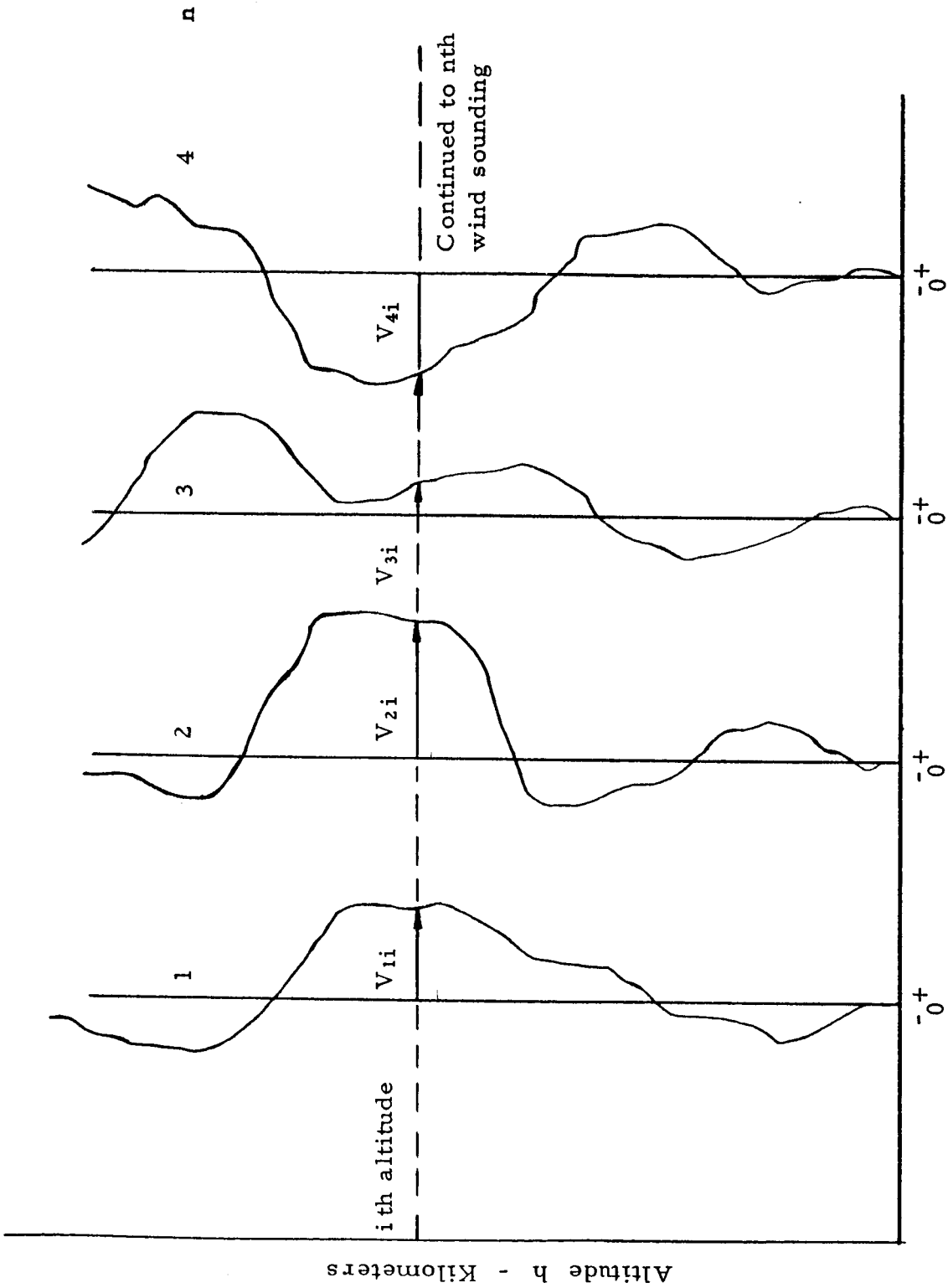
$$W_i(t_1, t_2) = f(Y^*)$$

These adjoint equations can be solved for $W_i(t_1, t_2)$ as a function of t_2 . This is a highly desirable form of the system weighting function because it allows direct computation of the variance and covariance (Reference (4)).

3. WIND AND TURBULENCE MODEL

The wind model to be used in conjunction with the combined system model must have a random output which has the same variance and covariance as the winds measured at Cape Kennedy by balloons and rockets. Typical wind data is illustrated in Figure 3.

Consider an ensemble of wind soundings which have been measured over a long period of time at regular intervals and which are said to be a statistical sample of the winds aloft.



TYPICAL ENSEMBLE OF WIND SOUNDINGS

FIGURE 3

At various altitudes two separate statistics can be computed. These are
 (1) mean wind values - $\overline{V_w(h_i)}$ which is approximated by

$$\overline{V_w(h_i)} \cong \frac{\sum_{j=1}^n V_w(h_i)_j}{n},$$

and, (2) the variance of the wind which is approximated by

$$C_{vw}(h_i, h_i) = \frac{\sum_{j=1}^n (V_w(h_i)_j - \overline{V_w(h_i)})^2}{n}$$

The variance of the winds at each altitude is also equal the standard deviation squared; i. e., $C_{vw}(h_i, h_i) = \sigma_{vw}^2(h_i)$. It was assumed throughout this analysis that the wind velocity amplitude characteristic across the ensemble of winds is normally distributed (Gaussian). This characteristic has been shown to be a good approximation to the probability density function in past experimental investigations.

Another statistic for the wind data can be computed by averaging products of corresponding wind velocities at different altitudes. This statistic is the wind correlation function. The covariance is similar to the correlation function, except it is computed for the process with the mean subtracted out and is defined by

$$C(h_r, h_s) = \frac{\sum_{j=1}^n [V_w(h_r) - \overline{V_w(h_r)}]_j [V_w(h_s) - \overline{V_w(h_s)}]_j}{n}$$

This function defines the degree of correlation between the winds at various altitudes. For a Gaussian process the three statistics defined above completely define the process.

Implicit in the wind data is the turbulence characteristic of the winds aloft data. This is merely another name for the short wavelength motions of the atmosphere.

The wind model used in this study is defined as follows:

- (1) Given a linear differential equation with altitude varying coefficients, such as

$$\sum_{k=0}^n a_k(h) \frac{d^k Y}{dh^k} = \sum_{i=0}^m b_i(h) \frac{d^i X}{dh^i}$$

- (2) For an input $X(h)$ which is white noise and begins at $h = 0$, the desired output $Y(t)$ is one wind trace,
- (3) If n runs are made, all beginning at $h = 0$, and we define these runs as an ensemble of wind data, then the variance of the ensemble for any h and the correlation for any h is the same as the measured winds, if the wind model coefficients are synthesized correctly.

The synthesis of a wind model of the form shown above from the Cape Kennedy wind data is described in detail in Chapter III.

4. COMBINED SYSTEM MODEL

The combined system model used in this report is composed of the vehicle equations of motion and the wind model equation. The system equations in

shorthand matrix notation are

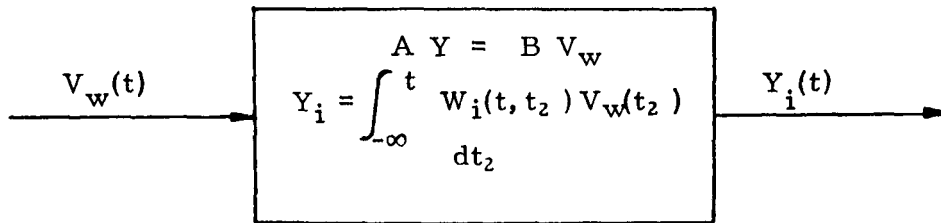
System Equations

$$[A] \{Y_i\} = \{B\} [V_w]$$

or

$$Y_i(t) = \int_{-\infty}^t W_i(t, t_2) V_w(t_2) dt_2$$

and in block diagram notation



with the supplemental equation

$$h = \int_0^t v(t) dt$$

which relates altitude of the wind model to time after vehicle launch.

Wind Equation

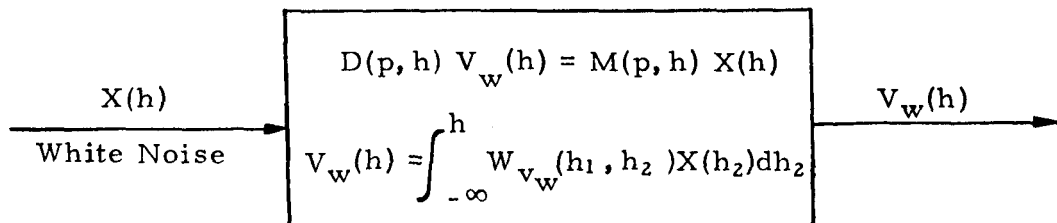
Using the notation defined previously, the wind equation may be expressed

$$\sum_{n=0}^k a_n(h) \frac{d^n V_w(h)}{dh^n} = \sum_{m=0}^l b_m(h) \frac{d^m X(h)}{dh^m}$$

or

$$D(p, h) V_w(h) = M(p, h) X(h)$$

and in block diagram notation

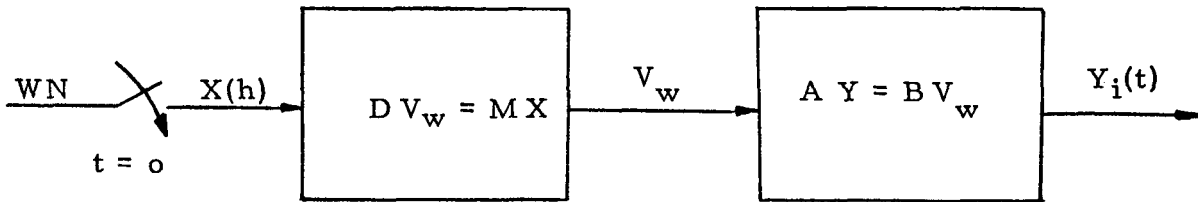


The combined system model is made up of a combination of the two systems of equations

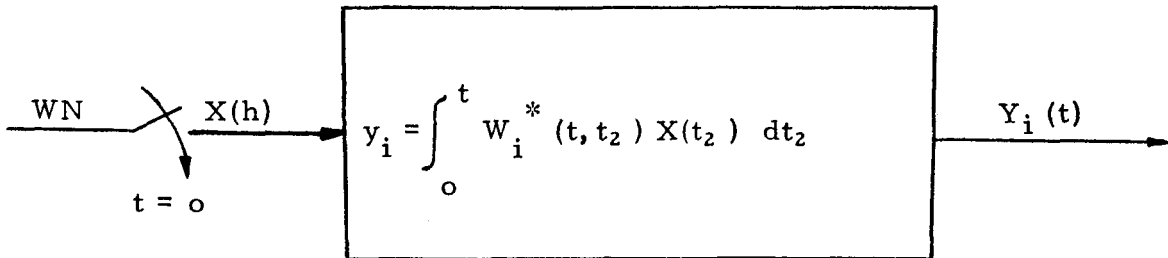
$$(1) \quad A Y(t) = B V_w(t) \quad \text{with} \quad h = \int_0^t v(t) dt$$

$$(2) \quad D V_w(h) = M X(h)$$

and in block diagram form is



or



where $W_i^*(t, t_2)$ is the combined system weighting function.

The equation for the correlation function of a system with a white noise input can then be written in terms of the combined system weighting function

$$R(t_1, t_1) = \int_0^{t_1} \{ W_i^*(t_1, \lambda) \}^2 d\lambda$$

and

$$R(t_1, t_2) = \int_0^{t_1} W_i^*(t_1, \lambda) W_i^*(t_2, \lambda) d\lambda \quad t_1 < t_2$$

It is seen then that the combined system concept has allowed the specification of all of the higher order statistics of the process in terms of integrals of the combined system weighting function. Shaping the weighting function shapes the variance and covariance.

III. THE WIND MODEL

The wind model as defined in this study is a higher order, variable coefficient, linear, differential equation which has a white noise input. The output of the wind model has been defined to have the same statistical properties as the winds aloft data. The task of synthesizing the wind model is discussed in this section and the initial results are presented.

The winds aloft data modeled in this study are the result of two hundred (200) wind soundings taken over an extended period of time using the Jimsphere with radar tracking (Reference (11)). Later wind models will use a larger wind sample of approximately six hundred (600) wind soundings. This preliminary wind model utilizes the east-west component of wind which is parallel to the surface of the earth at the given altitude. These winds are assumed to be acting perpendicular to the vehicle flight path. The dominant assumption made in computing the statistics of the winds is that the wind amplitude distribution at any one altitude is normal (Gaussian).

As mentioned in the previous section, the wind statistics which are approximated from the two hundred (200) wind samples are:

$$1. \quad \overline{V_w(h_i)} = \text{mean wind at altitude } h_i \\ \cong \sum_{j=1}^n V_w(h_i)_j / n$$

where n = number of winds in the ensemble ;

2.

$$\frac{\sum_{j=1}^n (V_w(h_i) - \overline{V_w(h_i)})^2}{n} \cong \text{variance of the wind at altitude } h_i;$$

3.

$$\frac{\sum_{j=1}^n (V_w(h_r) - \overline{V_w(h_r)})_j (V_w(h_s) - \overline{V_w(h_s)})_j}{n}$$

\cong covariance of the winds for the altitude range
in question.

If the winds are normally distributed at all altitudes the preceding averages have a good approximation to the ensemble statistics and higher order statistics can be defined in terms of these.

Plots of the statistics derived from the two hundred (200) wind samples are shown in Figures 4, 5, and 6.

There was a significant data scatter in the values derived for the variance and covariance. This was believed to be due to the relatively small sample size of the ensemble (200 soundings). The covariance was smoothed in two directions before it was used; otherwise, the data scatter would have caused serious difficulty during synthesis of the wind model. Figure 7 is a plot of the covariance between altitude 10 kilometers and other altitudes after smoothing. It is interesting to observe the following characteristics of the variance and covariance plots. The variance is maximum between 10 and 11 kilometers in altitude indicating important effects of winds in that altitude range. The covariance values are large for great ranges of altitude indicating

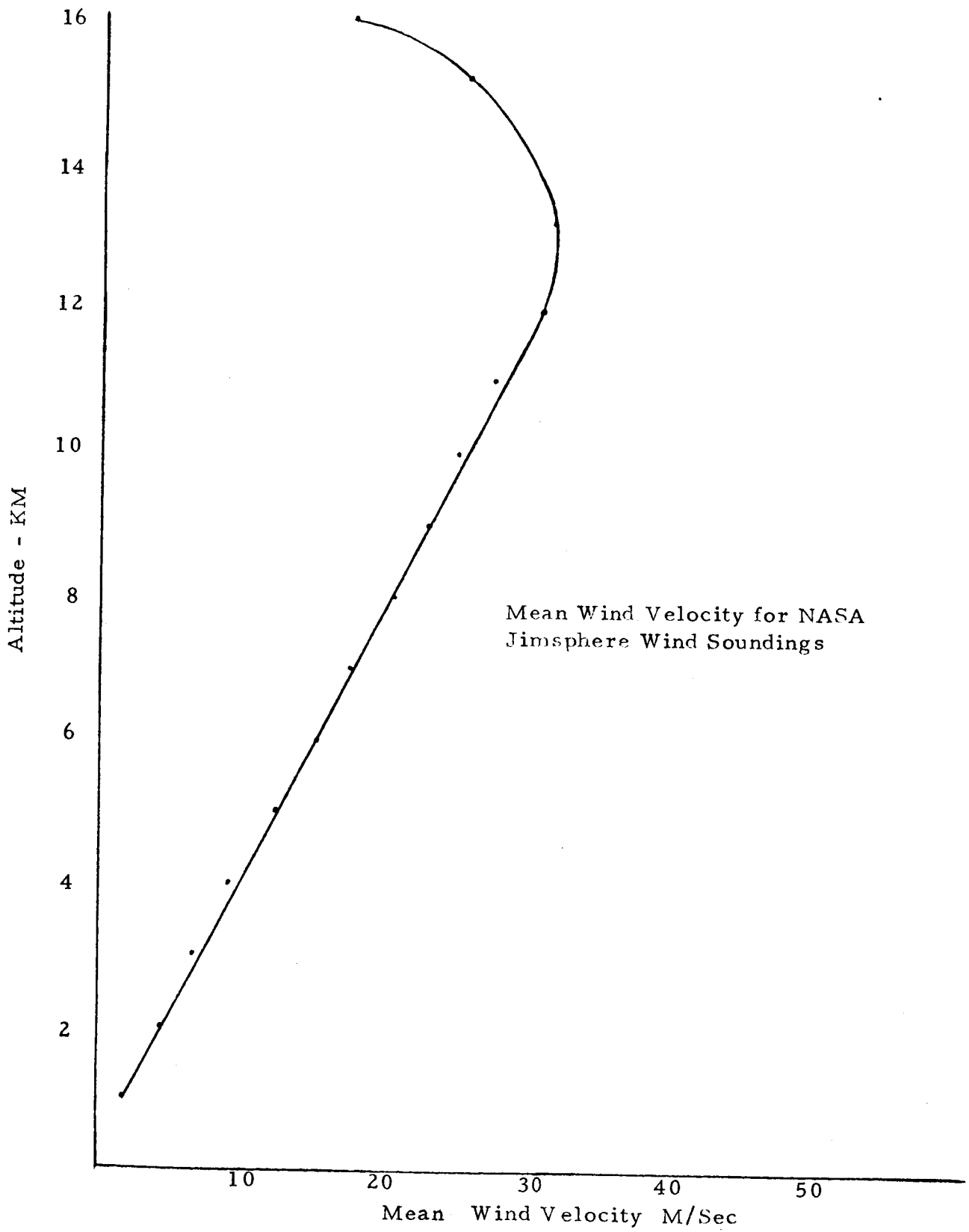


FIGURE 4

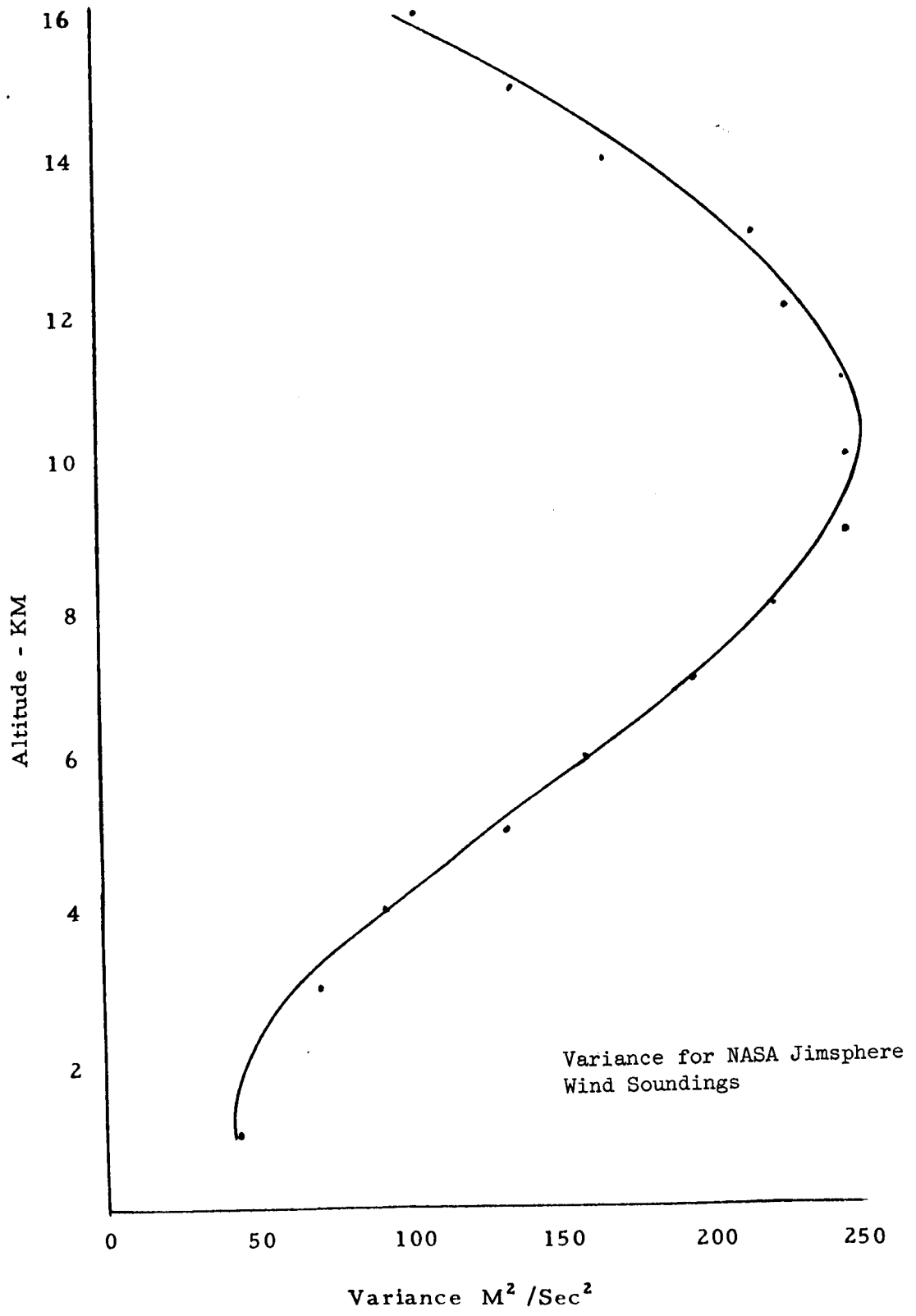


FIGURE 5

Covariance for NASA Jimsphere
Wind Soundings

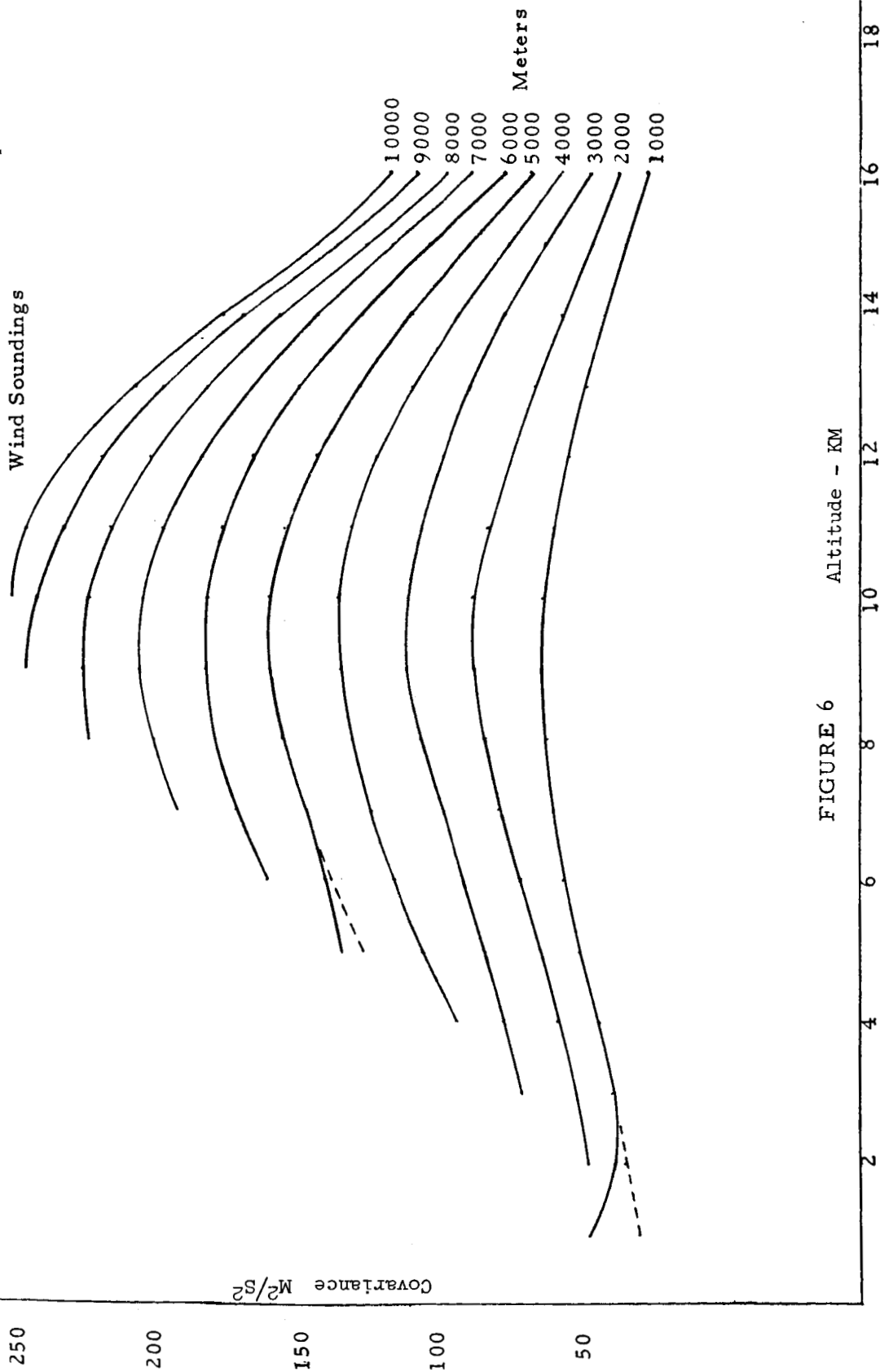
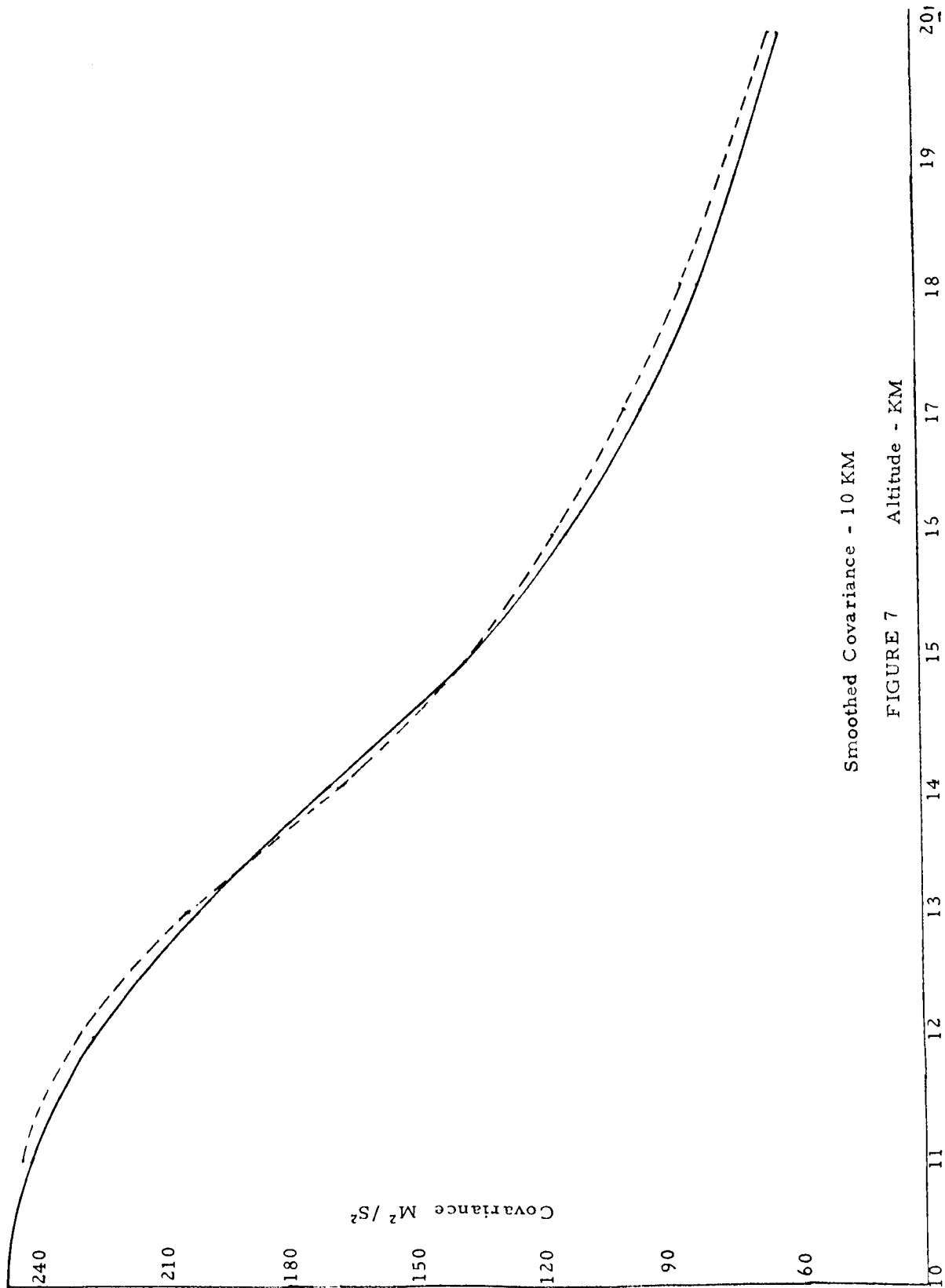


FIGURE 6 Altitude - KM



a high degree of correlation between winds at various altitudes. Correlation coefficients for winds are not presented.

1. SHAPING FILTER CONCEPT AND THEORY

The shaping filter is defined to be a higher order linear differential equation with variable coefficients. For this study it is as follows:

$$\begin{aligned} a_n(h) \frac{d^n y}{dh^n} + \dots + a_1(h) \frac{dy}{dh} + a_0(h)y &= \\ &= b_m(h) \frac{d^m x}{dh^m} + \dots + b_1(h) \frac{dx}{dh} + b_0(h)x \end{aligned} \quad (2)$$

or in operator notation

$$D(p, h) y(h) = M(p, h) x(h), \quad p = \frac{d}{dh}$$

$$\text{where } D(p, h) = a_n(h) \frac{d^n}{dh^n} + a_{n-1}(h) \frac{d^{n-1}}{dh^{n-1}} + \dots + a_0(h)$$

$$M(p, h) = b_m(h) \frac{d^m}{dh^m} + \dots + b_0(h)$$

Let $x(h)$ be a white noise input with correlation function $R(\tau) = \delta(h - \tau)$,

see Reference (1), Solodovnikov.

$$\begin{aligned} \text{Then } R_y(h, \tau) &= \int_{-\infty}^h g(h, \lambda) g(\tau, \lambda) d\lambda, \quad h < \tau \\ R_y(h, \tau) &= \int_{-\infty}^{\tau} g(h, \lambda) g(\tau, \lambda) d\lambda, \quad h > \tau \end{aligned} \quad (3)$$

where $g(h, \tau)$ is the weighting function for equation (2). Thus, equation (3) gives a relation between the shaping filter output covariance (correlation) function and the characteristic of the shaping filter differential equation which is represented by its weighting function, $g(h, \tau)$. It can easily be shown, by

multiplying equation (3) by $D(p, h)$, that the following relations are satisfied by $R_y(h, \tau)$ (See Appendix II).

$$(1) D(p, h) R_y(h, \tau) = 0 \quad h > \tau, \quad p = \frac{d}{dh}$$

$$(2) D(p, h) R_y(h, \tau) = M(p, h) g(\tau, h), \quad h < \tau, \quad p = \frac{d}{dh}$$

$$(3) D(p, \tau) R_y(h, \tau) = 0, \quad h < \tau, \quad p = \frac{d}{d\tau}$$

$$(4) D(p, \tau) R_y(h, \tau) = M(p, \tau) g(h, \tau), \quad h > \tau, \quad p = \frac{d}{d\tau}$$

These relations are extremely useful for determining $R_y(h, \tau)$ if $g(h, \tau)$ is known or for identifying the left-hand side coefficients $a_0(h), a_1(h) \dots a_n(h)$.

It is seen that equation (3) is the fundamental relation between the known output statistics $R_y(h, \tau)$ and the differential equation which is represented by its weighting function $g(h, \tau)$. This relation must be solved in order that $g(h, \tau)$ be determined. Then, of course, the differential equation must be defined from the $g(h, \tau)$.

2. WEIGHTING FILTER SYNTHESIS

Methods for synthesis of the shaping filter have not been developed in past literature and a combination of several synthesis methods were developed

and implemented during the course of this study. Because of the small wind sounding sample (200 winds) and the scatter in the derived statistics, the decision was made to concentrate all of the initial efforts to synthesize a shaping filter on a second order wind model differential equation. This shaping filter equation is

$$\frac{d^2 y(h)}{dh^2} + a_1(h) \frac{dy(h)}{dh} + a_0(h) y(h) = b_1(h) \frac{dx(h)}{dh} + b_0(h) x(h)$$

and the coefficients to be synthesized in the course of this study are

$$a_1(h), a_0(h), b_1(h), \text{ and } b_0(h).$$

Referring to Appendix II, it is known that $a_1(h)$ and $a_0(h)$ can be determined from the differential equation

$$D(p, h) R(h, \tau) = 0 \quad h > \tau.$$

$b_1(h)$ and $b_0(h)$ are more difficult to determine. $b_1(h)$ can be evaluated in terms of the first derivative of $R(h, \tau)$ at $h = \tau^+$ and $h = \tau^-$. $b_0(\tau)$ can either be identified after $g(h, \tau)$ has been determined in terms of initial conditions for $g(h, \tau)$ or it can be evaluated from the equation

$$D(p, \tau) R_{yy}(h, \tau) = M(p, \tau) g(h, \tau)$$

$$h > \tau \quad p = \frac{d}{d\tau}$$

For a theoretical discussion of the various relations for b_0 , b_1 , etc. see Appendix III.

The various synthesis methods which were used in this analysis are:

- (1) Regression analysis to get $a_1(h)$, $a_0(h)$, $b_1(h)$, $b_0(h)$, and a check of the results on the analog computer.

- (2) Determination of the best constant coefficient equation [$a_1(h)$, and $a_0(h)$] fit to $R_{yy}(h, \tau)$ by expansion of $R_{yy}(h, \tau)$ in a series of orthonormal functions. Then, regression analysis to determine $b_1(h)$ and $b_0(h)$.
- (3) Derivation of analytical relations for $b_1(h)$ and $b_0(h)$.
- (4) Analog computer synthesis of all coefficients using adjoint relationships and closed loop iterative technique.

Of all the methods tried, Method (1) gave the best results. It was found that good results were obtained from the regression analysis alone and that these results could be improved by a final iteration on $b_0(h)$ with the analog computer implementation of the adjoint equations for the shaping filter.

Multiple linear regression analysis is a procedure for finding the best linear relationship between a dependent variable y and a set of independent variables x_i , where the set x_i may be interpreted as the coordinates or basis of a vector space and the dependent variable y as a vector in that space. In this context, y is represented as a vector sum of basis vectors, the contribution of each component vector being the projection of y on the basis vector.

In the general theory of regression analysis it is assumed that y is normally distributed about an expected value μ with variance σ^2 and that the independent variables or observations are independent. However, these assumptions are misleading in that there is no requirement that the x_i be independent in a statistical sense. All that is required is that they be variables

whose values x_{ij} are known for each value of j . As far as the estimation of parameters is concerned, it does not require the assumption of normality. However, the assumption of normality and independence of variables is needed for the construction of confidence intervals and tests of hypotheses concerning the parameters in the linear equation.

The general model for estimating y in terms of x_i may be written as

$$y = \sum_{i=1}^n b_i x_i$$

Several different criteria may be used to determine the coefficients b_i . We will consider only the case where the coefficients are determined by the method of least squares. This method for estimating the coefficients has the desired property that the estimators obtained are unbiased, and among all unbiased linear estimators these have minimum variance. The sample estimates, b_i , are obtained by minimizing the sum of the squares of the deviations between the observed and the predicted values.

$$D^2 = \sum_{j=1}^m \left\{ y_j - \sum_{i=1}^n b_i x_{ij} \right\}^2$$

By differentiating with respect to b_i and setting equal to 0 (the necessary conditions for a minimum) a set of n simultaneous linear equations called normal equations are obtained.

$$\begin{aligned} b_1 \sum x_{1j}^2 + b_2 \sum x_{1j} x_{2j} + \dots + b_n \sum x_{1j} x_{nj} &= \sum y_j x_{1j} \\ b_1 \sum x_{1j} x_{2j} + b_2 \sum x_{2j}^2 + \dots + b_n \sum x_{2j} x_{nj} &= \sum y_j x_{2j} \\ \vdots & \\ b_1 \sum x_{1j} x_{nj} + b_2 \sum x_{2j} x_{nj} + \dots + b_n \sum x_{nj}^2 &= \sum y_j x_{nj} \end{aligned}$$

This set of equations can be solved for the b_i , the estimated coefficients in the linear regression model.

Linear regression analysis has been utilized in two respects to assist in obtaining the coefficients of the differential equation of the wind shaping filter. For an input of white noise it is known that the covariances satisfy the linear differential equations (see Appendix II):

$$\frac{d^n C(h, h_1)}{dh^n} + a_{n-1}(h) \frac{d^{n-1} C(h, h_1)}{dh^{n-1}} + \dots + \frac{a_1(h) d C(h, h_1)}{dh} + a_0(h) C(h, h_1) = 0 \quad h > h_1$$

and

$$\begin{aligned} \frac{d^n C(h, h_1)}{dh^n} + a_{n-1}(h) \frac{d^{n-1} C(h, h_1)}{dh^{n-1}} + \dots + a_1(h) \frac{dC(h, h_1)}{dh} \\ + a_0(h) C(h, h_1) = b_0(h) g(h_1, h) + b_1(h) \frac{dg(h_1, h)}{dh} \\ + \dots + b_m(h) \frac{d^m g(h_1, h)}{dh^m} \quad h < h_1 \end{aligned}$$

For a second order differential equation the linear model becomes

$$\frac{d^2 C(h, h_1)}{dh^2} + a_1(h) \frac{dC(h, h_1)}{dh} + a_0(h) C(h, h_1) = 0$$

or

$$\frac{d^2 C(h, h_1)}{dh^2} = -a_1(h) \frac{dC(h, h_1)}{dh} - a_0(h) C(h, h_1)$$

With this model for fixed h $\frac{d^2 C(h, h_1)}{dh^2}$ is considered as the dependent variable and $\frac{dC(h, h_1)}{dh}$ and $C(h, h_1)$ as the independent variables. All

data for $C(h, h_1)$, $\frac{d}{dh} C(h, h_1)$, and $\frac{d^2}{dh^2} C(h, h_1)$ are obtained by numerical procedures (Appendix III) for $h_1 < h$. Thus, for fixed values of h the coefficients $a_0(h)$, and $a_1(h)$ can be estimated by linear regression techniques.

Likewise, multiple linear regression techniques may be utilized to obtain the $b_0(h)$ and $b_1(h)$ in

$$Y = b_0(h) g(h, h_1) + b_1(h) \frac{dg(h, h_1)}{dh},$$

where Y is the dependent variable computed for each set of data from

$$Y = \frac{d^2 C(h, h_1)}{dh^2} + a_1(h) \frac{dC(h, h_1)}{dh} + a_2(h) C(h, h_1).$$

The results of the regression analysis are presented in Figures 8 through 13. $a_0(h)$ is presented in Figure 8, and the dashed line is the analog computer function generator representation of $a_0(h)$.

$a_1(h)$ is shown in Figure 9, and the dashed line is the analog computer representation of $a_1(h)$. Figure 10 shows the wind model coefficient $b_1(h)$, which was derived from the analytical expression for $b_1(h)$ presented in Appendix III. Figure 11 shows a plot of $b_0(h)$ which was obtained from the regression analysis. Also shown in the same figure is the $b_0(t)$ which was obtained by iteration on the analog computer. The starting point for the iteration was the coefficient values obtained by regression. Using the adjoint simulation of the wind model equation on the analog computer, $b_0(h)$ was modified slightly to give the best fit to the variance curve shown in Figure 12. Figure 13 illustrates the wind model variance taken from the reduced wind data and the dashed line is the wind model variance using the refined value

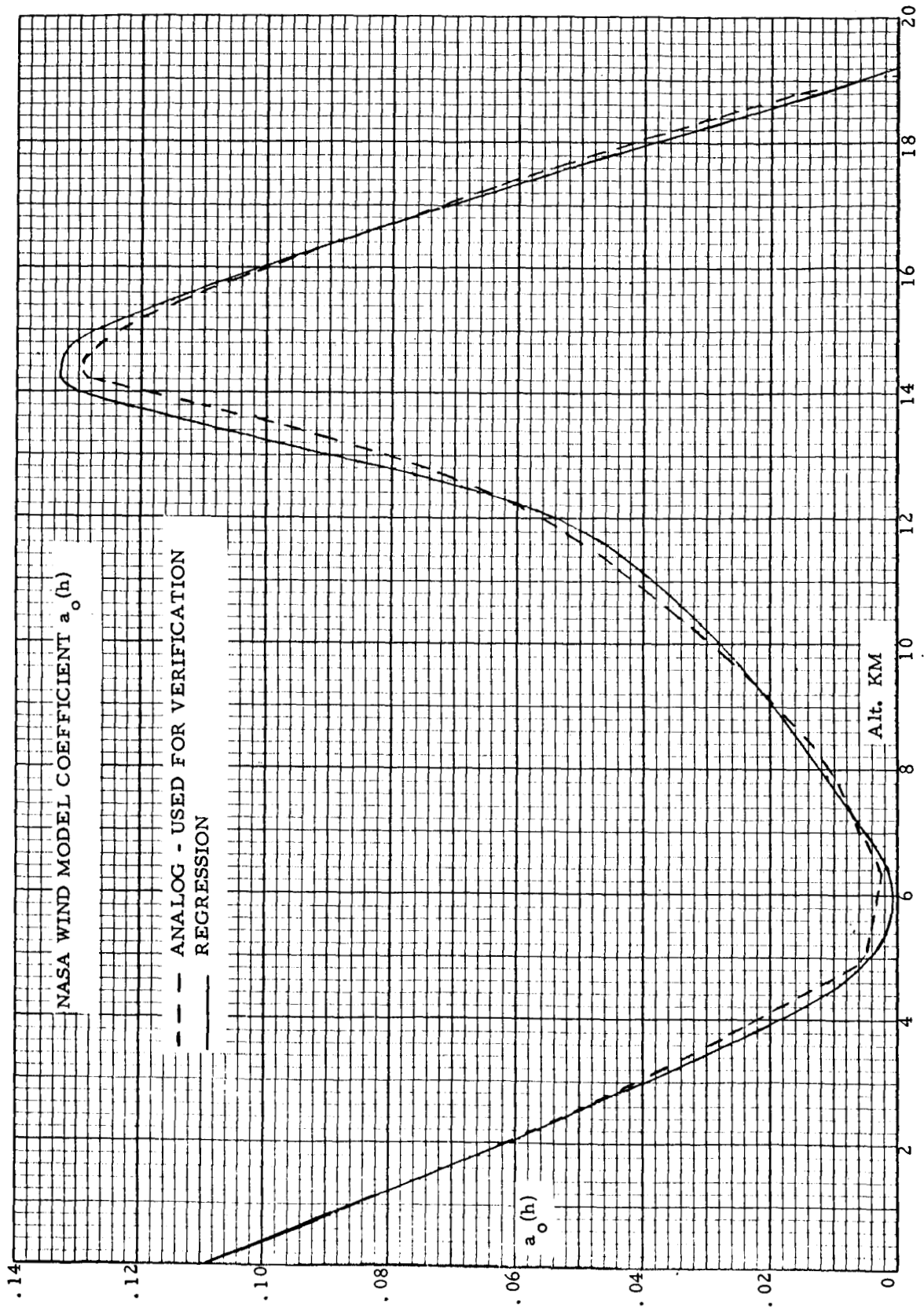


FIGURE 8

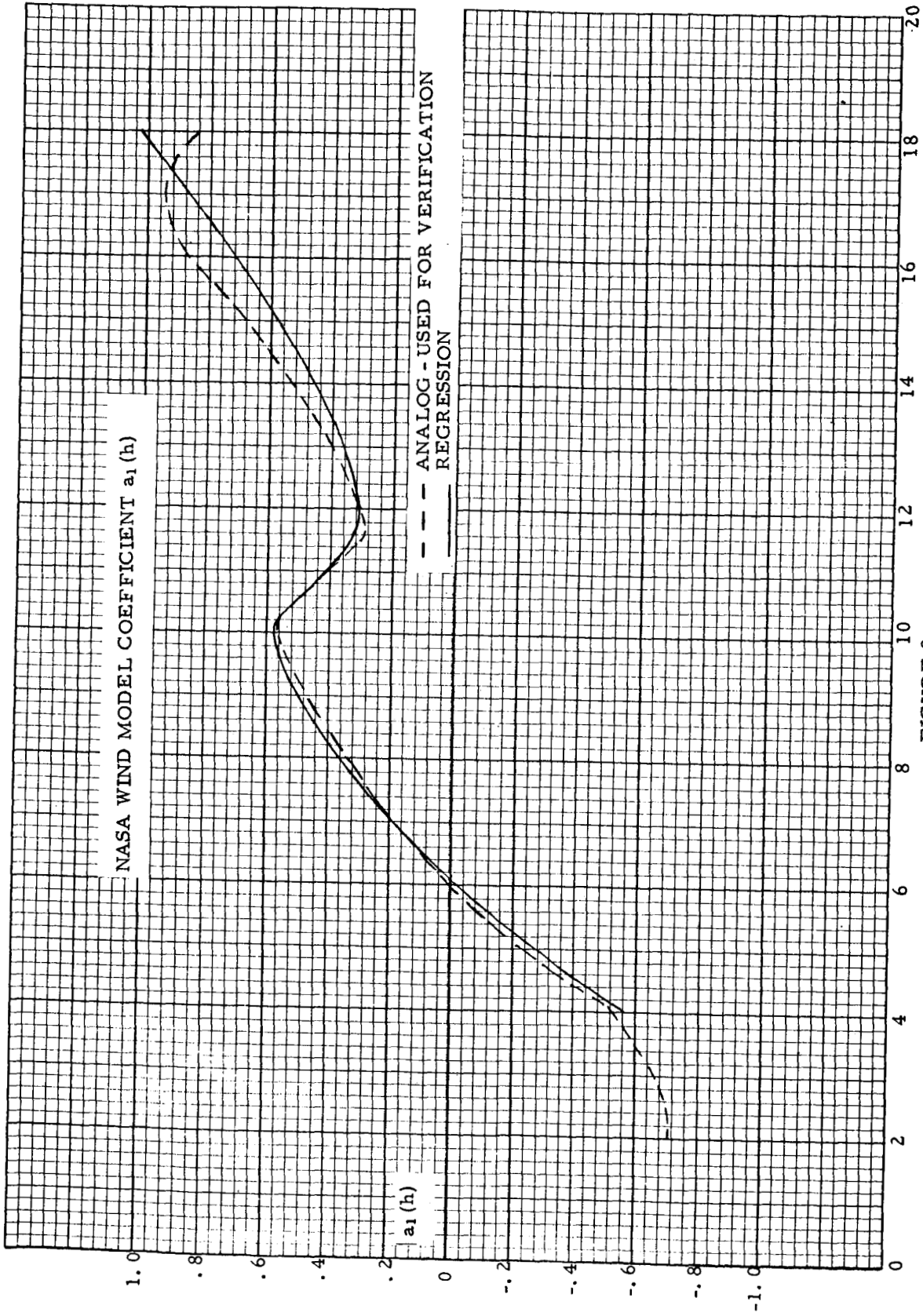


FIGURE 9



FIGURE 10

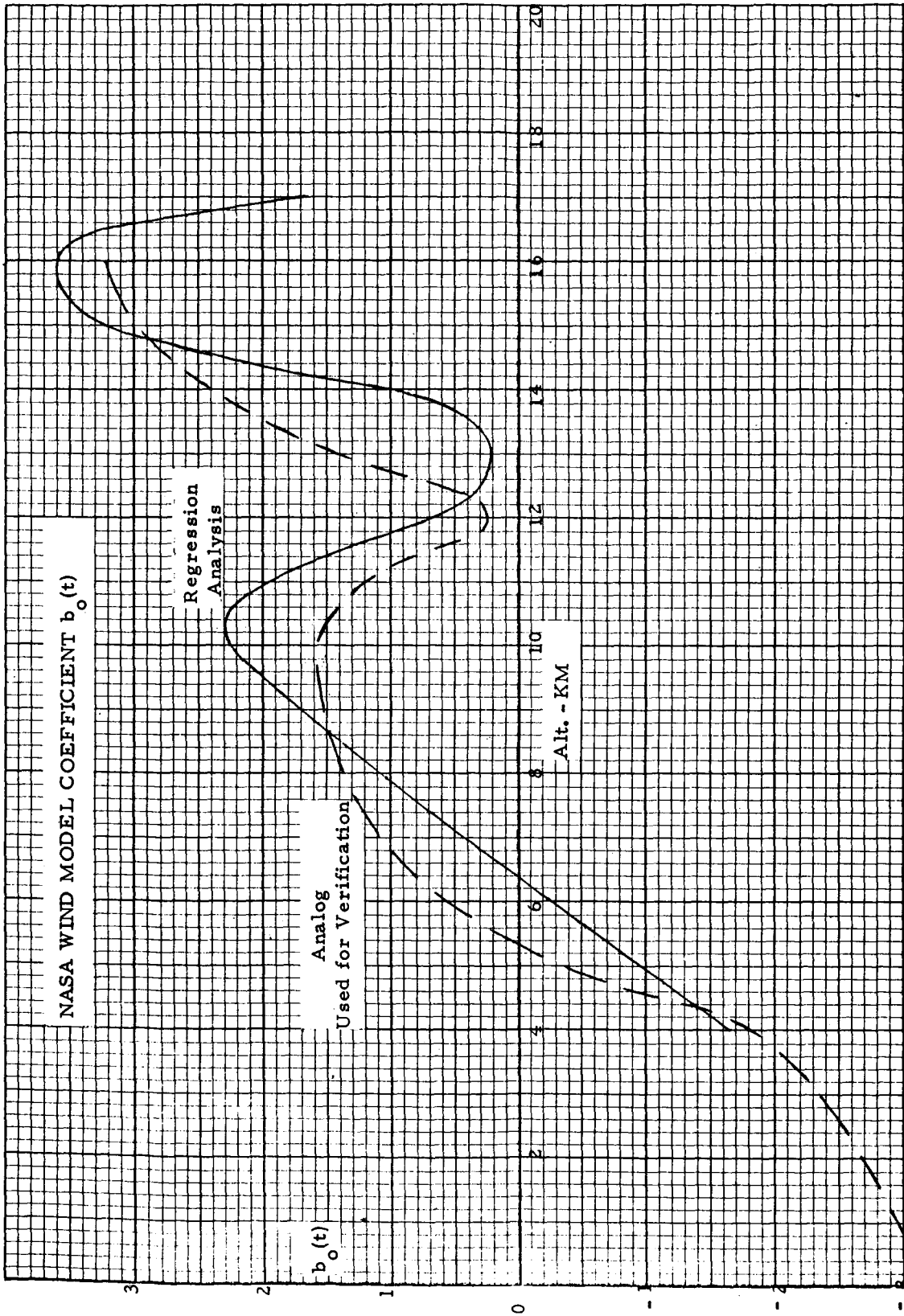


FIGURE 11

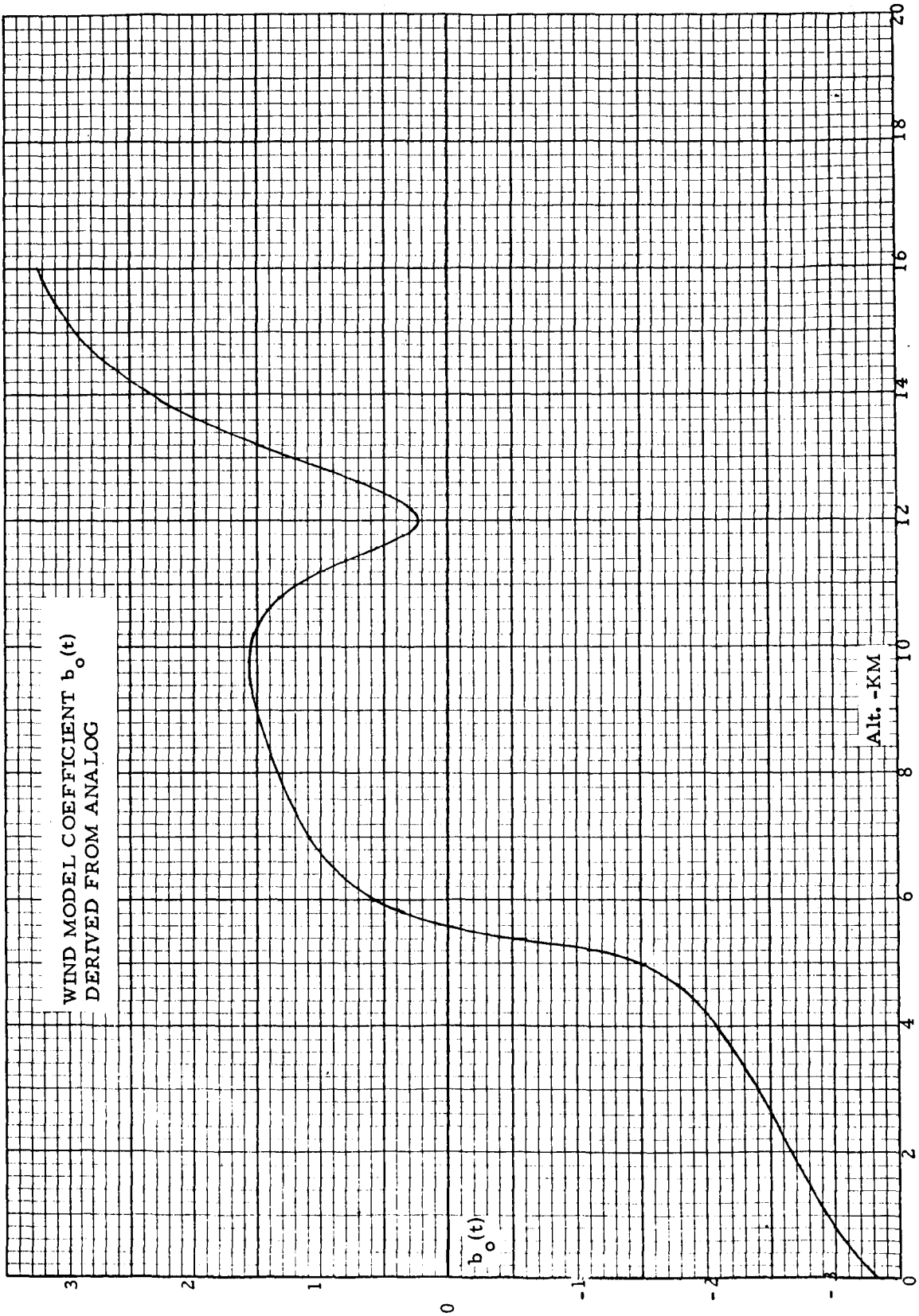


FIGURE 12

of $b_0(h)$. The variance is extremely sensitive to values of $b_0(h)$ and $b_1(h)$. A better fit could have been obtained in the curves of Figure 13 by adding another iteration on the analog, but was not considered to be practical until the refined wind statistics computed from the larger wind sample size is available. An analog check of the coefficients $a_1(h)$ and $a_0(h)$ determined by the regression analysis was made. The verification was made by solving

$$D(p, h) R_y(h, \tau) = 0 \quad h > \tau$$

for the proper initial conditions. Figure 14 illustrates the fit to the smoothed covariance data obtained with these coefficients. Reference is made to Appendix III for the theoretical aspects of this verification.

The wind covariance of Figure 14 was determined by considering each altitude in one thousand meter steps beginning with one thousand meters and determining the covariance of each altitude with all others above it. The curve marked (1) is the covariance between one thousand meters and all altitudes above one thousand meters up to ten thousand meters. The curve marked (2) is the covariance between two thousand meters and all altitudes above two thousand meters, all values were determined by the techniques explained in Section II-3.

In the areas 0-4, 10-18 kilometers no comparison to the NASA wind data covariance was performed on the analog computer due to insufficient data sample size, although coefficients for these altitudes were determined through regression analysis. The data point sample size increased steadily from five hundred meters up to its maximum at approximately eight thousand meters, and decreased steadily above ten thousand meters.

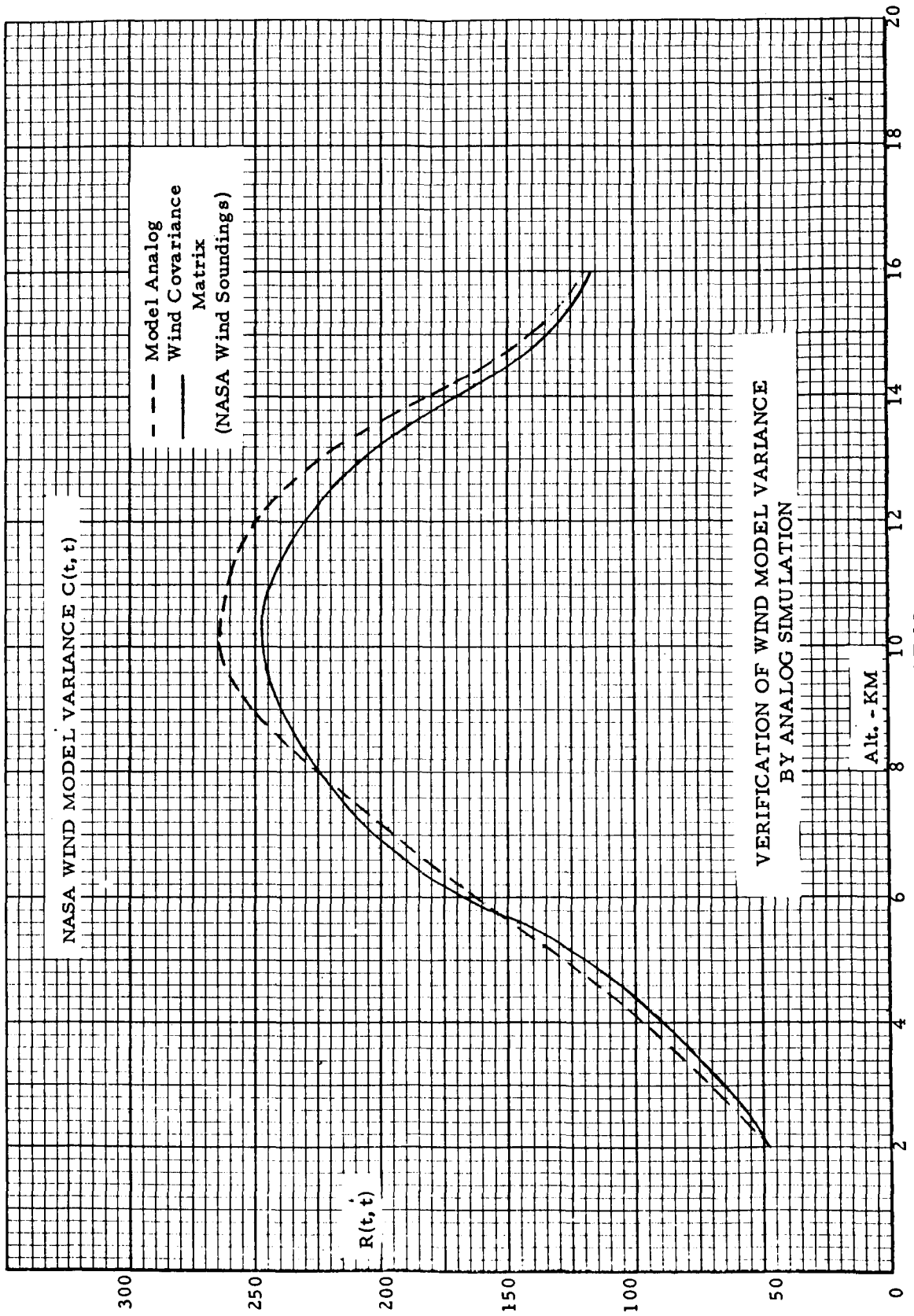


FIGURE 13

VERIFICATION OF SHAPING FILTER OUTPUT COVARIANCE
BY ANALOG SIMULATION

Shaping Filter Output
vs.
Wind Statistics

FIGURE 14

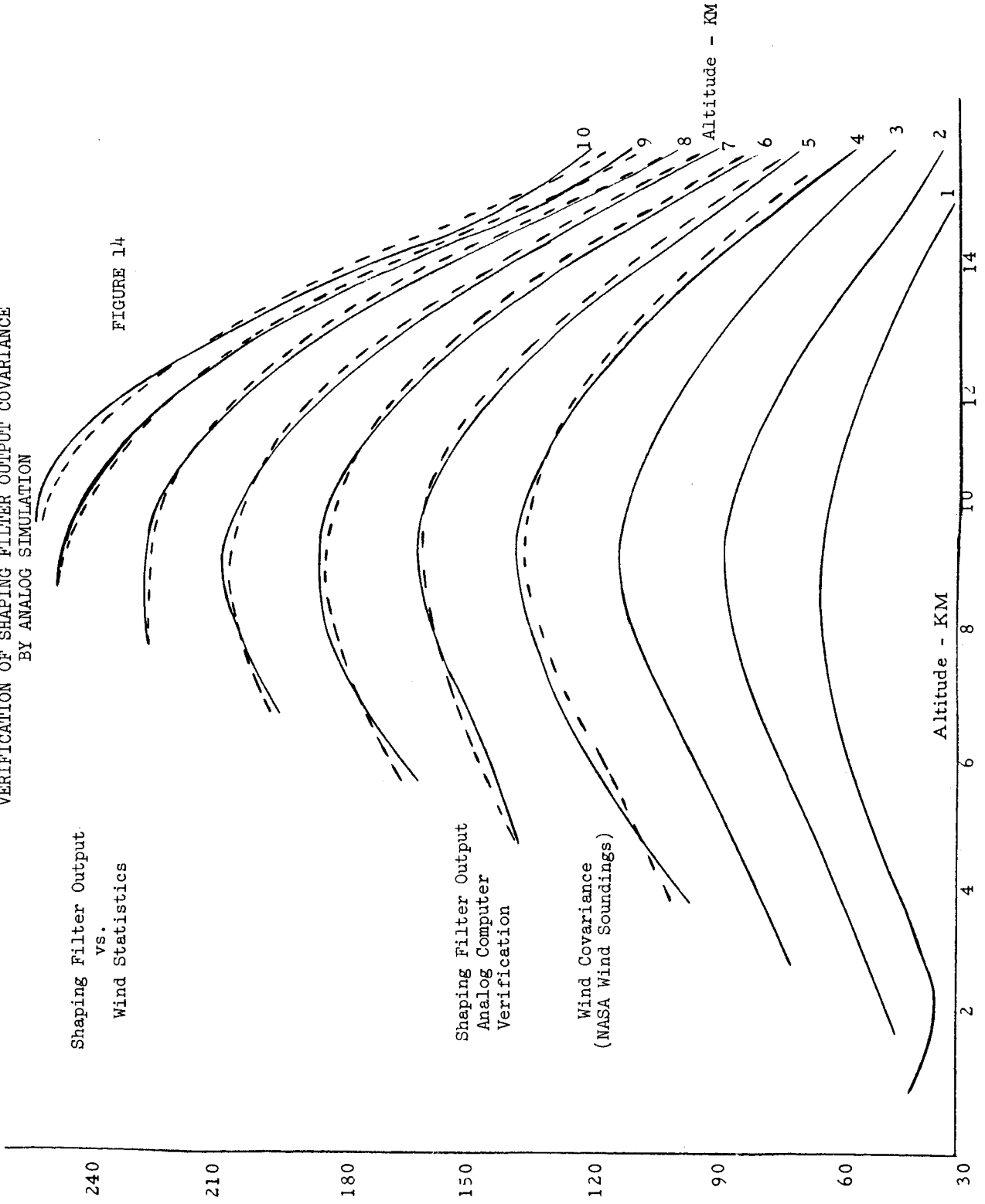
Covariance M^2/S^2

Shaping Filter Output
Analog Computer
Verification

Wind Covariance
(NASA Wind Soundings)

Altitude - KM

Altitude - KM



IV. EXTENSION TO THE FREQUENCY DOMAIN

1. POWER SPECTRA AND ZADEH SYSTEM FUNCTION

One approach to analysis of a system with time-varying coefficients is to "freeze" the coefficients at a given altitude and utilize the power spectra technique of analysis. This approach can give good results if the coefficients are sufficiently slowly varying.

For the wind model developed in this report

$$\frac{d^2 y}{dh^2} + a_1(h) \frac{dy}{dh} + a_0(h) y = b_1(h) \frac{dx}{dh} + b_0(h) x$$

if we fix the values of a_1 , a_0 , b_1 , and b_0 for a particular altitude h^* the frozen time transfer function for the system is

$$\frac{y(j\omega)}{x(j\omega)} = \frac{b_1(h^*) j\omega + b_0(h^*)}{(j\omega)^2 + a_1(h^*) j\omega + a_0(h^*)}$$

and $\frac{y(j\omega)}{x(j\omega)} = \lim_{\omega \rightarrow \infty} H(j\omega, t)$,

thus, $\frac{y(j\omega)}{x(j\omega)}$ and $H(j\omega, t)$ the system function, are asymptotic to each other as $\omega \rightarrow \infty$. For a system with transfer function $\frac{y(j\omega)}{x(j\omega)}$, with a white noise input, the output spectra is

$$G_y(\omega) = \left| \frac{y(j\omega)}{x(j\omega)} \right|^2$$

Straight line asymptotes for $G_Y(\omega)$ are shown in Figure 15 for various frozen time altitudes h^* . It is interesting to note that these spectra are in the same range as the NASA data. This result would be expected, although there is no reason to expect much closer correlation, even for the slopes. The altitudes near 8 KM compare best with the NASA data. This result is reasonable since the greater wind activity in the 6 to 10 KM altitude range would likely be more of a dominant influence on the NASA spectra.

To utilize fully the wind model in frequency domain analysis, a further extension to a time-varying transfer function may be realized by application of the Zadeh system function concept.

The system function is based on an extension of a stationary analysis technique. The conventional steady-state as well as transient analysis of fixed linear networks is based on the use of a function $H(s)$ or $H(j\omega)$ which is variously known as the transmission function, transfer function, frequency function, etc. $H(j\omega)$ may be regarded as the Fourier transform of the weighting function. Mathematically, this can be expressed as

$$H(j\omega) = \int_0^{\infty} W(t-\tau) e^{-j\omega(t-\tau)} d\tau. \quad (4)$$

The fundamental characteristic of fixed networks is that their impulsive response is dependent solely on the age variable $t - \tau$. No such property is possessed by variable networks, for in these the impulsive response is of the general form $W(t, \tau)$. Nevertheless, by analogy with equation (4) the time-varying transfer function, called the system function by Zadeh, is defined

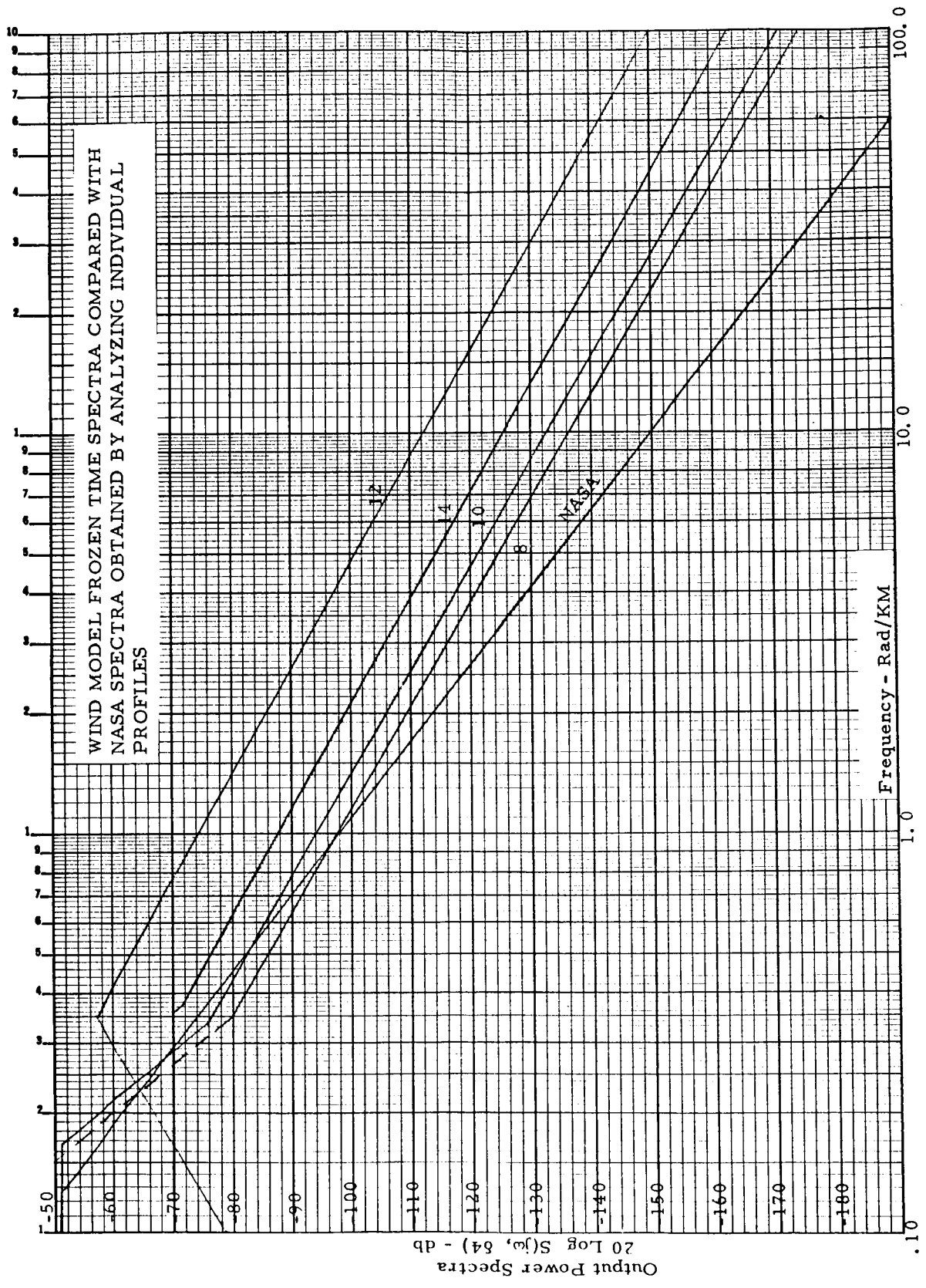


FIGURE 15

by the relation

$$H(j\omega, t) = \int_0^{\infty} W(t, \tau) e^{-j\omega(t-\tau)} d\tau . \quad (5)$$

In both equations (4) and (5) the weighting function $W(t - \tau) = W(t, \tau) = 0$ for $t < \tau$ is required for the realizability of the system, and the upper limit of integration is t . Making the change of variables $\lambda = t - \tau$, equations (4) and (5) become

$$H(j\omega) = \int_0^{\infty} W(\lambda) e^{-j\omega\lambda} d\lambda \quad (6)$$

and

$$H(j\omega, t) = \int_0^{\infty} W(t, t-\lambda) e^{-j\omega\lambda} d\lambda . \quad (7)$$

2. USES OF THE SYSTEM FUNCTION

In contrast to $H(j\omega)$, $H(j\omega, t)$ is a function of $j\omega$ involving t as a parameter. It has been shown that $H(j\omega, t)$ represents a natural extension of the system function of a fixed network. It appears that $H(j\omega, t)$ not only possesses many of the properties of $H(j\omega)$, but also can be used in a similar manner to obtain the steady-state and transient response to any prescribed input. Use of the system function in input-output relationships is considerably more complicated than for fixed systems since variable coefficient differential equations cannot be transformed directly to obtain the system function. Methods for obtaining system functions will be discussed later. Uses for the system function are as follows. The system output is

$$X(t) = \int_{-\infty}^{\infty} H(j\omega, t) M(j\omega) e^{-j\omega t} d\omega. \quad (8)$$

$M(j\omega)$, the input to equation (8), is the Fourier transform of $M(t)$, that is

$$M(j\omega) = \int_{-\infty}^{\infty} M(t) e^{-j\omega t} dt. \quad (9)$$

The statistical parameters (for stationary or non-stationary inputs) are

$$R_{xx}(t, \tau) = \int_{-\infty}^{\infty} H(j\omega, t) H^*(j\omega, t) S_{xx}(\omega) d\omega \quad (10)$$

and

$$\sigma^2(t) = \int_{-\infty}^{\infty} |H(j\omega, t)|^2 S_{xx}(\omega) d\omega \quad (11)$$

where $S_{xx}(\omega)$, the input power spectral density, is

$$S_{xx}(\omega) = \int_{-\infty}^{\infty} e^{-j\omega\tau} d\tau \left[\lim_{T \rightarrow \infty} \int_{-T}^T R_{xx}(t, t+\tau) dt \right]. \quad (12)$$

If, in addition, the input is a stationary process, equation (12) reduces to

$$S_{xx}(\omega) = \int_{-\infty}^{\infty} R_{xx}(t-\tau) e^{-j\omega(t-\tau)} d\tau. \quad (13)$$

If the input is further restricted to be white noise

$$R_{xx}(t-\tau) = \delta(t-\tau)$$

and

$$S_{xx}(\omega) = 1$$

which simplifies equations (10) and (11) to

$$R_{\infty}(t, \tau) = \int_{-\infty}^{\infty} H(j\omega, t) H^*(j\omega, \tau) d\omega \quad (14)$$

$$\sigma(t)^2 = \int_{-\infty}^{\infty} |H(j\omega, t)|^2 d\omega \quad (15)$$

3. COMBINED SYSTEM FUNCTION USING SHAPING FILTER

In order to take advantage of the simpler equations resulting when the input is white noise, the concept of a shaping filter was developed. If the system shown in Figure 16 is replaced with that shown by Figure 17, then the combined system can be

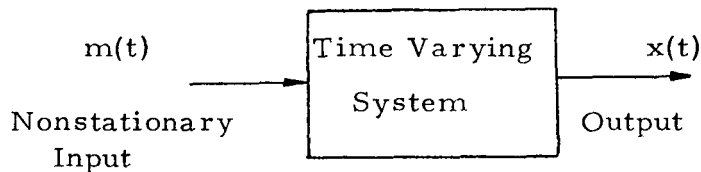


FIGURE 16
SYSTEM BLOCK DIAGRAM

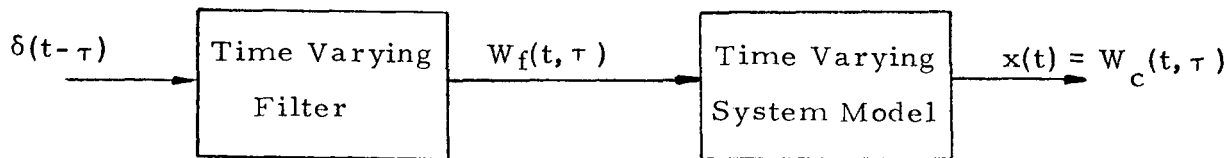


FIGURE 17
SHAPING FILTER SYSTEM BLOCK DIAGRAM

treated as a time-varying system with a stationary (white noise) input, shown by the block diagram in Figure 18.

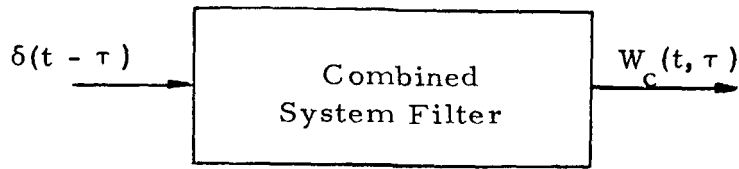


FIGURE 18
COMBINED SYSTEM BLOCK DIAGRAM

Mathematically, this combined weighting function $W_c(t, \tau)$ is obtained from W_f and the system weighting function W_s by convolution. That is

$$W_c(t, \tau) = \int_0^t W_s(t, \tau_1) W_f(\tau_1, \tau) d\tau_1 \quad (16)$$

The combined system function can be obtained mathematically either by transforming $W_c(t, \tau)$ or by combining the two system functions $H_s(j\omega, t)$ and $H_f(j\omega, t)$. Two equations for this combination of H_s and H_f are given by Reference (18):

$$H_c(j\omega, t) = H_s H_f + \frac{\partial H_s}{\partial (j\omega)} \frac{dH_f}{dt} + \dots + \frac{1}{n!} \frac{\partial^n H_s}{\partial (j\omega)^n} \frac{d^n H_f}{dt^n} \quad (17)$$

where n is the order of the original system, and

$$H_c(j\omega, t) = H_s \left(\frac{d}{dt} + j\omega, t \right) H_f(j\omega, t). \quad (18)$$

Equation (18) holds for any H_s which can be expressed as a power series. The mathematical difficulties of equations (17) and (18) are eliminated by an adjoint simulation of the combined system and filter to obtain $W_c(t, \tau)$ and transform this to get $H_c(j\omega, t)$.

4. OBTAINING THE SYSTEM FUNCTION

Consider the problem of obtaining the system function for an equation of the form

$$\begin{aligned}
 & a_n(t) \frac{d^n Y(t)}{dt^n} + a_{n-1}(t) \frac{d^{n-1} Y(t)}{dt^{n-1}} + \dots + a_1(t) \frac{dY(t)}{dt} + a_0(t) Y(t) \\
 = & b_m(t) \frac{d^m X(t)}{dt^m} + b_{m-1}(t) \frac{d^{m-1} X(t)}{dt^{m-1}} + \dots + b_1(t) \frac{dX(t)}{dt} + b_0(t) X(t)
 \end{aligned}
 \tag{19}$$

where $a_0(t), a_1(t), \dots, a_{n-1}(t), b_0(t), b_1(t), \dots, b_m(t)$ are functions of time, the leading coefficient a_n can always be set equal to one without loss of generality. In operator notation this equation can be shortened to

$$A(p, t) Y(t) = B(p, t) X(t) \text{ where } p = \frac{d}{dt}. \tag{20}$$

Note that the system function $H(j\omega, t)$ is the Fourier transform of the weighting function or impulsive response $W(t, \tau)$. In equation (20) if $X(t)$ is a unit impulse, then the output $Y(t)$ is the impulsive response. Mathematically, this is expressed

$$A(p, t) W(t, \tau) = B(p, t) \delta(t - \tau). \tag{21}$$

The system function is generally obtained from equation (21) either by solving for $W(t, \tau)$ and transforming, or by further manipulation to obtain $H(j\omega, t)$ directly.

In determining the system function by the Green's function method, the system function is obtained from the impulsive response by means of equation (7). The impulsive response is in turn determined by using the one-sided Green's function as follows. If a solution exists, it must be of the form

$$W(t, \tau) = \sum_{i=1}^n \phi_i(t) \psi_i(\tau)$$

where the $\phi_i(t)$ are the solutions to the homogeneous equation

$$A(p, t) \phi_i(t) = 0.$$

The $\psi_i(\tau)$ are not determined directly, but follow as a result of the following procedure. First calculate the Wronskian determinant, $W(\tau)$:

$$W(\tau) = \begin{vmatrix} \phi_1(\tau) & \phi_2(\tau) & \dots & \phi_n(\tau) \\ \phi_1'(\tau) & \phi_2'(\tau) & \dots & \dots \\ \vdots & \vdots & \dots & \vdots \\ \phi_1^{(n-1)}(\tau) & \dots & \dots & \phi_n^{(n-1)}(\tau) \end{vmatrix}$$

The Wronskian is used to determine the one-sided Green's function from the equation

$$G(t, \tau) = \frac{(-1)^{n-1}}{a_n(\tau) W(\tau)} \begin{vmatrix} \phi_1(t) & \phi_2(t) \dots \phi_n(t) \\ \phi_1(\tau) & \phi_2(\tau) \dots \phi_n(\tau) \\ \phi_1'(\tau) & \dots \dots \dots \\ \vdots & \vdots & \vdots \\ \phi_1^{(n-2)}(\tau) & \dots \dots \phi_n^{(n-2)}(\tau) \end{vmatrix} \quad (22)$$

The one-sided Green's function is related to the impulsive response by the equation

$$W(t, \tau) = \left\{ b_0(\tau) G(t, \tau) - \frac{\partial}{\partial \tau} [b_1(\tau) G(t, \tau)] + \dots + (-1)^m \frac{\partial^m}{\partial \tau^m} [b_m(\tau) G(t, \tau)] \right\} u(t-\tau). \quad (23)$$

Note here that if $B(p, t) = b_0(t)$, the impulsive response is the product of $b_0(\tau)$ and the one-sided Green's function $G(t, \tau)$. Derivations of the equations of this section can be found in References (16) and (18).

5. SAMPLE CALCULATIONS FOR SYSTEM FUNCTION

USING METHOD OF GREEN'S FUNCTION

Consider the problem of calculating the system function for the first order

Euler equation:

$$\dot{Y} + \left(\frac{1}{a+t} \right) Y = B(p, t) X(t)$$

The homogeneous equation

$$\dot{\phi}(t) + \left(\frac{1}{a+t} \right) \phi(t) = 0$$

has the solution

$$\phi(t) = \frac{1}{a+t} \cdot$$

Its Wronskian is

$$W(\tau) = \phi(\tau) = \frac{1}{a+\tau}$$

and the Green's function becomes

$$G(t, \tau) = \frac{\phi(t)}{W(\tau)} = \frac{a+\tau}{a+t}$$

If $B(p, t) \neq 1$, equation (22) must be used to determine the weighting function.

For simplicity $B(p, t) = 1$ is chosen and the weighting function becomes

$$\begin{aligned} W(t, \tau) &= G(t, \tau) \quad u(t - \tau) \\ &= G(t, \tau) \quad t \geq \tau \\ &= 0 \quad t < \tau \end{aligned}$$

The system function corresponding to this weighting function is now determined from equation (7).

$$\begin{aligned} H(j\omega, t) &= \int_0^{\infty} G(t, t - \lambda) e^{-j\omega\lambda} d\lambda = \int_0^{\infty} \left[\frac{a+(t-\lambda)}{a+t} \right] e^{-j\omega\lambda} d\lambda \\ &= \frac{a+t}{a+t} \int_0^{\infty} e^{-j\omega\lambda} d\lambda - \frac{1}{a+t} \int_0^{\infty} \lambda e^{-j\omega\lambda} d\lambda \\ &= \frac{1}{j\omega} - \left(\frac{1}{a+t} \right) \frac{1}{(j\omega)^2} \end{aligned} \quad (24)$$

Several interesting statements can be made about equation (24); first, the poles of the system function are constant (two poles at the origin) as required for realizability of the system. Another point of interest is that there are two poles for a first order system. In general, for time-variable systems the system function will have more poles than the order of the system. In fact, if the number of poles is the same as the order of the differential equation the coefficients must be constants .

Additional insight into the system response can be obtained by showing the system function as a family of Bode Plots. This is done for $a = 1$ in Figure 19; Figure 20 shows a three-dimensional plot of the same information.

6. A COMPUTER SOLUTION TO OBTAIN THE SYSTEM FUNCTION

If equation (21) is transformed with respect to τ , and the definition of $H(j\omega, t)$ is applied, the result is

$$A(p, t) H(j\omega, t) e^{j\omega t} = B(p, t) e^{j\omega t} . \quad (25)$$

Performing the indicated operations, noting that

$$\frac{\partial^u A(p, t) e^{j\omega t}}{\partial p^u} = \frac{\partial^u A(j\omega, t) e^{j\omega t}}{\partial (j\omega)^u}$$

and

$$B(p, t) e^{j\omega t} = B(j\omega, t) e^{j\omega t} ,$$

we obtain after minor simplifications, the differential equation

$$\left[\frac{1}{n!} \frac{\partial^n A(j\omega, t)}{\partial (j\omega)^n} \right] \frac{d^n H(j\omega, t)}{d + n} + \dots + \frac{\partial A(j\omega, t)}{\partial (j\omega)} \frac{dH(j\omega, t)}{dt} + A(j\omega, t) H(j\omega, t) = B(j\omega, t) . \quad (26)$$

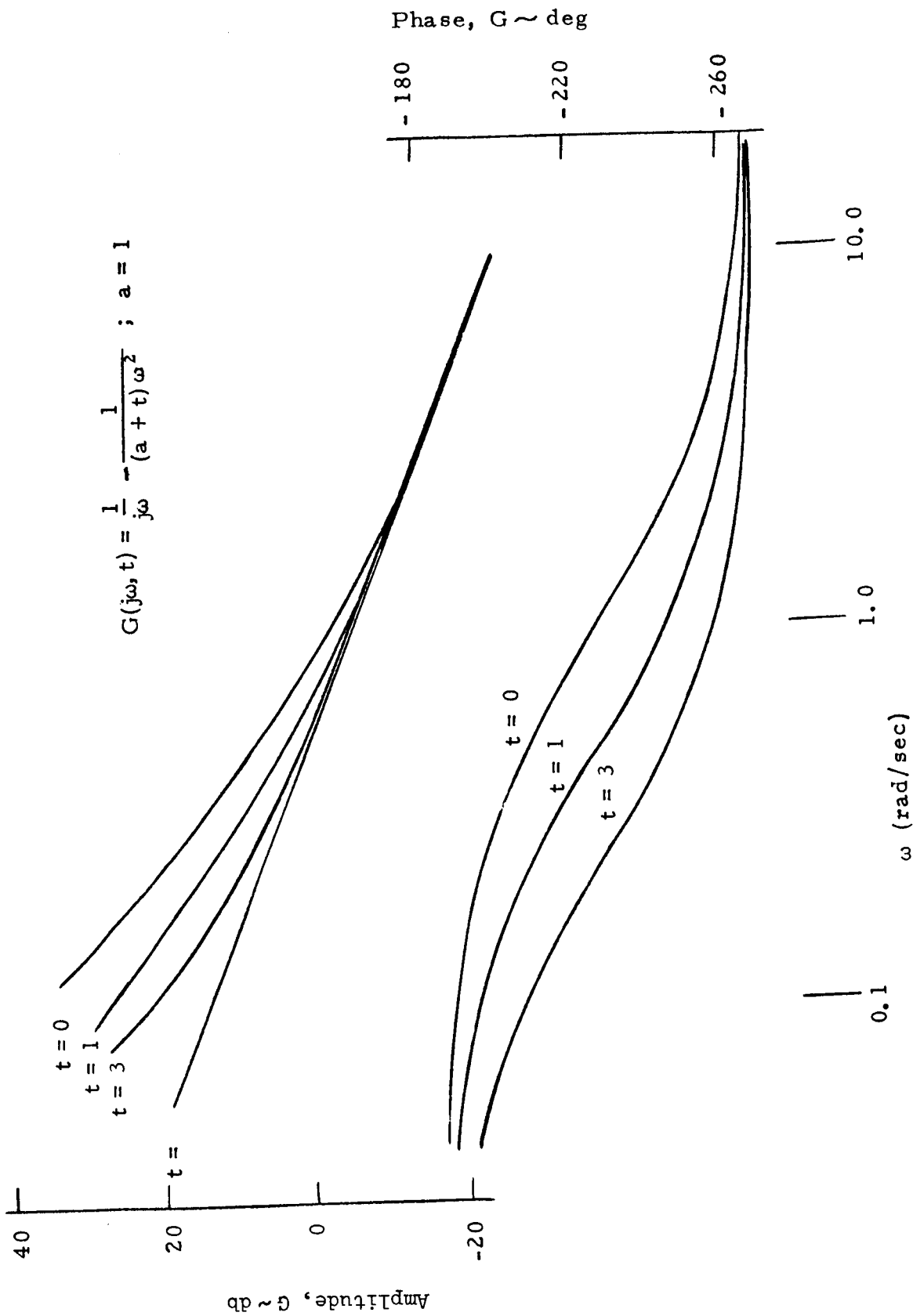


FIGURE 19. BODE DIAGRAM, AMPLITUDE RATIO AND PHASE FOR EULER EQUATION SYSTEM FUNCTION, $G(j\omega, t)$

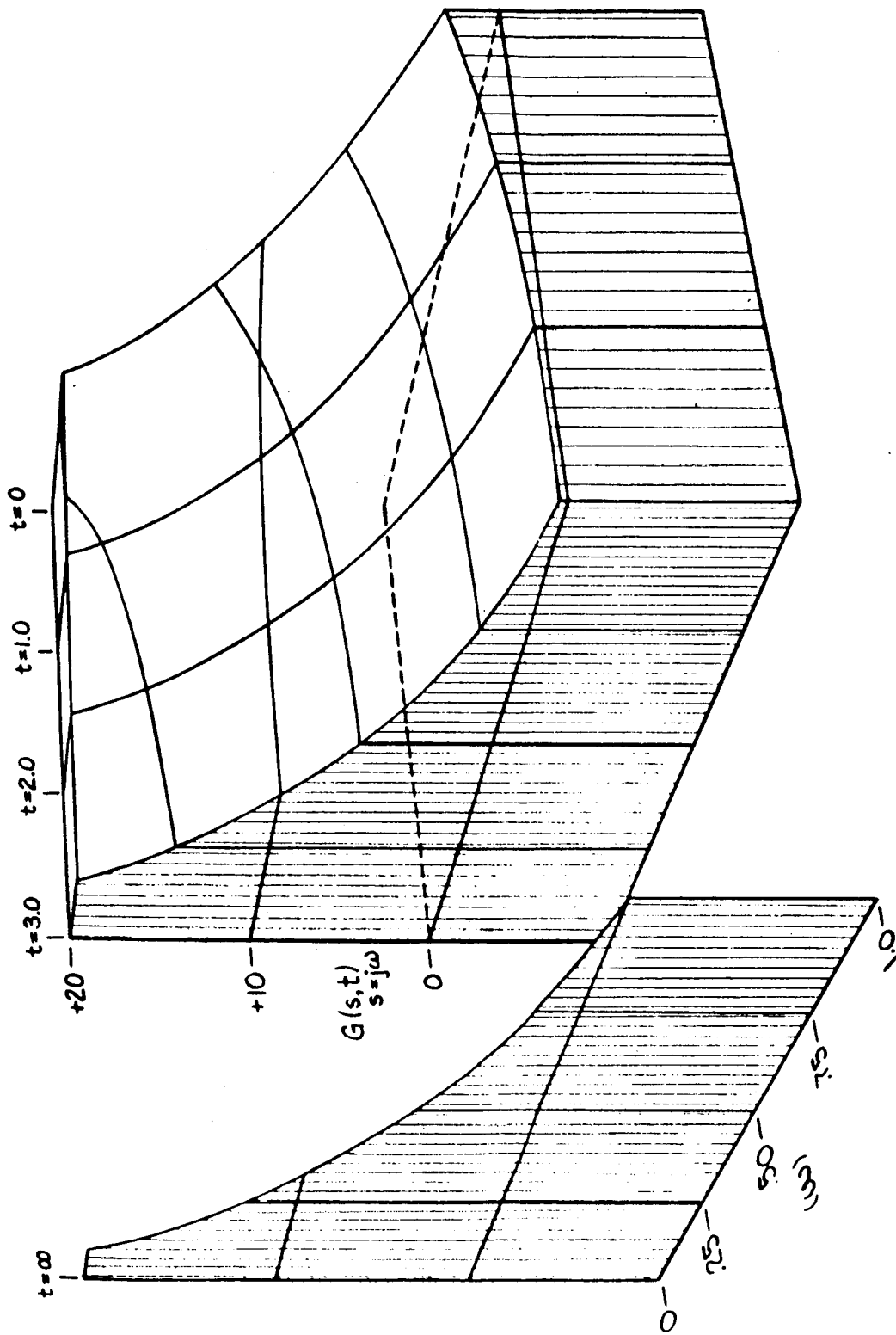


FIGURE 20. THREE-DIMENSIONAL REPRESENTATION OF THE EULER EQUATION SYSTEM FUNCTION

In general, this equation will be complex and its solution will be

$$H(j\omega, t) = H_r(j\omega, t) + jH_i(j\omega, t).$$

Separating equation (26) into real and imaginary parts results in two similar equations which must be solved simultaneously to obtain $H(j\omega, t)$. While this solution is not practical to obtain by hand, the equations can be solved by either analog or digital computer.

For the wind model differential equation, equation (26) is

$$\left[\frac{d^2}{dt^2} + a_1(t) \frac{d}{dt} + a_0(t) \right] H(j\omega, t) e^{j\omega t} = \left[b_0(t) + b_1(t) \frac{d}{dt} \right] e^{j\omega t}$$

which becomes

$$(j\omega)^2 H(j\omega, t) + 2j\omega \dot{H}(j\omega, t) + \ddot{H}(j\omega, t) + a_1(t) \left[\dot{H}(j\omega, t) + j\omega H(j\omega, t) \right] + a_0(t) H(j\omega, t) = j\omega b_1(t) + b_0(t). \quad (27)$$

Separating equation (27) into its real and imaginary parts

$$\ddot{H}_r + a_1 \dot{H}_r - 2\omega \dot{H}_i + (a_0 - \omega^2) H_r - a_1 \omega H_i = b_0 \quad (28)$$

$$\ddot{H}_i + a_1 \dot{H}_i + 2\omega \dot{H}_r + (a_0 - \omega^2) H_i + a_1 \omega H_r = \omega b_1 \quad (29)$$

results in the equations which are used later to obtain the system function for the wind model differential equation.

7. APPROXIMATE METHODS OF OBTAINING THE SYSTEM FUNCTION

The differential equation for the system function equation (26) can also be solved by several approximate methods (15, 18, 1). In general, the utility of all of these approaches is limited by restrictions on how the parameters vary. One method, which is restricted to slowly varying parameters, is especially

useful in showing the relationship between the system function and frozen system function. The frozen system function is obtained by conventional transform methods for stationary coefficients and is

$$H_f(j\omega, t_f) = \frac{B(p, t_f)}{A(p, t_f)} \quad (30)$$

Re-arranging equation (30) by solving for $H(j\omega, t)$,

$$H(j\omega, t) = \frac{B(j\omega, t)}{A(j\omega, t)} + \frac{1}{A(j\omega, t)} \frac{\partial A}{\partial (j\omega)} \frac{dH}{dt} + \dots + \frac{1}{n!} \frac{\partial^n A}{\partial (j\omega)^n} \frac{d^n H}{dt^n} \quad (31)$$

Thus, the frozen system function can be obtained from equation (31) under the assumption that the derivatives of $H(j\omega, t)$ are zero in the time interval under consideration. Thus, $H_f(j\omega, t)$ may be considered as a first approximation to $H(j\omega, t)$. This one approximation will be enough when the coefficients of equation (21) do not change appreciably during the interval in which the impulse response practically differs from zero. Furthermore, for high values of the input frequencies the exact transfer function tends asymptotically to that expressed by equation (30). This is so because where these components of the input are concerned, the system may be regarded as constant.

When the coefficients of equation (21) vary slowly, a recurrence formula for $H(j\omega, t)$ has been developed (1) so as to obtain

$$H_i(j\omega, t) = - \frac{1}{A(j\omega, t)} \left[\frac{1}{n!} \frac{\partial^n A}{\partial (j\omega)^n} \frac{d^n H_{i-1}}{dt^n} + \dots + \frac{\partial A}{\partial (j\omega)} \frac{dH_{i-1}}{dt} \right] \quad (32)$$

as successive approximations to the exact system function. With the quantities obtained from equation (30) as $H_0(j\omega, t)$ we can write the following series for

the system function

$$H(j\omega, t) = \sum_{i=0}^{\infty} H_i(j\omega, t) . \quad (33)$$

8. HIGHER DEGREE OF FREEDOM SYSTEMS

For an N-degree of freedom system with a single input, as might be encountered in the study of a missile/wind model, the preceding computer method in more general form is again applicable, although with much complexity. Consider the n simultaneous equations of motion

$$\begin{aligned} A_{11}(p, t) Y_1(t) + A_{12}(p, t) Y_2(t) + \dots + A_{1n}(p, t) Y_n(t) &= B_1(p, t) X(t) \\ A_{21}(p, t) Y_1(t) + A_{22}(p, t) Y_2(t) + \dots + A_{2n}(p, t) Y_n(t) &= B_2(p, t) X(t) \\ \vdots & \\ \vdots & \\ \vdots & \\ A_{n1}(p, t) Y_1(t) + A_{n2}(p, t) Y_2(t) + \dots + A_{nn}(p, t) Y_n(t) &= B_n(p, t) X(t) . \end{aligned} \quad (34)$$

By the same argument used in obtaining equation (25), n simultaneous equations for $H_i(j\omega, t)$ are obtained

$$\begin{aligned} A_{i1}(p, t) H_1(j\omega, t) e^{j\omega t} + A_{i2}(p, t) H_2(j\omega, t) e^{j\omega t} + \dots + A_{in}(p, t) H_n(j\omega, t) e^{j\omega t} \\ = B_i(p, t) e^{j\omega t} \end{aligned} \quad (35)$$

where $i = 1, 2, \dots, n$.

Equations (35) separate into $2n$ simultaneous equations in the real and imaginary parts of $H_i(j\omega, t)$. These equations will be similar to equations (28) and (29) in form, although more difficult to solve.

9. WIND MODEL SYSTEM FUNCTION SIMULATION

The objectives of the simulation of the system function of the wind model were: (1) to determine the feasibility of the computer method; (2) to investigate the inaccuracy of using the frozen system function as an approximation to the time-varying system function; and (3) to determine the system function for the wind model of Chapter III. Since the simulation was proceeding at the same time the wind model was being developed final coefficient values were not available and the third objective was by-passed. Plots of the interim values of wind coefficients used are shown by Figures 21 thru 24. Some work was done simulating the final wind model and these results are discussed.

The simulation was done on a REAC analog computer. The operating range of the independent variable (t), which for the wind model was altitude, was allowed to run from 0-20 km. Coefficients of the interim wind model were only specified over the range 0-12 km. Frequencies for which $H(j\omega, t)$ was simulated were $\omega = 0.1$ and $\omega = 0.01$.

In scaled form equations (28) and (29) become

$$\frac{\dot{H}_r}{\dot{H}_{rm}} = \frac{H_{rm} a_{1m}}{\ddot{H}_{rm}} \left(\frac{a_1}{a_{1m}} \right) \left(\frac{\ddot{H}_r}{\ddot{H}_{rm}} \right) + \frac{2\dot{H}_{rm}\omega}{\ddot{H}_{rm}} \left(\frac{\dot{H}_i}{\dot{H}_{im}} \right) - \frac{a_{0m}H_{rm}}{\ddot{H}_{rm}} \quad (36)$$

$$\left(\frac{a_0}{a_{0m}} \right) \left(\frac{H_r}{H_{rm}} \right) + \frac{H_{rm}\omega^2}{\ddot{H}_{rm}} \left(\frac{H_r}{H_{rm}} \right) + \frac{a_{1m}H_{im}\omega}{H_{rm}} \left(\frac{a_1}{a_{1m}} \right) \left(\frac{H_i}{H_{im}} \right) + \frac{b_{0m}}{H_{rm}} \left(\frac{b_0}{b_{0m}} \right)$$

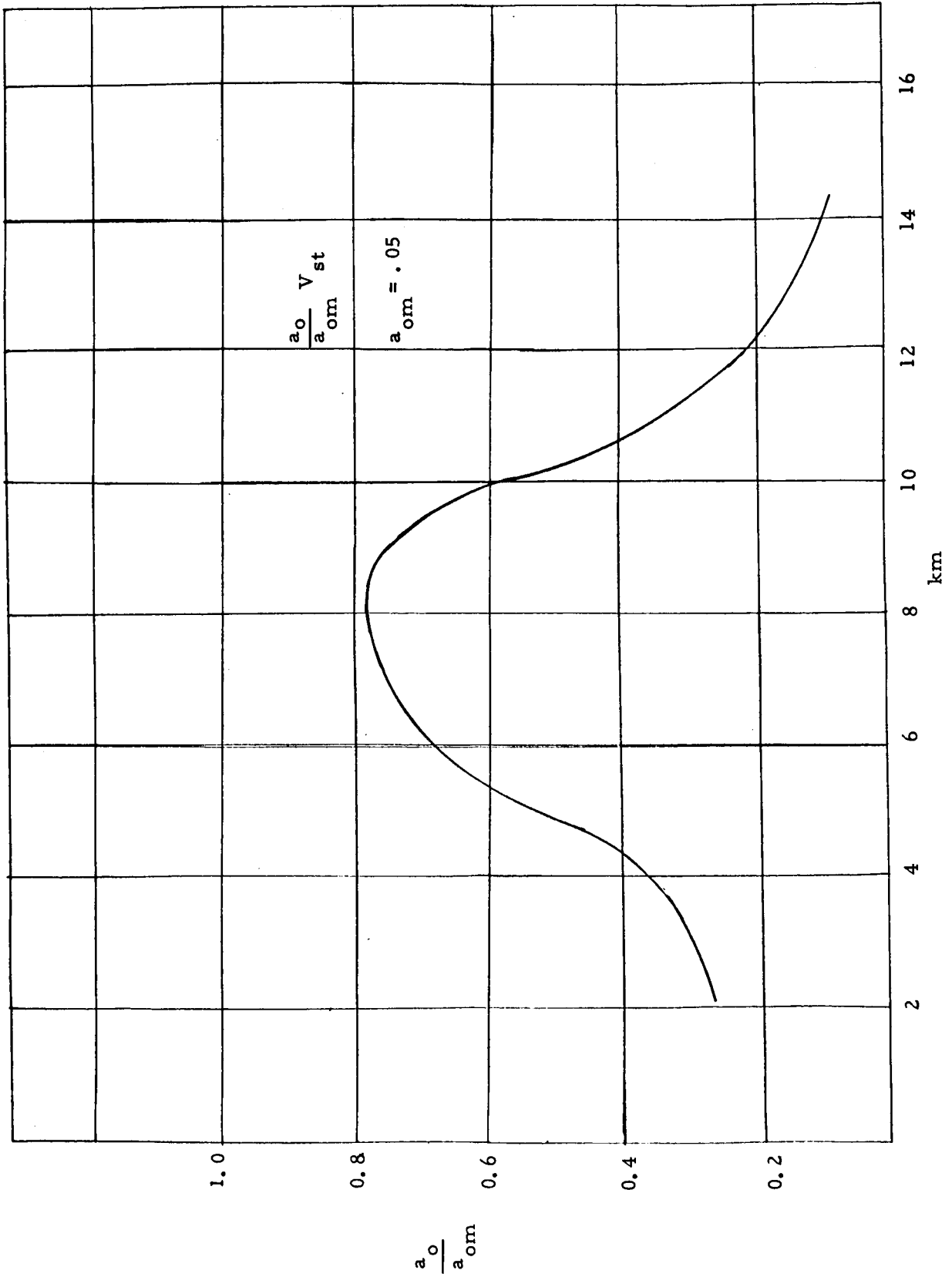


FIGURE 21. a_0 COEFFICIENTS FOR INTERIM WIND MODEL

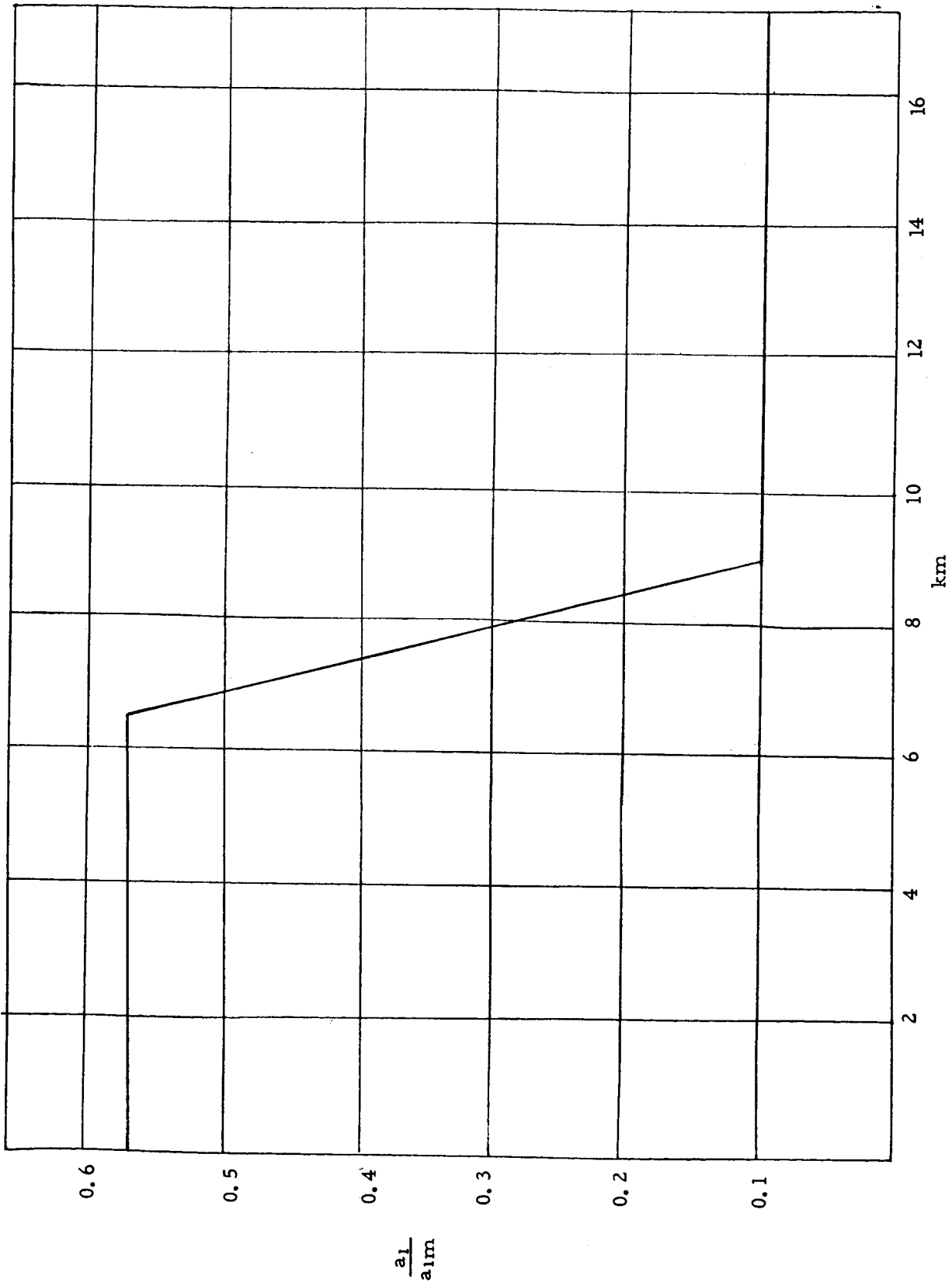


FIGURE 22. a_1 COEFFICIENTS FOR INTERIM WIND MODEL

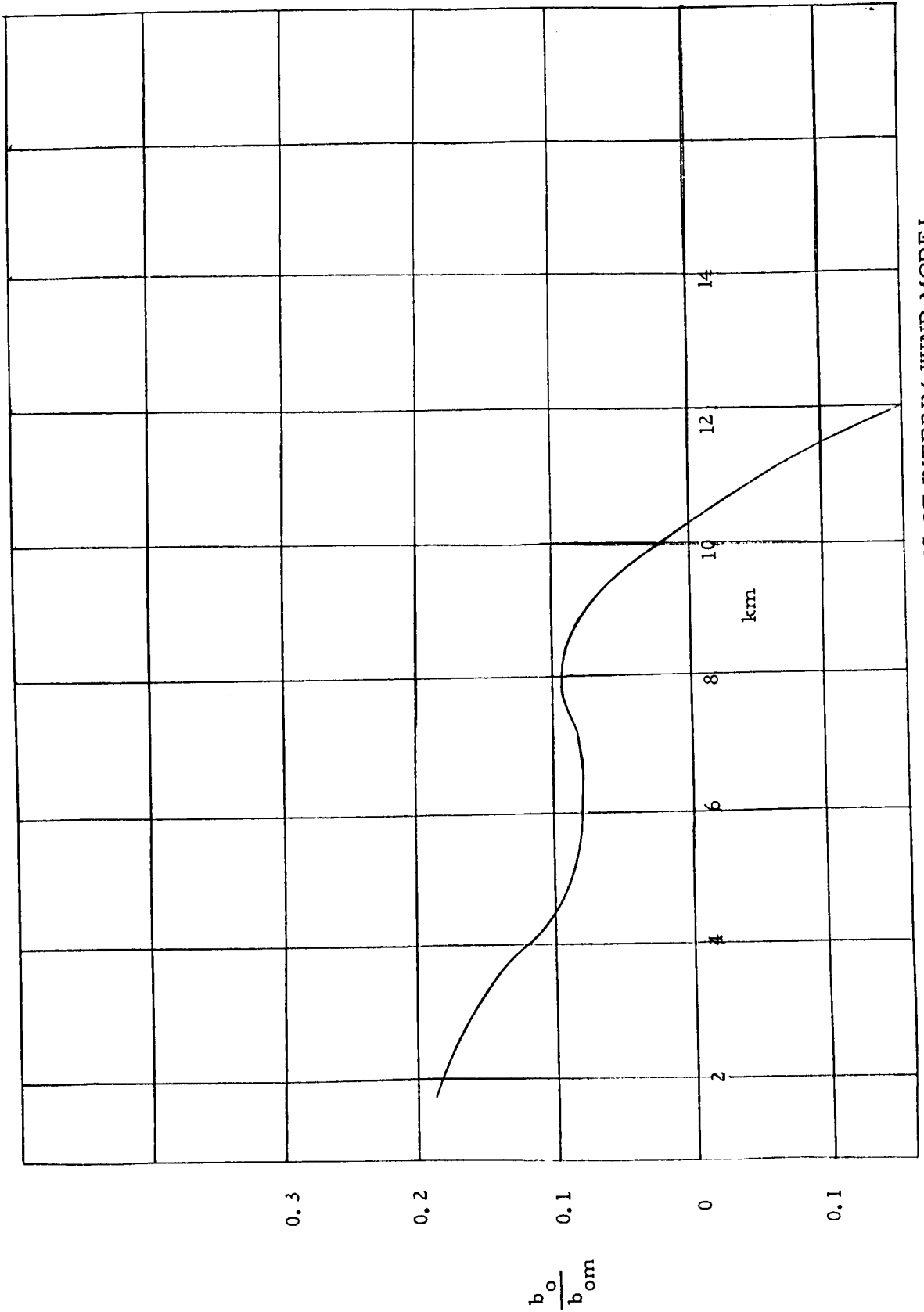


FIGURE 23. b_o COEFFICIENTS OF INTERIM WIND MODEL

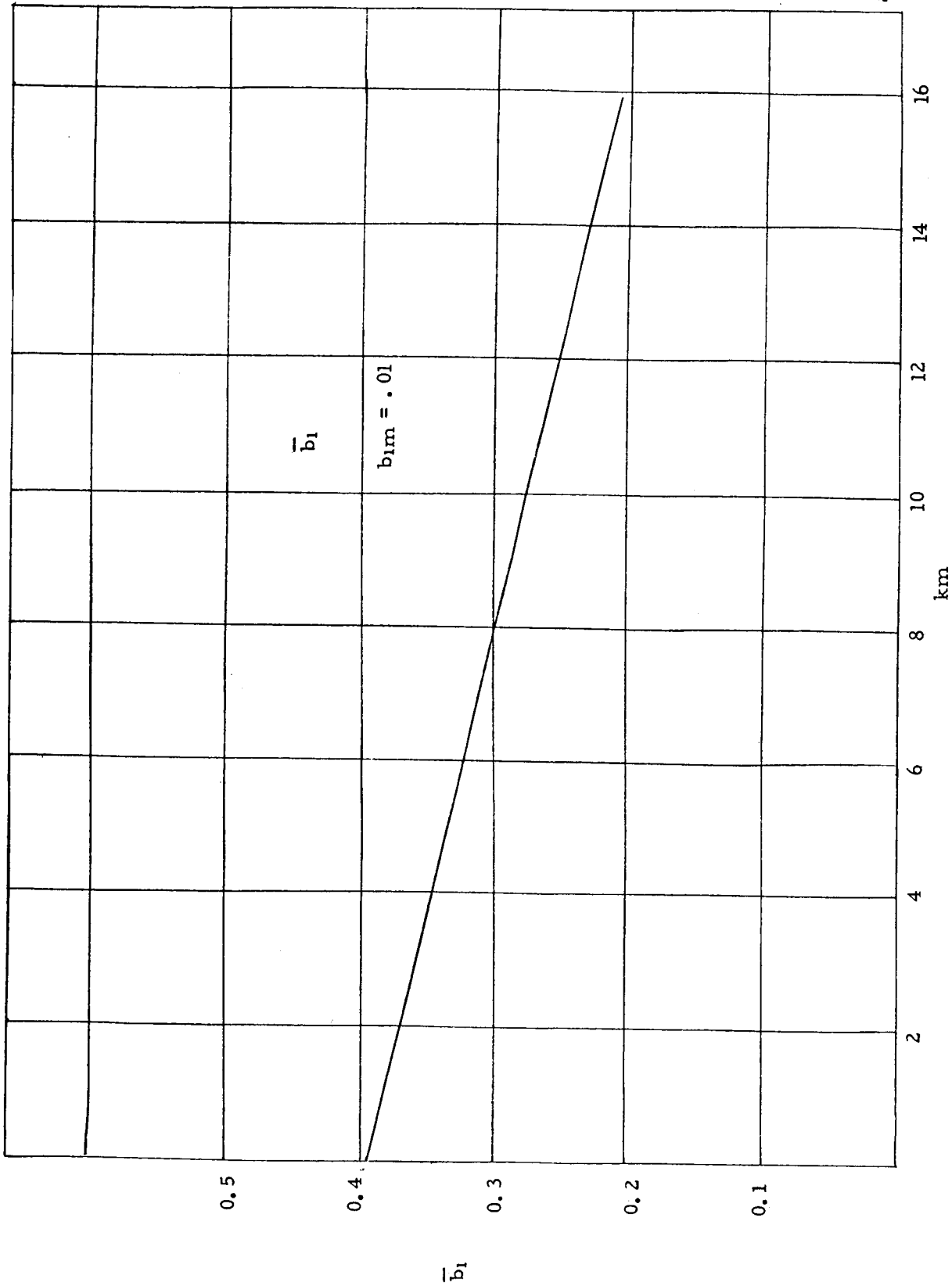


FIGURE 24. b_1 COEFFICIENTS FOR INTERIM WIND MODEL

$$\begin{aligned} \frac{\ddot{H}_i}{\dot{H}_{im}} = & - \frac{\dot{H}_{im} a_{1m}}{\dot{H}_{im}} \left(\frac{a_1}{a_{1m}} \right) \left(\frac{\dot{H}_i}{\dot{H}_{im}} \right) - \frac{2 \dot{H}_{rm} \omega}{\dot{H}_{im}} \left(\frac{\dot{H}_i}{\dot{H}_{im}} \right) - \frac{a_{0m} \dot{H}_{im}}{\dot{H}_{im}} \left(\frac{a_0}{a_{0m}} \right) \left(\frac{\dot{H}_i}{\dot{H}_{im}} \right) \\ & + \frac{H_{im} \omega^2}{\dot{H}_{im}} \left(\frac{H_i}{\dot{H}_{im}} \right) - \frac{a_{1m} H_{rm} \omega}{\dot{H}_{im}} \left(\frac{a_1}{a_{1m}} \right) \left(\frac{H_r}{H_{rm}} \right) + \frac{b_{1m} \omega}{\dot{H}_{im}} \left(\frac{b_1}{b_{1m}} \right) \end{aligned} \quad (37)$$

Substituting the appropriate maximum values into equations (36) and (37)

gives the equations to be programmed.

For $\omega = 0.1$ (H/H_m terms are written as \bar{H})

$$\ddot{\bar{H}}_r = (-0.5 \dot{\bar{H}}_r + 0.2 \bar{H}_i) \bar{a}_1 - (\bar{a}_0 - 0.2) \bar{H}_r + \dot{\bar{H}}_i + \bar{b}_0$$

$$\ddot{\bar{H}}_i = -(0.5 \dot{\bar{H}}_i + 0.2 \bar{H}_r) \bar{a}_1 - (\bar{a}_0 - 0.2) \bar{H}_i - \dot{\bar{H}}_r + 0.1 \bar{b}_1.$$

For $\omega = 0.01$

$$\ddot{\bar{H}}_r = (-0.5 \dot{\bar{H}}_r + 0.02 \bar{H}_i) \bar{a}_1 + 0.1 \dot{\bar{H}}_i + \bar{H}_r (-\bar{a}_0 + 0.002) + \bar{b}_0$$

$$\ddot{\bar{H}}_i = -(0.5 \dot{\bar{H}}_i + 0.02 \bar{H}_r) \bar{a}_1 - 0.1 \dot{\bar{H}}_r + \bar{H}_i (-\bar{a}_0 + 0.002) + 0.01 \bar{b}_1$$

Figures 25 and 26 show the computer diagrams for these simulations.

10. RESULTS OF SIMULATION

In order to check the accuracy of the simulation it was necessary, since $H(j\omega, t)$ was not calculable directly, to devise some other method of checking. As the system function must approach the frequency function, or frozen system function, as its coefficients become constant, the output of the simulation with constant coefficients must be the frozen system function. This was done by freezing the time input to the function generators, and the results compared

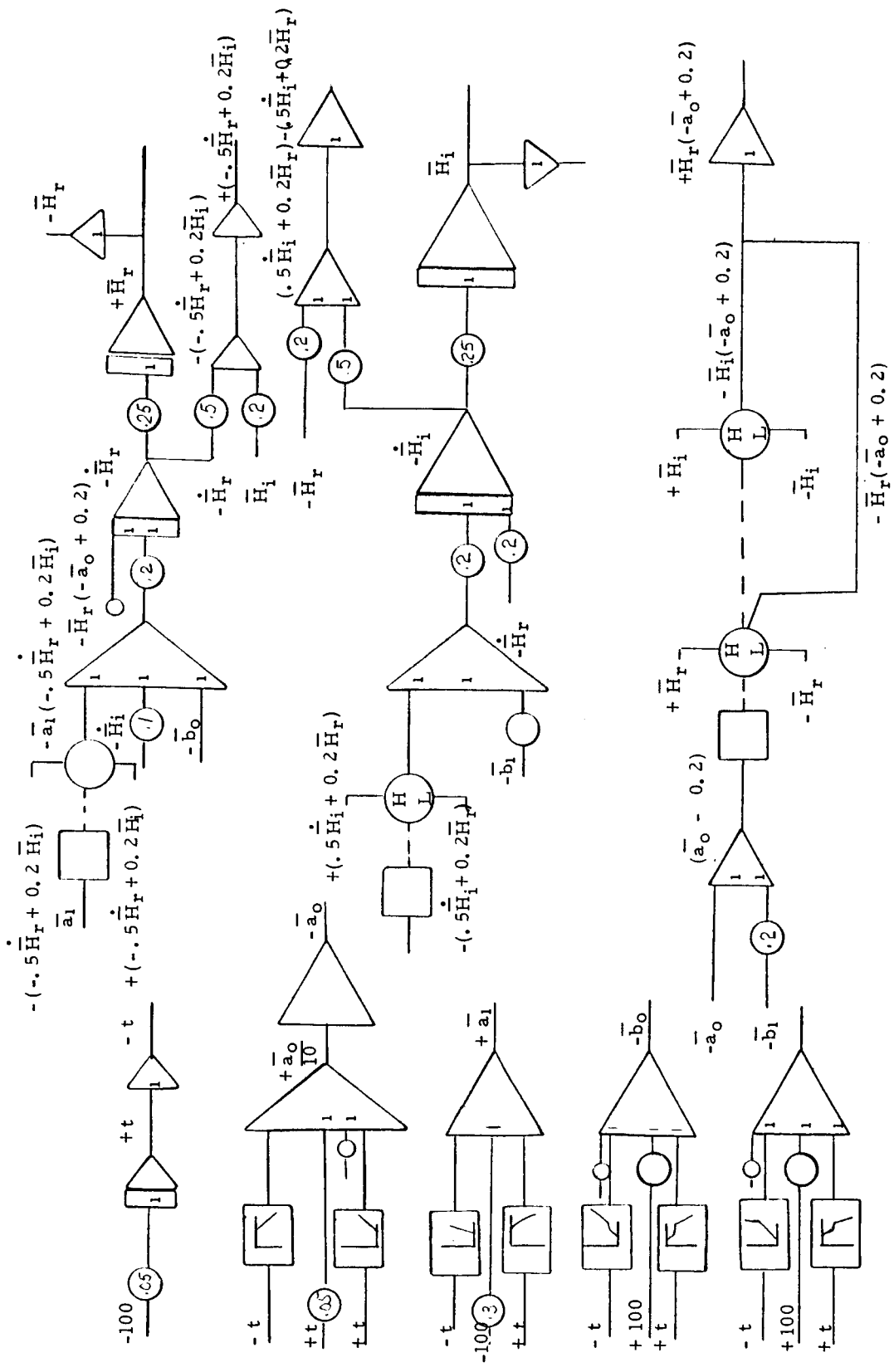


FIGURE 25. COMPUTER DIAGRAM FOR WIND MODEL SYSTEM FUNCTION
 $\omega = 0.1$

with the calculated frozen system function. This comparison is shown in Table 1 with some sample computer solutions shown by Figures 27. Agreement between calculated and computed values was good, and at least part of the error can be attributed to inaccuracies in the simulation. Discrepancies were reduced considerably for the $\omega = 0.01$ case by increased care in setting coefficients and potentiometers.

The results of the variable coefficient solution for $H(j\omega, t)$ are shown by Figures 28, 29 and 30 for $\omega = 0.1, 0.01$. Figures 28 and 29 show that the system function and frozen system differ considerably. The question of initial conditions on $H(j\omega, t)$ was considered, and Figure 30 shows several combinations of initial conditions which are based on the frozen system function at 2 km. The frozen system function at $t = 0$ was not used because the data used to generate the wind model coefficients tended toward less accuracy at $t = 0$. Use of the excessively large values of H_f would also have required re-scaling the equations (maximum values of H_r and H_i were both 0.2). Although these initial conditions did not produce entirely satisfactory results, one conclusion was apparent. The shape of the system function curves, which were much smoother than the frozen system function curves, show that the system function does not react as rapidly to rapid changes in coefficient values as the frozen system function. This confirms the fact that stationary analysis of rapidly varying systems can induce significant errors.

t	$\omega = 0.1$		$\omega = 0.01$	
	Computer $H_r + jH_i$	Calculated $H_r + jH_i$	Computer $H_r + jH_i$	Calculated $H_r + jH_i$
0		0.118 - 0.3267		1.63 - 1.105 j
2	0.168 - 0.214 j	0.137 - 0.202 j	0.127 - 0.001 j	0.127 - 0.00319 j
3	0.122 - 0.172 j	0.135 - 0.154 j	-	0.103 - 0.0019 j
4	-	0.123 - 0.079 j	0.071 + 0.000 j	0.072 - 0.00057 j
5	0.058 - 0.0015 j	0.062 - 0.0023 j	0.036 + 0.0005 j	0.036 + 0.00055 j
6	0.029 + 0.0063 j	0.0285 + 0.00635 j	0.021 + 0.000 j	0.019 - 0.0008 j
7	0.0265 + 0.0055 j	0.0284 + 0.00565 j	-	0.0205 + 0.00052 j
8	-	0.0285 + 0.0066 j	0.022 + 0.0008 j	0.022 + 0.00055 j
9	0.0126 + 0.0112 j	0.0115 + 0.01 j	-	0.0076 + 0.0007 j
10	-	-0.185 + 0.0147 j	-	0.0125 + 0.001 j

TABLE 1. FROZEN SYSTEM FUNCTIONS,
COMPUTER VS. CALCULATED VALUES

As final values of coefficients of the wind model became available, it was apparent that they were quite different in form. Re-programming the computer for final coefficients was undertaken in the time remaining and, while this study has not been completed, one additional result will be discussed.

For a stationary wind model using the same differential equation

$$\ddot{Y} + a_1 \dot{Y} + a_0 Y = b_0 X + b_1 \dot{X}$$

the transfer function by conventional Laplace transform methods is

$$H(s) = \frac{b_0 + b_1 s}{s^2 + a_1 s + a_0} \quad (38)$$

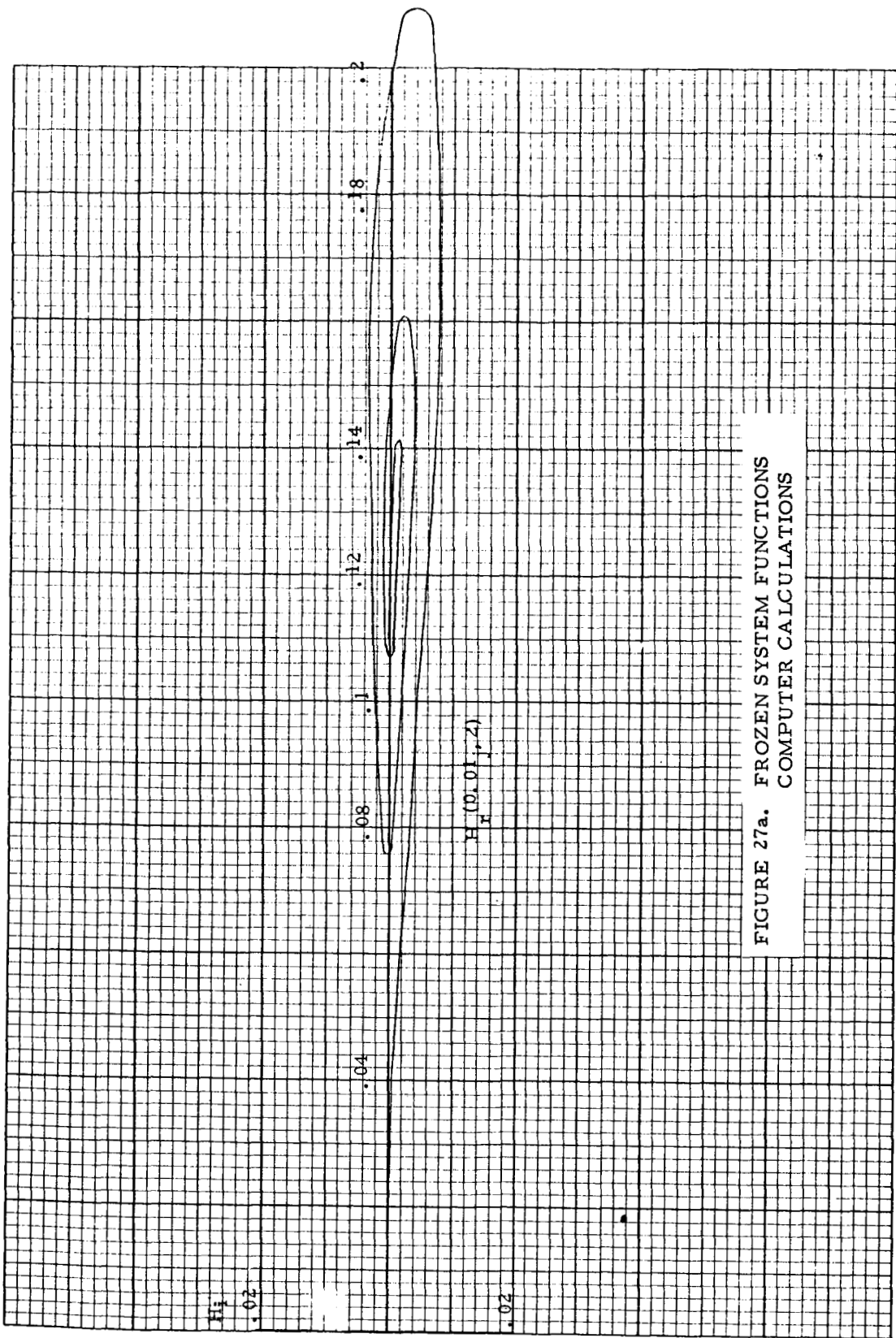


FIGURE 27a. FROZEN SYSTEM FUNCTIONS
COMPUTER CALCULATIONS

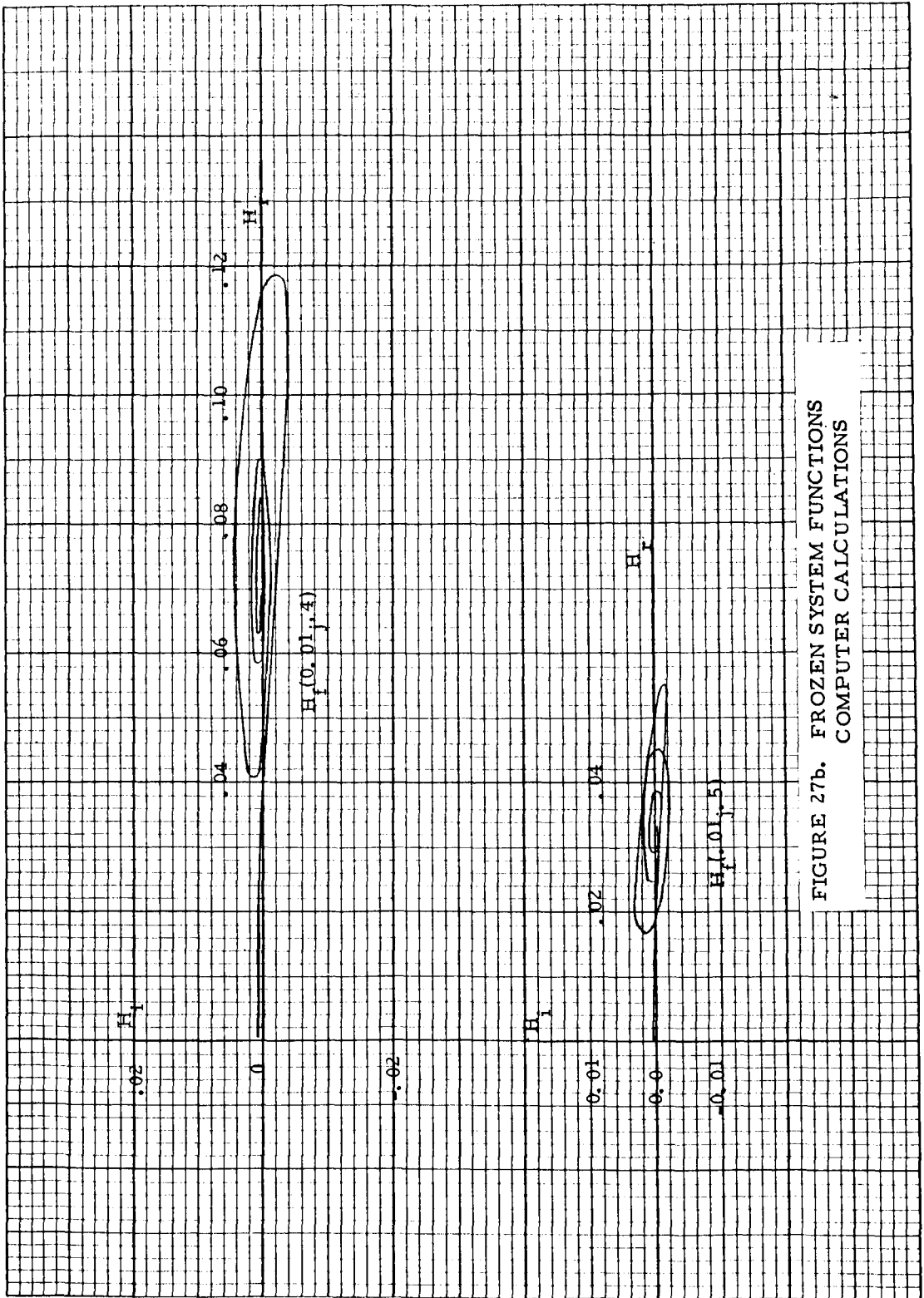


FIGURE 27b. FROZEN SYSTEM FUNCTIONS
COMPUTER CALCULATIONS

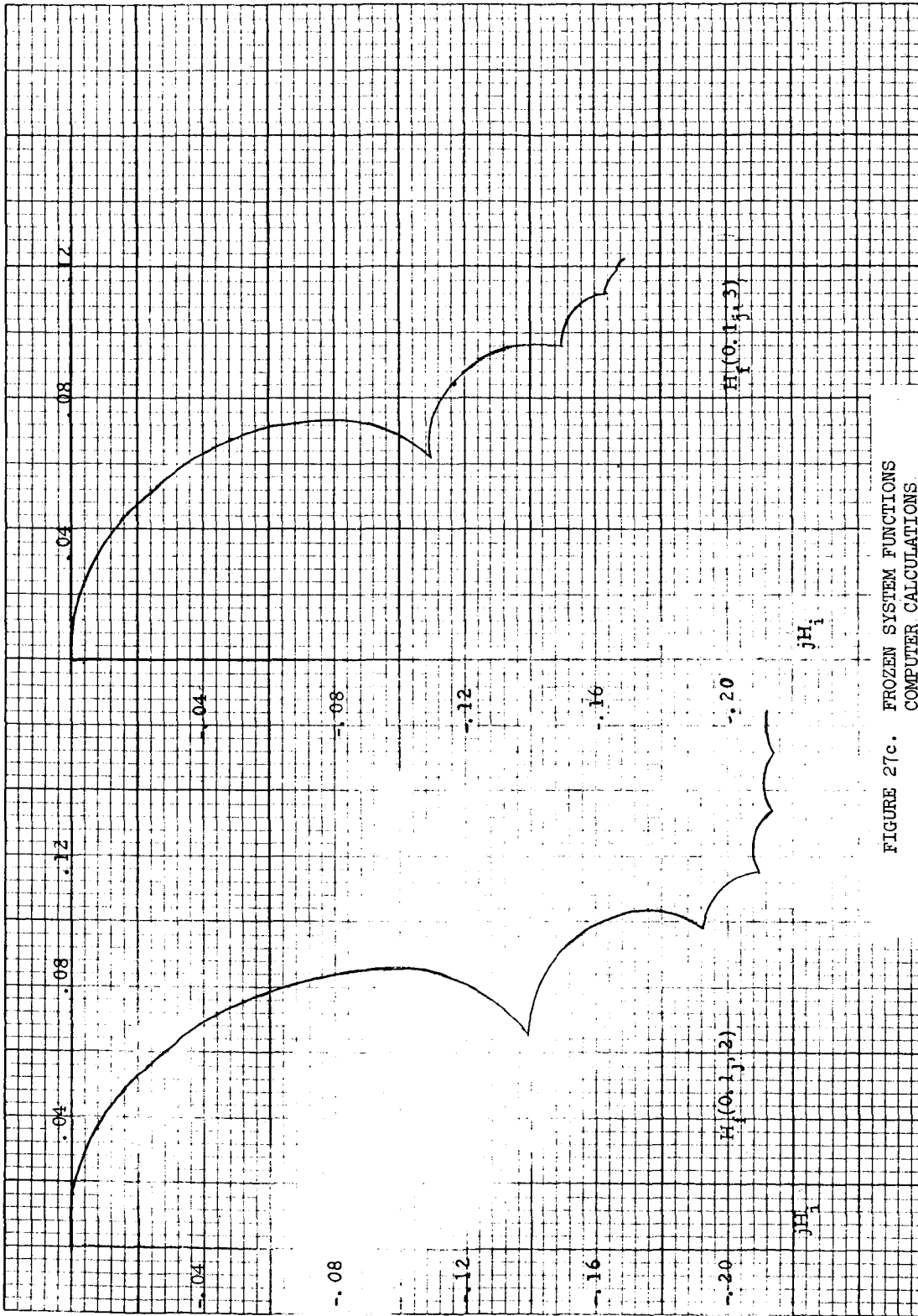


FIGURE 27c. FROZEN SYSTEM FUNCTIONS
COMPUTER CALCULATIONS

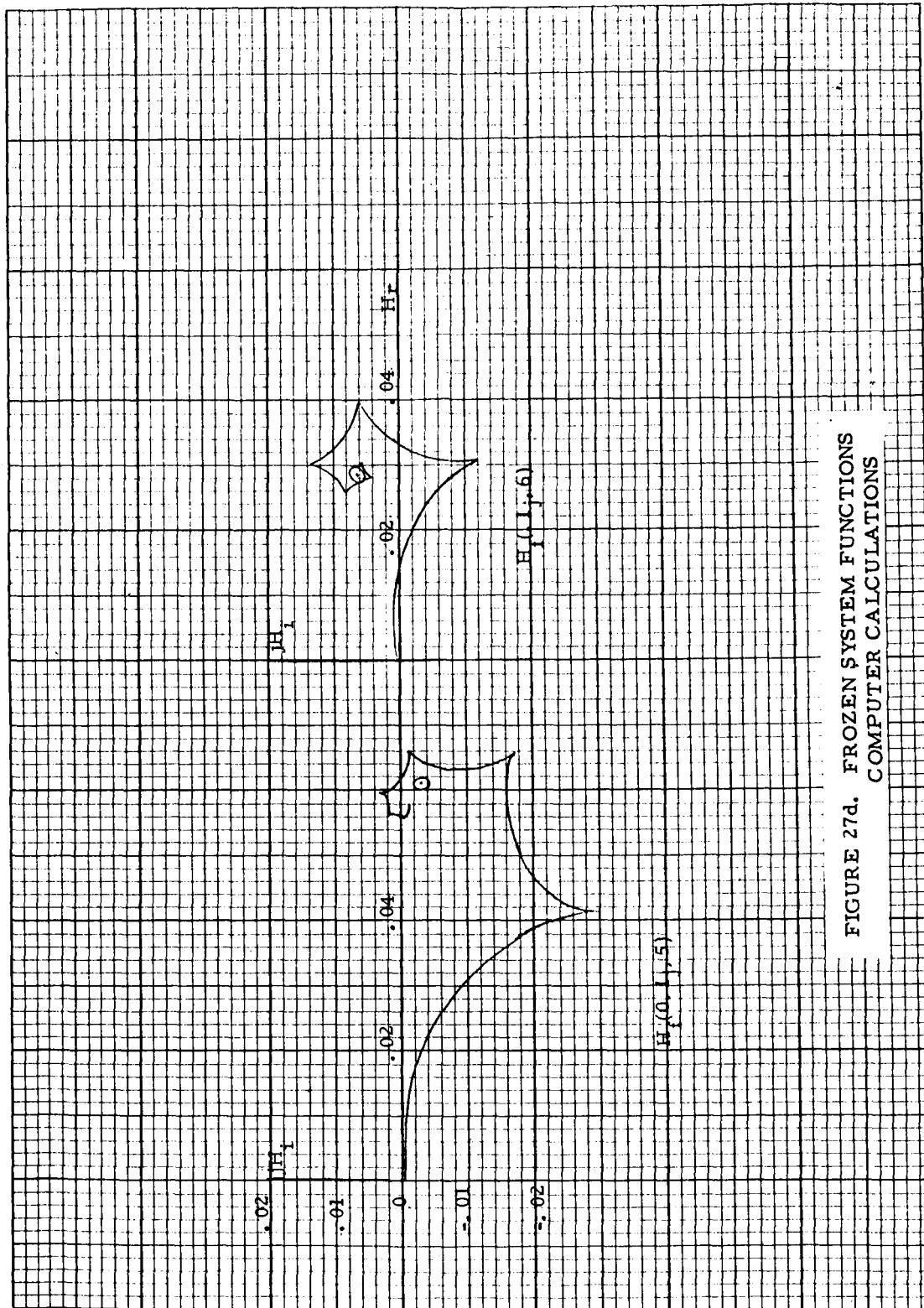


FIGURE 27d. FROZEN SYSTEM FUNCTIONS
COMPUTER CALCULATIONS

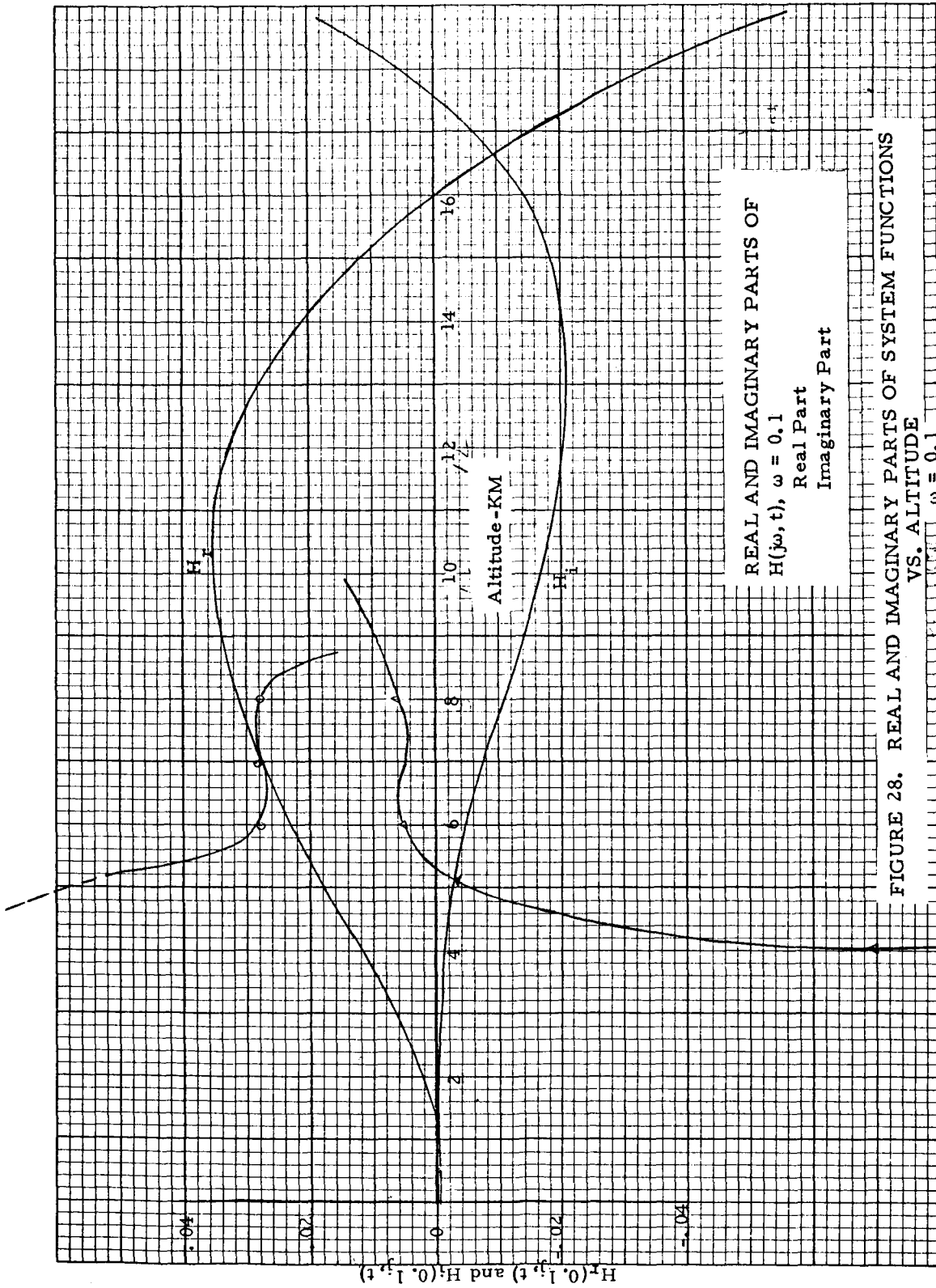


FIGURE 28. REAL AND IMAGINARY PARTS OF SYSTEM FUNCTIONS VS. ALTITUDE $\omega = 0.1$

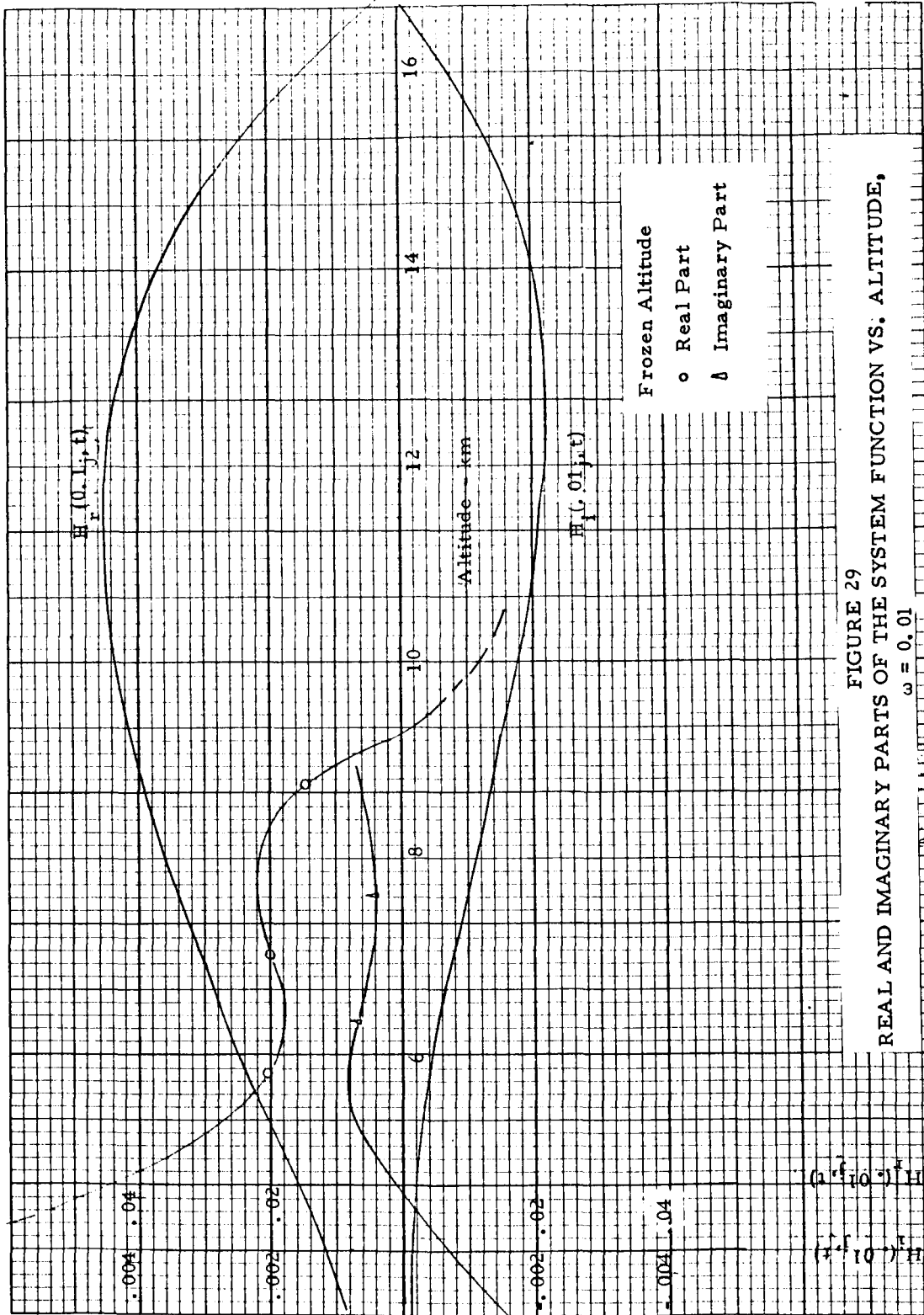


FIGURE 29
 REAL AND IMAGINARY PARTS OF THE SYSTEM FUNCTION VS. ALTITUDE,
 $\omega = 0.01$

REAL PART OF THE SYSTEM FUNCTION VS.
 ALTITUDE WITH VARIOUS INITIAL CONDITIONS,
 $\omega = 0.01$

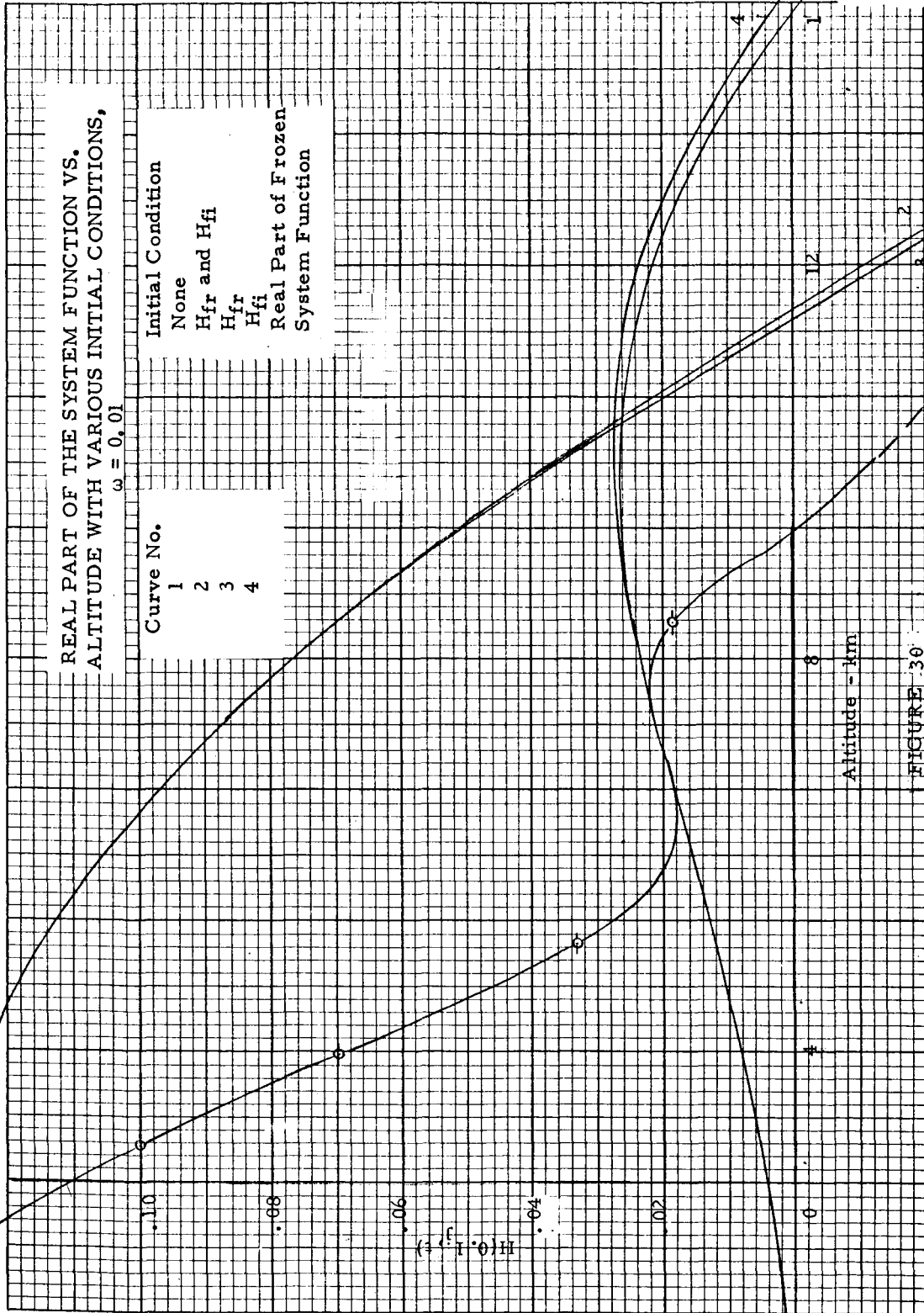


FIGURE 30

It can be shown by Routh's criterion that the characteristic equation must not have negative values of a_0 or a_1 if the transfer function poles are in the right half plane. If $s = j\omega$ this transfer function is identically the frozen system function. The frozen system is easily calculated from equation (38) even when it represents an unstable system, and instability is not readily obvious from the Bode plot. Final values of the wind model coefficients include negative values in the range of h from 0 to 6 km. When the computer simulation of the frozen system function for this range was attempted an unstable solution resulted for the range 0 - 6 km. The solution converged to the frozen system function in the range for which a_1 was positive. A tentative conclusion can be made then, that the simulation method will not produce frozen system functions for unstable situations. This also raises the question of realizability of the system as discussed by Reference (9), which requires that the poles of a time-varying system function have time-invariant singularities. Note also that the poles of the stationary and non-stationary systems are not generally the same, as was discussed previously.

The conclusions reached in this system function analysis may be restated as follows:

1. The system function is a useful tool in studying frequency response and statistical properties of time-varying systems when its use is justified by the difficulties involved in its determination.

2. The wind model studied has a degree of non-stationarity which makes stationary analysis techniques inaccurate and possibly misleading.

3. The computer simulation developed can be used to provide completely mechanized solution for the system function, its application to multi-degree of freedom systems becomes much more complex.

4. The combined system function for the Wind Model/Saturn V model cannot easily be generated using this computer technique, transforming the combined weighting function is an alternate method .

5. Initial conditions on the system function simulation are difficult to obtain for the wind model due to the built-in inaccuracy in the coefficients of the equations.

V. APPLICATION

The primary purpose of this study was the development of the techniques presented in the previous chapters. However, to insure that the wind model format was compatible with system analysis of a launch vehicle, a short digital computer study was conducted to determine the bending moment response of the Saturn V vehicle during a portion of its ascent through the atmosphere. The dynamic model utilized included rigid body equations of motion with a pitch, pitch rate and accelerometer feedback control system. Body bending was determined at station 25 from time $t = 40$ seconds to $t = 90$ seconds of flight.

The vehicle equations are obtained in the following form:

Rigid Body Equations

$$\begin{aligned}
 I(t) \ddot{\phi} &= -F_s X_E \beta - Q F_1(t) \alpha \\
 m(t) \ddot{Y} &= (F - X) \dot{\phi} + F_s \beta + Q F_0(t) \alpha
 \end{aligned}
 \tag{39}$$

Control Equation

$$\beta = a_0(t) \dot{\phi} + a_1(t) \phi + g_2(t) A
 \tag{40}$$

Accelerometer Equation

$$A = \ddot{Y} - g(t) \phi =
 \tag{41}$$

Angle of Attack Equation

$$\alpha = \phi - \frac{\dot{Y}}{v} + \frac{v_w}{v}
 \tag{42}$$

Bending Moment Equation

$$BM = M'_\beta(t) \beta + M'_\alpha(t) \alpha
 \tag{43}$$

The first five of these equations were then expressed in state variable form by introducing

$$\begin{aligned} \dot{\phi} &= p \\ \dot{Y} &= r \end{aligned} \quad (44)$$

and incorporation equations (40), (41) and (42) in equations (39) to yield the form

$$\begin{bmatrix} \dot{p} \\ p \\ \dot{\phi} \\ \phi \\ \dot{r} \\ r \end{bmatrix} = \begin{bmatrix} a_{11} & a_{12} & a_{13} \\ a_{21} & a_{22} & a_{23} \\ a_{31} & a_{32} & a_{33} \end{bmatrix} \begin{bmatrix} p \\ \phi \\ r \end{bmatrix} + \begin{bmatrix} c_1^* \\ 0 \\ c_2^* \end{bmatrix} v_w \quad (45)$$

Equation (45) were then solved on the digital computer using a deterministic wind input to obtain a check of the computer program. The bending moment equation (45) was expanded in terms of the state variables through equations (40), (41) and 42). This give the form

$$BM = a_{61} p + a_{62} \phi + a_{63} r \quad (46)$$

The deterministic wind profile utilized was an approximation to the 95% wind speed 99% wind shear profile developed by MSFC for launch vehicle design and analysis and is shown in Figure 31.

The nonstationary wind input program was then set up by adding the wind equation, developed in Chapter III, to equation (45)

$$\dot{v}_w(t) + a_1(t) \dot{v}_w(t) + a_0 v_w(t) = b_1(t) \dot{\delta}(t) + b_0 \delta(t) \quad (47)$$

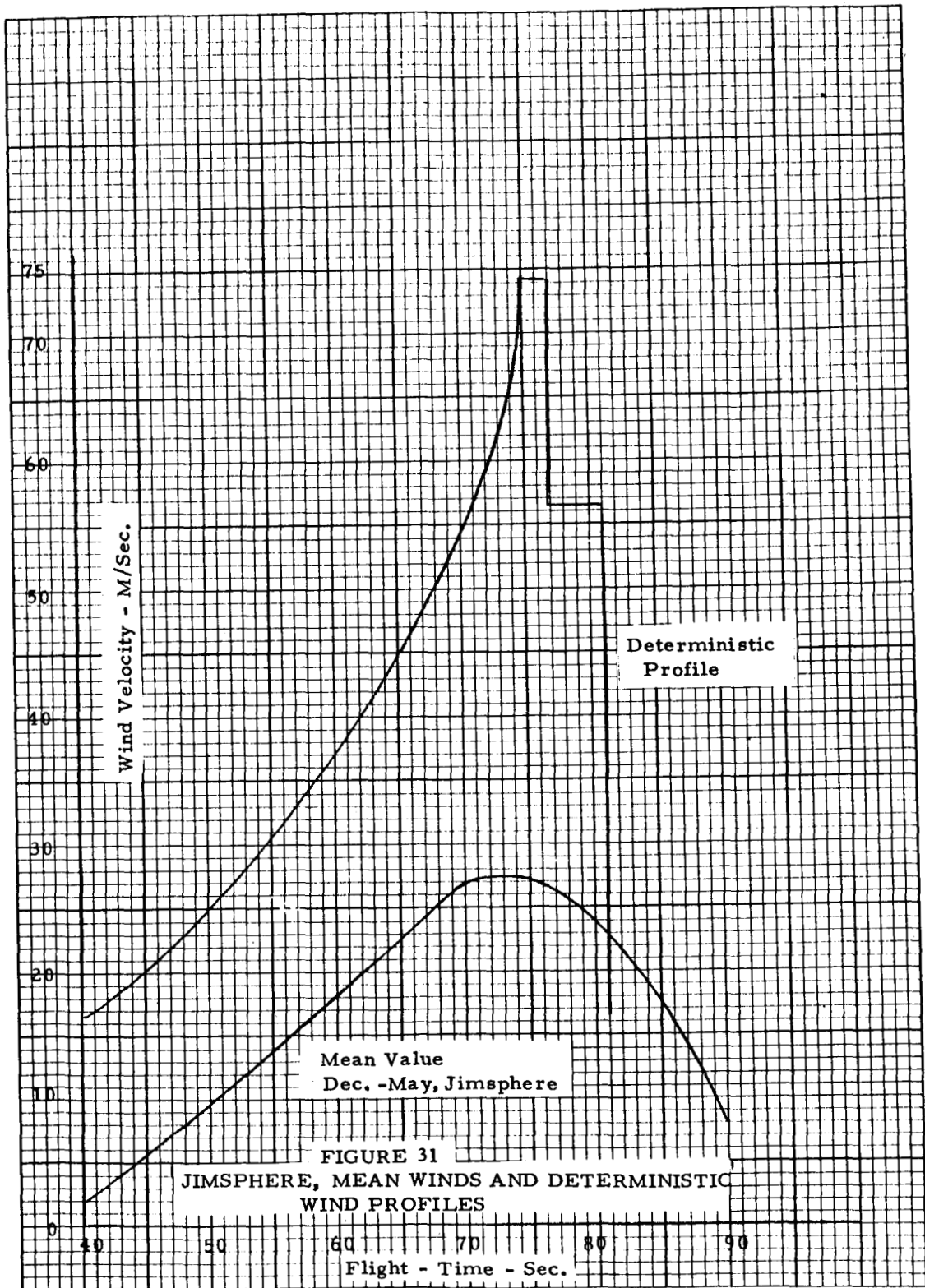


FIGURE 31
 JIMSPHERE, MEAN WINDS AND DETERMINISTIC
 WIND PROFILES

In setting up this program, full advantage was made of the fact that equation (47) could be replaced by its homogeneous form with initial conditions on the proper variables. The equations programmed were then

$$\begin{bmatrix} p \\ \dot{\phi} \\ \dot{r} \\ \dot{w} \\ \dot{\bar{w}} \end{bmatrix} = \begin{bmatrix} a_{11} & a_{12} & a_{13} & 0 & a_{15} \\ a_{21} & 0 & 0 & 0 & 0 \\ a_{31} & a_{32} & a_{33} & a_{34} & 0 \\ 0 & 0 & 0 & 0 & a_{44} \\ 0 & 0 & 0 & a_{54} & a_{55} \end{bmatrix} \begin{bmatrix} p \\ \phi \\ r \\ w \\ \bar{w} \end{bmatrix} \quad (48)$$

where $\bar{w} = \dot{v}_w$, $w = v_w$ and the bending moment is calculated from equation (46). The coefficients used in equations (45) and (48) are presented in Table 2.

The coefficients of the wind model, equation (47) are time-varying in order to be compatible with the time variation of the study. However, the independent variable of the wind model equation developed in Chapter III was altitude. Consequently, it was necessary to change the independent variable from altitude to time. This was accomplished by incorporating the altitude equation

$$h = \int_0^t v \, dt$$

which converts the altitude-varying equation

$$\frac{d^2 w}{dh^2} + a_1(h) \frac{dw}{dh} + a_0(h) w = b_1(h) \frac{dm}{dh} + b_0(h) m$$

TABLE 2

VEHICLE AND WIND MODEL COEFFICIENTS

$$a_{11} = \frac{-F_S X_E a_1^*}{I} \quad ; \quad a_{12} = \frac{-F_S X_E}{I} \left[a_0^* + g_2 \left(\frac{F-X}{m} + \frac{QF_0}{m} - g \right) \right] - \frac{QF_1}{I},$$

$$a_{13} = \frac{Q}{IV} \left[F_1 + \frac{F_S F_0 X_E g_2}{(m - F_S g_2)} \right] \quad ; \quad a_{21} = 1$$

$$a_{31} = \frac{a_1^* F_S}{m - F_S g_2} \quad a_{32} = \frac{F - X + QF_0 + F_S (a_0^* - g_2 g)}{m - F_S g_2}$$

$$a_{33} = \frac{-QF_0}{v(m - F_S g_2)} \quad a_{34} = \frac{QF_0}{v(m - F_S g_2)}$$

$$a_{44} = 1 \quad a_{54} = -a_0(t) \text{ Wind Coef.}$$

$$a_{55} = a_1(t) \text{ Wind Coef.} \quad a_{61} = \frac{m M_\beta a_1^*}{m - F_S g_2}$$

$$a_{62} = \frac{M'_\beta g_2 [F - X + QF_0 - gm] + m M'_\beta a_0^*}{m - F_S g_2} + M'_\alpha \quad ; \quad a_{63} = \frac{-M'_\beta g_2 QF_0}{v(m - F_S g_2)} - \frac{M'_\alpha}{v}$$

$$c_1^* = -a_{13} \quad c_2^* = -a_{33}$$

to

$$\frac{d^2 w}{dt^2} \frac{1}{v^2} + \left[a_1(t) \frac{1}{v^2} - \frac{1}{v^3} \frac{dv}{dt} \right] \frac{dw}{dt} + a_0(t) \frac{1}{v^2} w =$$

$$\frac{1}{v^2} b_1(t) \frac{dm}{dt} + \left[b_0(t) \frac{1}{v^2} - \frac{1}{v^3} \frac{dv}{dt} \right] m$$

or

$$\frac{dw^2}{dt^2} + \left[a_1(t) - \frac{1}{v} \frac{dv}{dt} \right] \frac{dw}{dt} + a_0(t) = b_1(t) \frac{dm}{dt} + \left[b_0(t) - \frac{1}{v} \frac{dv}{dt} \right] m$$

where

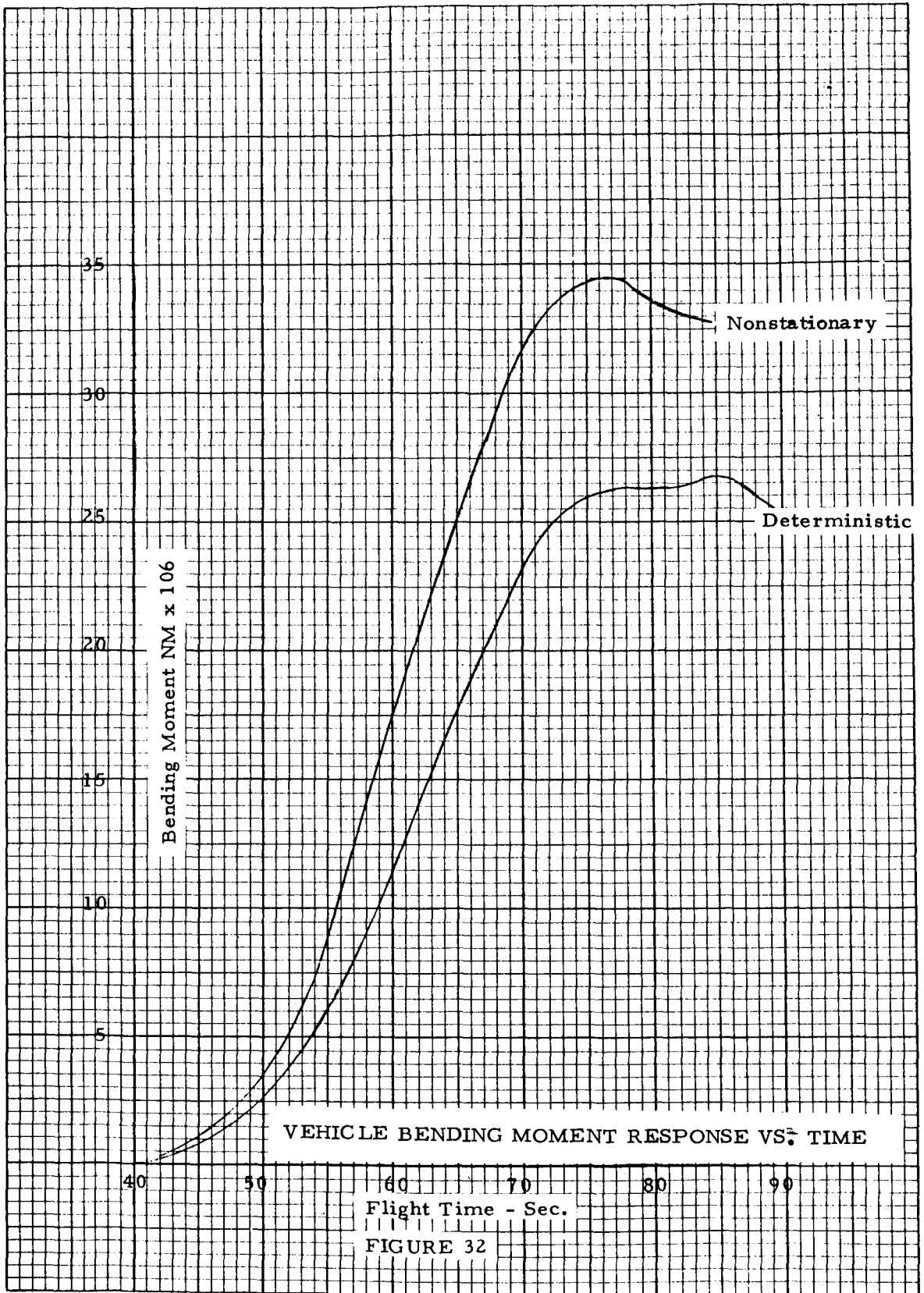
$$a_1(h) = a_1(t) \frac{1}{v}$$

$$a_0(h) = a_0(t) \frac{1}{v^2}$$

$$b_0(h) = b_0(t) \frac{1}{v}$$

$$b_1(h) = b_1(t)$$

The results of this study are presented in Figure 32 in the form of the variation of the bending moment at station 25 with flight time. Although the deterministic program was run strictly to check out the computer program, the close resemblance of the two curves is quite encouraging. However, the limited wind data available for constructing the nonstationary model, the approximate nature of the deterministic profile and the roughness of the integration program used here, precludes any comparison of the actual values



of the bending moments.

This computer study does indicate that a wind model developed by the techniques discussed herein is compatible with a launch vehicle system when utilized in a forward computation scheme as well as with the adjoint technique for which it was developed.

VI. CONCLUSIONS AND RECOMMENDATIONS

1. CONCLUSIONS

In general, the results of this study are most favorable, and it is believed that proper implementation of this model will open up the way to radical new design concepts for complicated systems. Concrete conclusions of this study are:

- (1) An accurate nonstationary wind model can be synthesized by the techniques developed during this study.
- (2) The present model, presented in this report, is believed to approximately represent the statistics implicit in the wind data to within 10 per cent. As more refined wind data becomes available, much higher accuracy can be developed in the synthesis procedure.
- (3) Combined system equations have been developed which can be implemented directly for computer applications.

2. RECOMMENDATIONS

The outstanding potential of the system design concepts which are illustrated in the report can be realized only if steps are taken to refine the existing model and develop confidence in the modeling by systematic verification studies. Several recommendations which are prompted by the results of this study are:

- (1) That the same synthesis techniques which have been used in this study be used to define a wind model for the 600 wind sample which is being made available at the present

time. This development should use smaller altitude variations in determining the covariance to insure the inclusion of high frequency turbulence information in the model.

- (2) That a more sophisticated error analysis of the approximate wind statistics be conducted utilizing the 600 wind ensemble. Confidence limits on the data and computed statistics should be carefully investigated.
- (3) That the order of the differential equations defining the wind shaping filter should be increased if greater accuracy is needed to represent more sensitive aspects of the wind model which may show up with more and better data.
- (4) Hybrid analog computer, high-speed real time digital computer, and conventional analog computer implementation of the system modeling presented in this report should be investigated thoroughly.
- (5) Verification and comparison studies of the results which are obtained using this method should be begun immediately so that confidence in the model can be developed and experience in application of the modeling concepts can be gained.
- (6) Extension of the present techniques for cases where discrete non-linearities are present is highly desirable.

VII. LIST OF REFERENCES

1. Solodovnikov, V. V.; Statistical Dynamics of Automatic Control Systems; D. Van Nostrand Co., Ltd.; 1965.
2. Bendat, J. S.; Principals and Applications of Random Noise Theory; John Wiley and Sons, Inc.; 1958.
3. Lee, Y. W.; Statistical Theory of Communication; John Wiley and Sons, Inc.; 1960.
4. Lanning, J. H. and Battin, R. H.; Random Processes in Automatic Control; McGraw-Hill Book Company, Inc.; 1956.
5. Papoulis, A.; Probability, Random Variables, and Stochastic Processes; McGraw-Hill Book Co.; 1965.
6. Bailey, J. E.; "Launch Vehicle Wind Response by Statistical Methods;" Hayes International Corp. Engineering Report 1193; 1965.
7. Bieber, R. E.; "Missile Structural Loads by Nonstationary Statistical Methods;" Journal of Aerospace Sciences; April, 1961.
8. Stubberud, A. R.; "A Technique for the Synthesis of Linear Nonstationary Feedback Systems;" AIEE Transactions; July, 1963.
9. Cruz, J. B.; "Some Techniques for the Analysis and Synthesis of Nonstationary Networks;" 1961 IRE International Convention Record.
10. Cruz, J. B.; "Linear Systems with Time-Varying Components;" Proceedings of the National Electronics Conference; 1961; Volume 17.

VII. LIST OF REFERENCES (Cont'd.)

11. Scoggins, James R. and Susko, Michael; "FPS-16 Radar/Jim Sphere Wind Data Measured at the Eastern Test Range;" NASA TMX-53290; July, 1965.
12. Ince, E. L.; Ordinary Differential Equations; New York; Dover Publications, Inc.; 1956.
13. James, H. M., N. B. Nichols, and R. S. Phillips; Theory of Servomechanisms; New York; McGraw-Hill Book Company, Inc.; 1947.
14. Lanning, J. H., Jr., and R. H. Battin; An Application of Analog Computers to the Statistical Analysis of Time-Varying Systems. Transactions of the IRE, CT2. Number 1 (March, 1955).
15. Zadeh, L. A.; Frequency Analysis of Variable Networks ; Proceedings of the IRE, Volume 38, Number 3 (March, 1950), 292-299.
16. Zadeh, L. A.; The Determination of Impulsive Response of Variable Networks; Journal of Applied Physics, Volume 21, No. 7 (July, 1950); 642-645.
17. Truxal, J. G.; Control System Synthesis; New York, McGraw-Hill Book Company, Inc., 1955, 421-424.
18. Graham, D., E. J. Brunelle, Jr., W. Johnson, and H. Passmore, III; Engineering Analysis Methods for Linear Time-Varying Systems; ASD TDR-62-362, January, 1963.
19. Cruz, J. B., Jr.; On the Realizability of Linear Differential Systems; Transactions of the IRE, CT7, No. 3 (September, 1960).

VII. LIST OF REFERENCES (Cont'd.)

20. Johnson, W. A., D T McRuer, and A. V. Phatak; Extension of Linear Analysis Methods to Time-Varying Systems; RTD-TDR-63-4178, September, 1964.
21. Kaplan, W.; Operational Methods for Linear Systems; Reading Massachusetts: Addison-Wesley Pub. Company, Inc., 1962.

APPENDIX I

DESCRIPTION OF LINEAR SYSTEMS

Linear systems with variable parameters have been discussed throughout this report. No fixed mathematical method exists for the solution of linear differential equations with varying coefficients although digital and electronic analog techniques have facilitated and influenced the study of such systems. The mathematical or statistical methods discussed in this report which allow quantitative study of such systems depend on two basic assumptions.

If the system is defined by the differential equation:

$$a_n(t) \frac{d^n y(t)}{dt^n} + a_{n-1}(t) \frac{d^{n-1} y(t)}{dt^{n-1}} + \dots + a_1(t) \frac{dy(t)}{dt} + a_0(t) y(t) = b_0(t) x(t) + \dots + b_m(t) \frac{d^m x(t)}{dt^m}$$

then:

(1) The deterministic function $\bar{Y}(t)$ satisfies the differential equation

$$a_n(t) \frac{d^n \bar{Y}(t)}{dt^n} + a_{n-1}(t) \frac{d^{n-1} \bar{Y}(t)}{dt^{n-1}} + \dots + a_1(t) \frac{d\bar{Y}(t)}{dt} + a_0(t) \bar{Y}(t) = b_0(t) \bar{X}(t) + \dots + b_m(t) \frac{d^m \bar{X}(t)}{dt^m}$$

where $\bar{Y}(t) = E\{y(t)\}$ and $\bar{X}(t) = E\{x(t)\}$ with appropriate initial conditions.

(2) If the input to a linear system, $x(t)$, is normal, then the output of the system is normal.

The truth of these statements will be indicated by the following considerations. Suppose that $\frac{dy(t)}{dt}$ exists and can be defined as the limit

$$\frac{dy(t)}{dt} = \lim_{h \rightarrow 0} \left[\frac{y(t+h) - y(t)}{h} \right] .$$

Then, taking the expected value on both sides,

$$E \left[\frac{dy(t)}{dt} \right] = E \left\{ \lim_{h \rightarrow 0} \left[\frac{y(t+h) - y(t)}{h} \right] \right\}$$

then, since the expected value of the limit is equal to the limit of the expected value, this becomes

$$E \left[\frac{dy(t)}{dt} \right] = \lim_{h \rightarrow 0} \left\{ \frac{E [y(t+h)] - E(yt)}{h} \right\}$$

giving

$$E \frac{dy(t)}{dt} = \frac{dE [y(t)]}{dt}$$

The above may be extended to higher order derivatives to yield

$$E \left\{ \frac{d^k y(t)}{dt^k} \right\} = \frac{d^k E \{ y(t) \}}{dt^k} .$$

Thus, taking expected value of both sides of differential equation of the system yields

$$\begin{aligned} a_n(t) \frac{d^n \bar{Y}(t)}{dt^n} + a_{n-1}(t) \frac{d^{n-1} \bar{Y}(t)}{dt^{n-1}} + \dots + a_1(t) \frac{d \bar{Y}(t)}{dt} \\ + a_0(t) \bar{Y}(t) = b_0(t) \bar{X}(t) + \dots + b_m(t) \frac{d^m \bar{X}(t)}{dt^m} \end{aligned}$$

subject to the appropriate initial conditions.

In order to demonstrate that if the input to a linear system is normal then the output is normal consider the linear system as being defined by the

impulse response function.

$$y(t) = \int_0^t g(t, \tau) x(\tau) d\tau$$

Suppose this integral is approximated by the sum

$$y(t) = \sum_i g(t, \tau_i) x(\tau_i) \Delta \tau_i$$

$y_j(t_j)$ is now a linear combination of normally distributed variables $x_i(\tau_i)$. It is well known in statistics that the linear combination or sum of normally distributed variables is normally distributed. We omit details but it is now evident that $y(t)$ is the limit $y_j(t_j)$ as $\Delta \tau_i \rightarrow 0$ and thus is normally distributed.

APPENDIX II

DEVELOPMENT OF COVARIANCE DIFFERENTIAL EQUATION

In Reference (5) it is shown that

$$E \left\{ \frac{d^n x(t_1)}{dt_1^n} \cdot \frac{d^m y(t_2)}{dt_2^m} \right\} = \frac{\partial^{n+m} R_{xy}(t_1, t_2)}{\partial t_1^n \partial t_2^m} .$$

Now, multiply both sides of the differential equation

$$a_n(t_1) \frac{d^n y(t_1)}{dt_1^n} + \dots + a_0(t_1) y(t_1) = b_0(t_1) x(t_1) + \dots + b_m(t_1) \frac{d^m x(t_1)}{dt_1^m}$$

by $y(t_2)$, and then take the expected value of both sides of the equation to obtain the following result

$$\begin{aligned} a_n(t_1) \frac{d^n}{dt_1^n} R_{yy}(t_1, t_2) + \dots + a_1(t_1) \frac{d}{dt_1} R_{yy}(t_1, t_2) \\ + a_0(t_1) R_{yy}(t_1, t_2) = b_0(t_1) R_{xy}(t_1, t_2) + \dots + b_m(t_1) \frac{d^m}{dt_1^m} R_{xy}(t_1, t_2) \end{aligned}$$

Now, consider the case where the input $x(t)$ is white noise and the output some variable y when $y(t_2)$ is defined by

$$y(t_2) = \int_0^{t_2} g(t_2, \tau) x(\tau) d\tau \quad t_2 > \tau$$

Multiply both sides of this equation by $x(t_1)$ and take the expected value to obtain

$$R_{xy}(t_1, t_2) = \int_0^{t_2} g(t_2, \tau) R_{xx}(t_1, \tau) d\tau = \int_0^{t_2} g(t_2, \tau) \delta(\tau - t_1) d\tau$$

If $t_1 > t_2$ then $R_{xy}(t_1, t_2) = 0$.

Thus

$$a_n(t_1) \frac{d^n R_{yy}(t_1, t_2)}{dt_1^n} + \dots + a_1(t_1) \frac{d}{dt_1} R_{yy}(t_1, t_2) + a_0(t_1) R_{yy}(t_1, t_2) = 0 \quad \text{for } t_1 > t_2$$

If $t_1 < t_2$, $R_{xy}(t_1, t_2) = g(t_2, t_1)$.

Thus

$$a_n(t_1) \frac{d^n R_{yy}(t_1, t_2)}{dt_1^n} + \dots + a_1(t_1) \frac{d}{dt_1} R_{yy}(t_1, t_2) + a_0(t_1) R_{yy}(t_1, t_2) = b_0(t_1) g(t_2, t_1) + b_1(t_1) \frac{d}{dt_1} g(t_2, t_1) + \dots + b_m(t_1) \frac{d^m g(t_2, t_1)}{dt_1^m} \quad \text{for } t_1 < t_2$$

In Appendix I it was shown that $\bar{Y}(t)$ and $\bar{X}(t)$ satisfied the differential equation of the shaping filter. Thus $Y(t) - \bar{Y}(t)$ and $x(t) - 0$ will satisfy the differential equation of the system where $x(t)$ is white noise with zero mean. Therefore, repeating the same argument as presented for $R(t_1, t_2)$, one can easily show that

$$a_n(t_1) \frac{d^n C(t_1, t_2)}{dt_1^n} + \dots + a_1(t_1) \frac{dC(t_1, t_2)}{dt_1} + a_0(t_1) C(t_1, t_2) = 0 \quad \text{for } t_1 > t_2,$$

and

$$a_n(t_1) \frac{d^n C(t_1, t_2)}{dt_1^n} + \dots + a_1(t_1) \frac{dC(t_1, t_2)}{dt_1} + a_0(t_1) C(t_1, t_2) = b_0(t_1) g(t_2, t_1) + b_1(t_1) \frac{d}{dt_1} g(t_2, t_1) + \dots + b_m(t_1) \frac{d^m g(t_2, t_1)}{dt_1^m} \quad \text{for } t_1 < t_2.$$

APPENDIX III
WEIGHTING FILTER SYNTHESIS
INITIAL CONDITIONS

In Reference (1) it is shown that the following boundary conditions or initial conditions hold for the derivatives of the function $C(h_1, h_2)$. Consider $C(h_1, h_2)$ as being defined by

$$C(h_1, h_2) = \int_0^{h_2} g(h_1, \lambda) g(h_2, \lambda) d\lambda \quad \text{for } h_1 > h_2$$

$$C(h_1, h_2) = \int_0^{h_1} g(h_1, \lambda) g(h_2, \lambda) d\lambda \quad \text{for } h_1 < h_2$$

Since $g(h_1, h_2)$ is a weighting function or impulse response function for a second order system, it has the following initial conditions

$$\left. \frac{d^i g(h_1, h_2)}{dh_1^i} \right|_{h_1 = h_2^+} = \begin{cases} b_1(h_2) & \text{for } i = 0 \\ b_0(h_2) - a_1 g(h_2^+, h_2) & \text{for } i = 1 \end{cases}$$

$$\left. \frac{dC(h_1, h_2)}{dh_1} \right|_{h_1 = h_2^+} = \int_0^{h_2} g(h_2, \lambda) \frac{dg(h_1, \lambda)}{dh_1} d\lambda \Big|_{h_1 = h_2^+}$$

and

$$\left. \frac{dC(h_1, h_2)}{dh_1} \right|_{h_1 = h_2^-} = \int_0^{h_1} g(h_2, \lambda) \frac{dg(h_1, \lambda)}{dh_1} d\lambda \Big|_{h_1 = h_2^-}$$

$$+ g(h_2, h_1) g(h_1, h_1) \Big|_{h_1 = h_2^-}$$

Subtracting the last two derivatives yields

$$\left. \frac{dC(h_1, h_2)}{dh_1} \right|_{h_1 = h_2^-} - \left. \frac{dC(h_1, h_2)}{dh_1} \right|_{h_1 = h_2^+} = g^2(h_2, h_2^-) = [b_1(h_2)]^2$$

$$\text{or } b_1(h_2) = \sqrt{\left. \frac{dC(h_1, h_2)}{dh_1} \right|_{h_1 = h_2^-} - \left. \frac{dC(h_1, h_2)}{dh_1} \right|_{h_1 = h_2^+}}$$

From the derivatives given in the preceding development, and taking a second derivative,

$$\left. \frac{\partial^2 C(h_1, h_2)}{\partial h_1^2} \right|_{h_1 = h_2^+} = \int_0^{h_2} \frac{\partial^2 g(h_1, \lambda)}{\partial h_1^2} g(h_2, \lambda) d\lambda \Big|_{h_1 = h_2^+}$$

and

$$\begin{aligned} \left. \frac{\partial^2 C(h_1, h_2)}{\partial h_1^2} \right|_{h_1 = h_2^-} &= g(h_2, h_1) \left[\frac{\partial}{\partial h_1} g(h_1, h_2^-) + \frac{\partial}{\partial h_1} g(h_2^-, h_1) \right] \\ &+ g(h_1, h_1) \frac{\partial}{\partial h_1} g(h_2, h_1) + \frac{\partial g(h_1, h_2^-)}{\partial h_1} g(h_2, h_1) \\ &+ \int_0^{h_1} \frac{\partial^2 g(h_1, \lambda)}{\partial h_1^2} g(h_2, \lambda) d\lambda \Big|_{h_1 = h_2^-} \end{aligned}$$

it is seen that

$$\left. \frac{\partial^2 C(h_1, h_2)}{\partial h_1^2} \right|_{h_1 = h_2^-} - \left. \frac{\partial^2 C(h_1, h_2)}{\partial h_1^2} \right|_{h_1 = h_2^+} =$$

$$2g(h_1, h_1) \left[\frac{\partial}{\partial h_1} g(h_1, h_2^-) + \frac{\partial}{\partial h_1} [g(h_2^-, h_1)] \right] \Big|_{h_1 = h_2^-}$$

For a second order system,

$$a_0(h_1) C(h_1, h_2) + a_1(h_1) \frac{\partial}{\partial h_1} C(h_1, h_2) + \frac{\partial^2}{\partial h_1^2} C(h_1, h_2) = 0 \text{ for } h_1 > h_2$$

and

$$\begin{aligned} a_0(h_1) C(h_1, h_2) + a_1(h_1) \frac{\partial}{\partial h_1} C(h_1, h_2) + \frac{\partial^2}{\partial h_1^2} C(h_1, h_2) &= b_0(h_1) g(h_2, h_1) \\ &+ b_1(h_1) \frac{d}{dh_1} g(h_2, h_1) \text{ for } h_1 < h_2 \end{aligned}$$

$$\begin{aligned} & \text{Thus } \left[a_0(h_1) C(h_1, h_2) + a_1(h_1) \frac{\partial}{\partial h_1} C(h_1, h_2) + \frac{\partial^2}{\partial h_1^2} C(h_1, h_2) \right] \Big|_{h_1 = h_2^+} \\ & - \left[a_0(h_1) C(h_1, h_2) + a_1(h_1) \frac{\partial}{\partial h_1} C(h_1, h_2) + \frac{\partial^2 C(h_1, h_2)}{\partial h_1^2} \right] \Big|_{h_1 = h_2^-} \\ & = - \left[b_0(h_1) g(h_2, h_1) + b_1(h_1) \frac{d}{dh_1} g(h_2, h_1) \right] \Big|_{h_1 = h_2^-} \end{aligned}$$

$$\text{Since } a_0(h_1) R(h_1, h_2) \Big|_{h_1 = h_2^+} = a_0(h_1) R(h_1, h_2) \Big|_{h_1 = h_2^-} \quad \text{and}$$

$$\text{since } \frac{\partial}{\partial h_1} C(h_1, h_2) \Big|_{h_1 = h_2^+} - \frac{\partial}{\partial h_1} C(h_1, h_2) \Big|_{h_1 = h_2^-} = -g^2(h_2, h_2^-)$$

this equation simplifies to

$$\begin{aligned} & - a_1(h_2) g^2(h_2, h_2^-) + \frac{\partial^2 C(h_1, h_2)}{\partial h_1^2} \Big|_{h_1 = h_2^+} - \frac{\partial^2 C(h_1, h_2)}{\partial h_1^2} \Big|_{h_1 = h_2^-} \\ & = - \left[b_0(h_1) g(h_2, h_1) + b_1(h_1) \frac{\partial g(h_2, h_1)}{\partial h_1} \right] \Big|_{h_1 = h_2^-} \end{aligned}$$

$$\text{Since } \frac{dg(h_1, h_2^-)}{dh_1} \Big|_{h_1 = h_2^-} = b_0(h_1) - a_1(h_1) b_1(h_1)$$

and since $g(h_1, h_1) = b_1(h_1)$, then

$$\begin{aligned} & - a_1(h_2) b_1^2(h_2) + \frac{\partial^2 C(h_1, h_2)}{\partial h_1^2} \Big|_{h_1 = h_2^+} - \frac{\partial^2 C(h_1, h_2)}{\partial h_1^2} \Big|_{h_1 = h_2^-} = \\ & - b_0(h_2) b_1(h_2) - b_1 \frac{\partial g(h_2, h_1)}{\partial h_1} \Big|_{h_1 = h_2^-} \end{aligned}$$

Substituting for

$$\frac{\partial^2 C(h_1, h_2)}{\partial h_1^2} \Big|_{h_1 = h_2^+} - \frac{\partial^2 C(h_1, h_2)}{\partial h_1^2} \Big|_{h_1 = h_2^-}$$

as developed from the boundary conditions, yields

$$- a_1(h_2) g(h_1, h_2) \Big|_{h_1 = h_2^+} - 2g(h_1, h_2) \frac{\partial g(h_1, h_2)}{\partial h_1} \Big|_{h_1 = h_2^+} - \frac{\partial g(h_2, h_1)}{\partial h_1} \Big|_{h_1 = h_2^-}$$

$$= - b_0(h_2) g(h_1, h_2) - g(h_1, h_2) \frac{\partial}{\partial h_1} g(h_2, h_1) \Big|_{h_1 = h_2^-}$$

$$g(h_2, h_2) [+ b_0(h_2) - a_1(h_2) g(h_2, h_2)] - \{ 2g(h_1, h_2) [\frac{\partial g(h_1, h_2)}{\partial h_1} - \frac{\partial g(h_2, h_1)}{\partial h_1}] \} \Big|_{h_1 = h_2^-}$$

$$= - g(h_2, h_2) \frac{\partial g(h_2, h_1)}{\partial h_1} \Big|_{h_1 = h_2^-}$$

$$g(h_1, h_2) [\frac{\partial g(h_1, h_2)}{\partial h_1} - \frac{\partial g(h_2, h_1)}{\partial h_1}] \Big|_{h_1 = h_2^-} = 0$$

$$\text{Thus } \frac{\partial^2 C(h_1, h_2)}{\partial h_1^2} \Big|_{h_1 = h_2^-} - \frac{\partial^2 C(h_1, h_2)}{\partial h_1^2} \Big|_{h_1 = h_2^+} = 0$$

It should be noted that the data did not fit this condition which indicates that the data is rather erratic or a second order differential equation is of too low an order.

A more detailed explanation of derivatives will now be given in terms of $R(h_1, h_2)$, instead of $C(h_1, h_2)$.

Differentiation of $R(t, \tau)$

$$R(t, \tau) = \int_{-\infty}^t g(t, \lambda) g(\tau, \lambda) d\lambda$$

First Derivative

$$\frac{dR(t, \tau)}{dt} = \lim_{\Delta t \rightarrow 0} \left\{ \frac{\int_{-\infty}^{t+\Delta t} g(t+\Delta t, \lambda) g(\tau, \lambda) d\lambda - \int_{-\infty}^t g(t, \lambda) g(\tau, \lambda) d\lambda}{\Delta t} \right\}$$

$$= \lim_{\Delta t \rightarrow 0} \left\{ \int_{-\infty}^t g(t+\Delta t, \lambda) g(\tau, \lambda) d\lambda + \int_t^{t+\Delta t} g(t+\Delta t, \lambda) g(\tau, \lambda) d\lambda - \int_{-\infty}^t g(t, \lambda) g(\tau, \lambda) d\lambda \right\} \frac{1}{\Delta t}$$

$$= \lim_{\Delta t \rightarrow 0} \left\{ \int_{-\infty}^t \left[\frac{g(t+\Delta t, \lambda) - g(t, \lambda)}{\Delta t} \right] g(\tau, \lambda) d\lambda + \int_t^{t+\Delta t} \frac{g(t+\Delta t, \lambda) g(\tau, \lambda)}{\Delta t} d\lambda \right\}$$

$$= \int_{-\infty}^t \frac{dg(t, \lambda)}{dt} g(\tau, \lambda) d\lambda + \lim_{\Delta t \rightarrow 0} \left\{ \int_t^{t+\Delta t} \frac{g(t+\Delta t, \lambda) g(\tau, \lambda)}{\Delta t} d\lambda \right\}$$

$$= \int_{-\infty}^t \frac{dg(t, \lambda)}{dt} g(\tau, \lambda) d\lambda + g(t, t) g(\tau, t)$$

Second Derivative

$$\frac{d^2}{dt^2} [R(t, \tau)] = \frac{d}{dt} \left\{ \int_{-\infty}^t \frac{dg(t, \lambda)}{dt} g(\tau, \lambda) d\lambda + g(t, t) g(\tau, t) \right\}$$

$$\text{First } \frac{d}{dt} [g(t, t) g(\tau, t)] = g(t, t) \frac{d}{dt} g(\tau, t) + g(\tau, t) \frac{d}{dt} g(t, t)$$

$$\frac{d}{dt} [g(\tau, t)] = \lim_{\Delta t \rightarrow 0} \left\{ \frac{g(\tau, t + \Delta t) - g(\tau, t)}{\Delta t} \right\}$$

$$\frac{d}{dt} [g(t, t)] = \lim_{\Delta t \rightarrow 0} \left\{ \frac{g(t + \Delta t, t + \Delta t) - g(t, t)}{\Delta t} \right\}$$

$$= \lim_{\Delta t \rightarrow 0} \left\{ \frac{g(t + \Delta t, t + \Delta t) - g(t + \Delta t, t) + g(t + \Delta t, t) - g(t, t)}{\Delta t} \right\}$$

$$= \lim_{\Delta t \rightarrow 0} \left\{ \frac{g(t + \Delta t, t + \Delta t) - g(t + \Delta t, t)}{\Delta t} + \frac{g(t + \Delta t, t) - g(t, t)}{\Delta t} \right\}$$

$$= \frac{d}{d\tau} [g(t, \tau)] \Big|_{\tau=t} + \frac{d}{dt} g(t, \tau) \Big|_{\tau=t}$$

$$= \frac{d}{dt} [g(\tau, t)] \Big|_{\tau=t} + \frac{d}{d\tau} g(\tau, t) \Big|_{\tau=t}$$

$$\frac{d}{dt} [g(t, t) g(\tau, t)] = g(t, t) \frac{d}{dt} g(\tau, t) + g(\tau, t) \left[\frac{d}{d\tau} g(t, \tau) \Big|_{\tau=t} + \frac{d}{dt} g(t, \tau) \Big|_{\tau=t} \right]$$

Now

$$\frac{d}{dt} \int_{-\infty}^t \frac{dg(t, \lambda)}{dt} g(\tau, \lambda) d\lambda = \lim_{\Delta t \rightarrow 0} \left\{ \frac{\int_{-\infty}^{t+\Delta t} \frac{dg(t+\Delta t, \lambda)}{dt} g(\tau, \lambda) d\lambda - \int_{-\infty}^t \frac{dg(t, \lambda)}{dt} g(\tau, \lambda) d\lambda}{\Delta t} \right\}$$

$$= \lim_{\Delta t \rightarrow 0} \left\{ \int_t^{t+\Delta t} \frac{dg(t+\Delta t, \lambda)}{dt} g(\tau, \lambda) d\lambda + \frac{\int_{-\infty}^t \frac{dg(t+\Delta t, \lambda)}{dt} g(\tau, \lambda) d\lambda - \int_{-\infty}^t \frac{dg(t, \lambda)}{dt} g(\tau, \lambda) d\lambda}{\Delta t} \right\}$$

$$= \frac{dg(t, \lambda)}{dt} g(\tau, \lambda) + \int_{-\infty}^t \frac{d^2 g(t, \lambda)}{dt^2} g(\tau, \lambda) d\lambda$$

So now

$$\frac{d^2}{dt^2} [R(t, \tau)] = \int_{-\infty}^t \frac{d^2 g(t, \lambda)}{dt^2} g(\tau, \lambda) d\lambda + g(\tau, \lambda) \frac{dg(t, \lambda)}{dt} \\ + g(t, t) \frac{d}{dt} g(\tau, t) + g(\tau, t) \frac{d}{dt} g(t, t)$$

$$\frac{d^2}{dt^2} [R_x(t, \tau)] = \int_{-\infty}^t \frac{d^2 g(t, \lambda)}{dt^2} g(\tau, \lambda) d\lambda \\ + 2g(\tau, t) \left\{ \frac{d}{d\tau} g(t, \tau) \Big|_{\tau=t} + \frac{d}{dt} [g(t, \tau)] \Big|_{\tau=t} \right\} + g(t, t) \frac{d}{dt} g(\tau, t)$$

$$\text{also, } \frac{d^2}{dt^2} [R_x(t, \tau)] = \int_{-\infty}^t \frac{d^2 g(t, \lambda)}{dt^2} g(\tau, \lambda) d\lambda + \frac{dg(t, \lambda=t)}{dt} g(\tau, \lambda=t) \\ + g(t, t) \frac{d}{dt} g(\tau, t) + g(\tau, t) \left\{ \frac{d}{d\tau} g(t, \tau=t) + \frac{d}{dt} g(t, \tau=t) \right\}$$

$$\text{so } \frac{d^2}{dt^2} [R_x(t, \tau)] \Big|_{t=\tau} - \frac{d^2}{dt^2} R_x(t, \tau) \Big|_{t=\tau} = \Delta R'' \\ = \left[\frac{dg(t, \lambda=t)}{dt} g(\tau, \lambda=t) + g(t, t) \frac{d}{dt} g(\tau, t) \right. \\ \left. + g(\tau, t) \left\{ \frac{d}{d\tau} [g(t, \tau=t)] + \frac{d}{dt} g(t, \tau=t) \right\} \right] \Big|_{t=\tau^-} \\ = g(\tau, \tau) \left[\frac{dg(t, \lambda=t)}{dt} + \frac{dg(t, \tau=t)}{dt} \right] \Big|_{t=\tau^-} \\ + g(\tau, \tau) \left[\frac{dg(\tau, t)}{dt} + \frac{dg(t, \tau=t)}{d\tau} \right] \Big|_{t=\tau^-}$$

Evaluate $\frac{dg(t, \lambda)}{d\lambda}$ from adjoint equation

$$D^* (p, \tau) \quad g_0(t, \tau) = \delta(t - \tau) \quad \tau > t$$

$$D^* (p, \tau) x = \frac{d}{d\tau^2} [a_2(\tau) x(\tau)] - \frac{d}{d\tau} [a_1(\tau) x(\tau)] + a_0(\tau) x(\tau) = 0$$

Expanding

$$\frac{d^2 g_0(t, \tau)}{d\tau^2} - a_1(\tau) \frac{dg_0(t, \tau)}{d\tau} + [a_0(\tau) - a_1(\tau)] g_0(t, \tau) = \delta(t - \tau)$$

it may be seen that

$$g_0(t, \tau) \Big|_{t=\tau=\tau^+} = 0 = g_0(t, \tau) \Big|_{t=\tau^-}$$

$$\frac{\partial g_0(t, \tau)}{\partial \tau} \Big|_{t=\tau=\tau^+} = -1 = \frac{\partial g_0(t, \tau)}{\partial \tau} \Big|_{t=\tau^-}$$

$$\frac{\partial g_0(t, \tau)}{\partial \tau} \Big|_{t=\tau^+} = -1 \text{ because } \delta(t - \tau) \text{ is effectively a negative impulse.}$$

Think of as derivative of $u(t - \tau)$ and $u(\tau - t)$.

It is further known that

$$g(t, \tau) = b_0(\tau) g_0(t, \tau) - \frac{\partial}{\partial \tau} [b_1(\tau) g_0(t, \tau)]$$

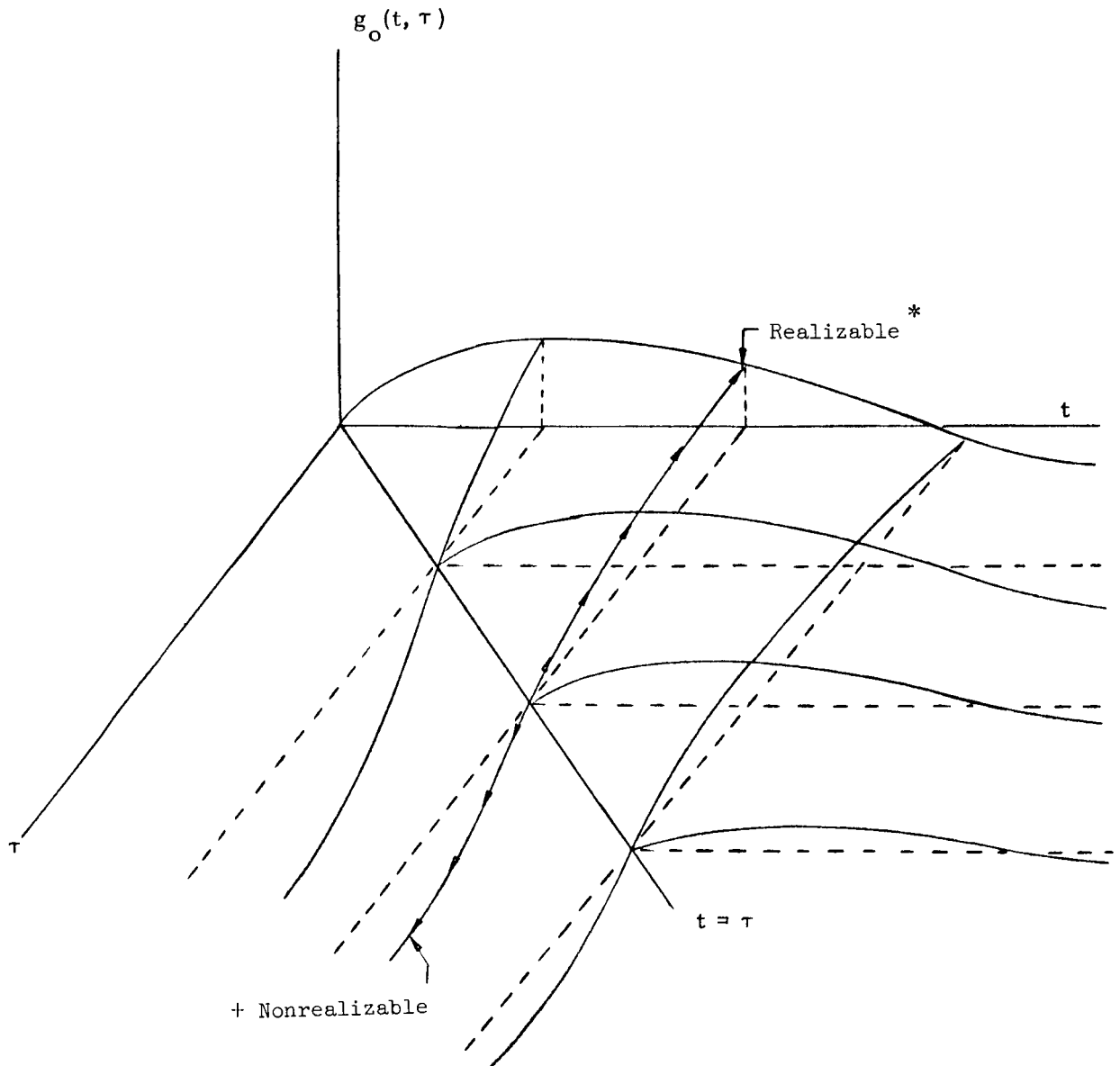
Evaluating at $t = \tau^+ = \tau$

$$\begin{aligned} g(t, \tau) \Big|_{t=\tau^+} &= b_0(\tau) g_0(t, \tau) - \frac{\partial}{\partial \tau} [b_1(\tau) g_0(t, \tau)] \Big|_{t=\tau^+} \\ &= \left\{ - \left[\frac{\partial}{\partial \tau} b_1(\tau) \right] g_0(t, \tau) - b_1(\tau) \frac{\partial}{\partial \tau} g_0(t, \tau) \right\} \Big|_{t=\tau^+} \\ &= + b_1(\tau). \text{ (This is in region of nonrealizable} \\ &\quad \text{weighting function.)} \end{aligned}$$

+ Solution of $D^*(p, \tau) g_o(t, \tau) = \delta(t - \tau)$

* Solution of $D_1(p, \theta) g_o(t, t-\theta) = \delta(\theta)$

where $p = \frac{d}{d\theta}$, replace τ by θ in $D^*(p, t) g_o(t, \tau) = \delta(t - \tau)$



Now

$$\begin{aligned}
 \frac{\partial g(t, \tau)}{\partial \tau} &= \frac{d b_0(\tau)}{d \tau} [g_0(t, \tau)] + \frac{d}{d \tau} [g_0(t, \tau)] b_0(\tau) \\
 &\quad - \frac{\partial^2}{\partial \tau^2} [b_1(\tau) g_0(t, \tau)] \\
 &= \frac{\partial b_0(\tau)}{\partial \tau} g_0(t, \tau) + \frac{\partial g_0(t, \tau)}{\partial \tau} b_0(\tau) - \frac{\partial^2 b_1(\tau)}{\partial \tau^2} g_0(t, \tau) \\
 &\quad - \frac{\partial g_0(t, \tau)}{\partial \tau} \frac{\partial b_1(\tau)}{\partial \tau} - \frac{\partial^2 g_0(t, \tau)}{\partial \tau^2} b_1(\tau) - \frac{\partial b_1(\tau)}{\partial \tau} \frac{\partial g_0(t, \tau)}{\partial \tau} \\
 &= -b_0(\tau) + \frac{\partial b_1(\tau)}{\partial \tau} - \frac{\partial^2 g_0(t, \tau)}{\partial \tau^2} - b_1(\tau) + \frac{\partial b_1(\tau)}{\partial \tau}
 \end{aligned}$$

since

$$\begin{aligned}
 \frac{\partial^2 g_0(t, \tau)}{\partial \tau^2} \Big|_{t=\tau=\tau^+} &= -a_1(\tau) \Big|_{t=\tau=\tau^+} \\
 &= -\left\{ b_0(\tau) + 2 \frac{\partial b_1(\tau)}{\partial \tau} + a_1(\tau) b_1(\tau) \right\} \Big|_{t=\tau=\tau^+}
 \end{aligned}$$

Using

$$g(\tau^-, \tau^-) = b_1(\tau)$$

$$\frac{\partial g(t, \lambda)}{\partial t} \Big|_{t=\lambda=\tau^-} = b_0(\tau) - a_1(\tau) b_1(\tau)$$

$$\begin{aligned}
 \frac{\partial g(t, \tau)}{\partial \tau} \Big|_{t=\lambda=\tau=\tau^+} &= -b_0(\tau) + 2b_1'(\tau) + a_1(\tau) b_1(\tau) \\
 &= \frac{\partial g(t, \lambda)}{\partial \tau} \Big|_{t=\lambda=\tau^+}
 \end{aligned}$$

Evaluate

$$\frac{d^2}{dt^2} [R_x(t, \tau)] \Big|_{t=\tau} - \frac{d^2}{dt^2} [R_x(t, \tau)] \Big|_{t=\tau^+} = \Delta R''$$

$$\Delta R'' = b_1(\tau) \{ 2 [b_0(\tau) - a_1(\tau) b_1(\tau)] + 2 \dot{b}_1(\tau) \}$$

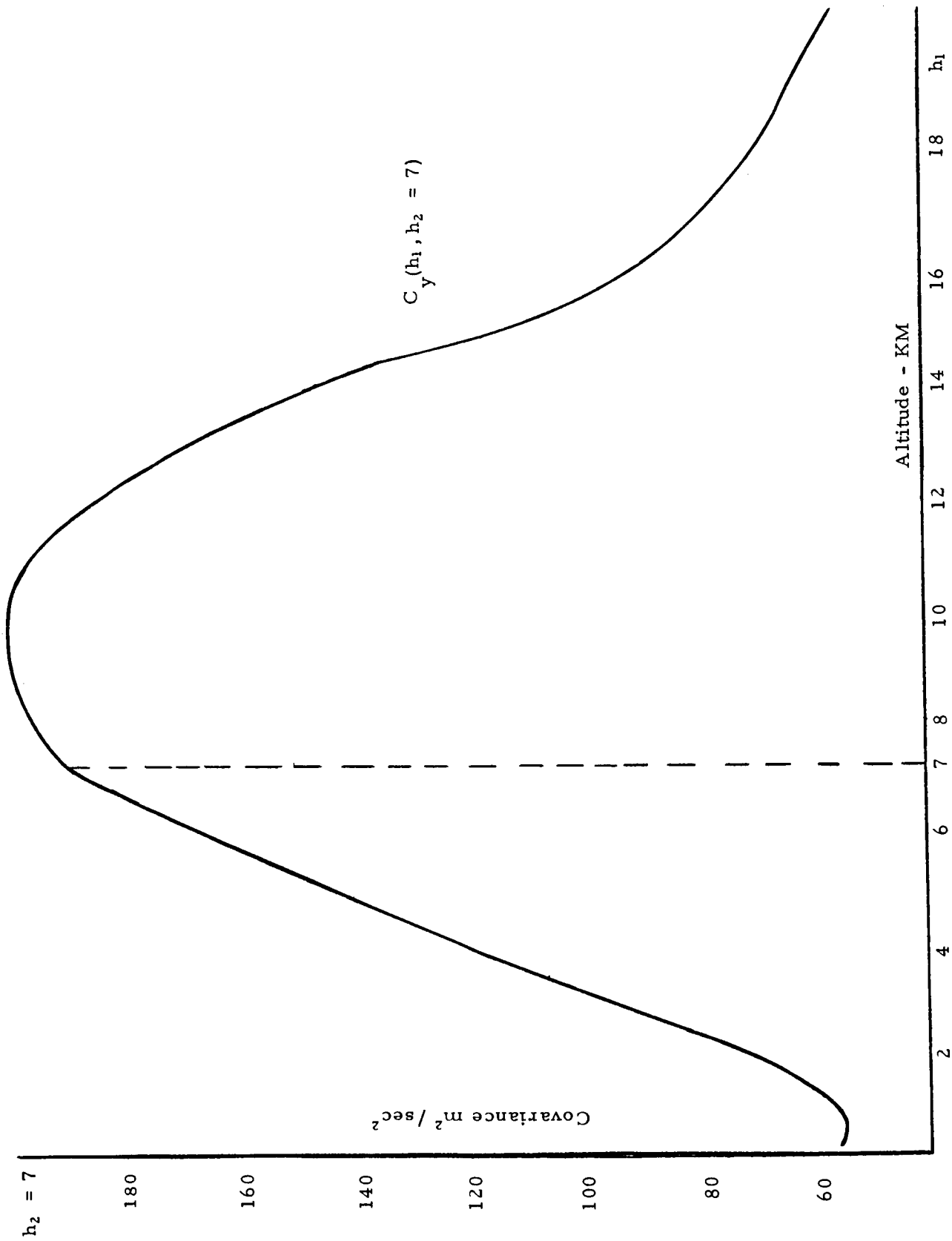
$$b_0(\tau) = \frac{\Delta R''}{2 b_1(\tau)} + a_1(\tau) b_1(\tau) + \frac{\partial b_1(\tau)}{\partial \tau}$$

Numerical Procedures

To obtain the values for $C(h_1, h_2)$, $\frac{d}{dh_1} C(h_1, h_2)$ and $\frac{d^2}{dh_1^2} C(h_1, h_2)$, as well as $g(h_2, h_1)$ and $\frac{d}{dh_1} g(h_2, h_1)$ to be utilized in finding the coefficients of the second order differential equation of the shaping filter using regression analysis, demanded smooth data. The data as presented by the 200 wind profiles produced an erratic distribution of $C(h_1, h_2)$'s. Thus, smoothing procedures were necessary in order to utilize numerical techniques to find $\frac{d C(h_1, h_2)}{dh_1}$ and $\frac{d^2 C(h_1, h_2)}{dh_1^2}$.

The first smoothing technique involved fitting a third degree polynomial to the data. However, this digital computer smoothing technique did not prove to be as useful as expected, since it smoothed out certain needed slope characteristics of the curves near $h_1 = h_2$. A method was then devised to involve a large number of points near $h_1 = h_2$ and to fit a typical curve as indicated in the figure on the next page.

The data was smoothed in two directions; namely, $C(h_1, h_2)$ for h_2 fixed and then $C(h_1, h_2)$, h_1 fixed. This double smoothing technique enabled the utilization of very erratic data in the process of obtaining first and second derivatives. The smoothing was handled separately for $h_1 > h_2$ and $h_1 < h_2$ because of the discontinuity of the derivatives of $C(h_1, h_2)$ across the line $h_1 = h_2$. Also, certain mathematical developments, developed later, were useful in the data analysis. The smoothed values for $C(h_1, h_2)$, $\frac{dC(h_1, h_2)}{dh_1}$



and $\frac{d^2 C(h_1, h_2)}{dh_1^2}$ are given in the following tables.

The usual finite difference formulas as found in most numerical analysis texts were used to approximate the derivatives, $\frac{dC(h_1, h_2)}{dh_1}$ and $\frac{d^2 C(h_1, h_2)}{dh_1^2}$. The smoothed values of $\frac{dC(h_1, h_2)}{dh_1}$ and $\frac{d^2 C(h_1, h_2)}{dh_1^2}$ for different values of $h_2 < h_1$ were used in the regression analysis to find $a_0(h_1)$, $a_1(h_1)$. The $a_0(h_1)$ and $a_1(h_1)$ as computed by this method for different values of h_1 are indicated in Figures 8 and 9 presented previously.

Both linear regression and the numerical procedure which will now be developed were used to find the $b_0(t)$ and $b_1(t)$ in the linear second order differential equation, $a_0(h) y(h) + a_1(h) \frac{dy(h)}{dh} + \frac{d^2 y(h)}{dh^2} = b_0(h) x(h) + b_1(h) \frac{dx(h)}{dh}$, used to represent the linear shaping filter converting white noise to random winds.

Since $g(h_1, h_2)$ is the impulse response function or weighing function for this filter

$$a_0(h_1) g(h_1, h_2) + a_1(h_1) \frac{dg(h_1, h_2)}{dh_1} + \frac{d^2 g(h_1, h_2)}{dh_1^2} = 0 \text{ for } h_1 > h_2.$$

By approximating $\frac{dg(h_1, h_2)}{dh_1}$ and $\frac{d^2 g(h_1, h_2)}{dh_1^2}$ in terms of differences representing three points a system of equations may be obtained to be utilized for numerically obtaining $g(h_1, h_2)$ for points near $h_1 = h_2$. If h_{10} , h_{11} and h_{12} are three consecutive values of h_1 near $h_1 = h_2$, then

$$\left. \frac{d g(h_1, h_2)}{dh_1} \right|_{h_1=h_{10}} = \frac{1}{2} [- 3 g(h_{10}, h_2) + 4 g(h_{11}, h_2) - g(h_{12}, h_2)]$$

h_1	h_2	1	2	3	4	5	6	7	8	9	10	11	12	13	14	15	16	17	18	19	20
1	1.6	-2	3.6	4.5	5	5.5	5.1	3.8	2.1	0	-2.9	-4.2	-6.0	-7.6	-7.5	-7	-5.5	-4	-3.1	-2.5	-2.1
2	2	3.6	4.5	6	6.4	6.1	5.6	4.3	1.4	-2.5	-5	-7.5	-1.0	-1.1	-1.12	-7.1	-5.5	-4.5	-3.7	-2.8	-2.8
3	3	6	7.5	8.0	7.5	6.7	5.5	2	-2.2	-5.8	-9	-12.3	-15.5	-15	-9.1	-7	-5.6	-4.4	-3.4	-3.4	-3.4
4	4	8.4	8.7	8.4	8.3	7.5	6	2.6	-2.3	-6.6	-10.5	-14.7	-20	-18.5	-11.4	-8.7	-6.6	-5.2	-4	-4	-4
5	5	9.3	8.9	8.3	6.2	2.5	-2.4	-7.4	-1.18	-17	-24	-21.6	-14	-10	-7.5	-5.7	-4.5	-4.5	-4.5	-4.5	-4.5
6	6	9.4	8.9	6.2	2	-2.8	-8.2	-1.35	-1.93	-27	-24.5	-16.4	-11.6	-8.4	-6.3	-5	-5	-5	-5	-5	-5
7	7	9.5	6	1.5	-3.3	-9	-1.5.1	-2.15	-2.92	-27.5	-18.5	-12.7	-9.1	-6.9	-5.5	-5.5	-5.5	-5.5	-5.5	-5.5	-5.5
8	8	3	0	-4.2	-9.8	-1.6.7	-2.4	-3.1	-2.8	-2.05	-1.3.4	-9.7	-7.4	-5.9	-5.9	-5.9	-5.9	-5.9	-5.9	-5.9	-5.9
9	9	-2	-5.1	-10.6	-1.8.8	-2.6.5	-3.2.3	-2.8	-2.0.7	-1.4.1	-1.0.3	-7.8	-6.3	-6.3	-6.3	-6.3	-6.3	-6.3	-6.3	-6.3	-6.3
10	10	-6.8	-1.1.3	-2.0.7	-2.9	-3.3	-2.7.4	-2.0.6	-1.4.7	-1.0.8	-8.1	-6.6	-6.6	-6.6	-6.6	-6.6	-6.6	-6.6	-6.6	-6.6	-6.6
11	11	-1.2.1	-2.3.5	-3.2	-3.3.5	-2.6.6	-2.0.5	-1.5.2	-1.1.3	-8.5	-7	-7	-7	-7	-7	-7	-7	-7	-7	-7	-7
12	12	-2.7	-3.5.8	-3.4.2	-2.5.8	-2.0.3	-1.5.5	-1.1.7	-8.8	-7.3	-7.3	-7.3	-7.3	-7.3	-7.3	-7.3	-7.3	-7.3	-7.3	-7.3	-7.3
13	13	-3.9.7	-3.4.5	-2.4.2	-2.0.1	-1.5.8	-1.2.1	-9.1	-7.6	-7.6	-7.6	-7.6	-7.6	-7.6	-7.6	-7.6	-7.6	-7.6	-7.6	-7.6	-7.6
14	14	-3.5	-2.4	-1.9.8	-1.6.1	-1.2.5	-9.4	-7.9	-7.9	-7.9	-7.9	-7.9	-7.9	-7.9	-7.9	-7.9	-7.9	-7.9	-7.9	-7.9	-7.9
15	15	-2.3	-1.9.5	-1.6.3	-1.2.8	-9.7	-8.2	-8.2	-8.2	-8.2	-8.2	-8.2	-8.2	-8.2	-8.2	-8.2	-8.2	-8.2	-8.2	-8.2	-8.2
16	16	-1.9.2	-1.6.4	-1.3.1	-1.0	-8.5	-8.5	-8.5	-8.5	-8.5	-8.5	-8.5	-8.5	-8.5	-8.5	-8.5	-8.5	-8.5	-8.5	-8.5	-8.5
17	17	-1.6.5	-1.3.4	-1.0.2	-8.8	-8.8	-8.8	-8.8	-8.8	-8.8	-8.8	-8.8	-8.8	-8.8	-8.8	-8.8	-8.8	-8.8	-8.8	-8.8	-8.8
18	18	-1.3.7	-1.0.8	-9	-9	-9	-9	-9	-9	-9	-9	-9	-9	-9	-9	-9	-9	-9	-9	-9	-9
19	19	-1.0.7	-9.2	-9.2	-9.2	-9.2	-9.2	-9.2	-9.2	-9.2	-9.2	-9.2	-9.2	-9.2	-9.2	-9.2	-9.2	-9.2	-9.2	-9.2	-9.2
20	20	9.4	9.4	9.4	9.4	9.4	9.4	9.4	9.4	9.4	9.4	9.4	9.4	9.4	9.4	9.4	9.4	9.4	9.4	9.4	9.4

TABLE FOR SMOOTHED VALUES OF $\frac{dC(h_1, h_2)}{dh_1}$

h_2	1	2	3	4	5	6	7	8	9	10	11	12	13	14	15	16	17	18	19	20
1	3.5	2.5	2	1.3	.5	-.1	-.7	-1.5	-2.1	-2.3	-2.1	-1.6	-.8	.3	2	1.5	.6	.2	.2	.3
2		2.8	2.1	1.3	.5	-.3	-1	-1.8	-2.5	-3	-2.9	-2.6	-1.8	-.4	2.5	2.5	1.6	.8	.6	.5
3			2.3	1.1	.3	-.5	-1.2	-2.1	-3.1	-3.8	-3.6	-3.3	-2.8	-1.4	3.2	3.5	2.4	1.3	.9	.7
4				1.4	.5	-.5	-1.6	-2.5	-3.6	-4.3	-4.4	-4.2	-3.8	-2	3.7	4.6	3.2	1.8	1.1	.9
5					.5	-.5	-1.9	-2.9	-4	-4.7	-5	-5.1	-4.7	-2.4	4.2	5.4	3.8	2.2	1.3	1
6						-.5	-2.1	-3.2	-4.3	-5.1	-5.7	-6	-5.4	-2.6	4.7	6.4	4.3	2.5	1.6	1.1
7							-2.2	-3.4	-4.4	-5.2	-6.2	-6.7	-6	-2.5	5.2	6.9	4.8	2.8	1.8	1.3
8								-3	-4	-5	-6.4	-7	-6.4	-2	5.6	7	5.1	3	1.9	1.4
9									-2.5	-4.8	-7	-7.7	-6.6	-1	6	6.8	5.1	3.1	2	1.5
10										-4.3	-7.1	-7.8	-6.4	.6	6.3	6.5	4.9	3.2	2.2	1.6
11											-7	-8	-5.2	2.5	6.6	6.1	4.6	3.2	2.3	1.7
12												-8.4	-3.7	5	6.8	5.7	4.3	3.1	2.4	1.8
13													-1.6	7.6	6.9	5.1	3.9	3	2.4	1.8
14														10.2	7	5	3.6	2.6	2	1.9
15															7	4.5	3.2	2.4	2	1.9
16																3.1	2.8	2.4	2.2	1.9
17																	2.9	2.5	2.1	1.9
18																		2.3	1.9	1.8
19																			1.6	1.4
20																				1.6

TABLE FOR SMOOTHED VALUES OF $\frac{d^2 C(h_1, h_2)}{dh_1^2}$

h_2	h_1	1	2	3	4	5	6	7	8	9	10	11	12	13	14	15	16	17	18	19	20	
1	64																					
2	86	135																				
3	11	153	174																			
4	13.4	17.1	18.9	19.5																		
5	15.6	18.8	20.4	20.7	19.8																	
6	17.6	20.3	21.6	22.0	21.4	19.2																
7	19.3	21.6	22.7	23.0	22.8	21.8	20.9															
8	20.9	22.8	23.7	23.9	23.8	23.3	22.4	20.4														
9	21.8	23.6	24.4	24.4	24.2	23.8	22.3	20.0	17.7													
10	22.7	24	24.8	24.5	24.3	23.2	21.6	19.0	14.6	9.2												
11	22.6	24	24.8	24.4	24.0	22.5	20.3	17.6	12.8	7.9	4.7											
12	21.4	23.1	23.9	23.6	23.0	21.	18.8	15.8	10.8	6.4	4.2	2.9										
13	19.1	21.5	22	21	21.0	19	16.7	13.8	9.3	5.1	3.4	2.3	3.2									
14	15.4	17.4	18.5	18.8	18.0	16.2	14.0	11.6	7.9	4.0	2.6	1.6	2.0	2.1								
15	12.5	13.7	14.2	14.4	14.0	13.0	11.5	9.7	6.8	3.0	2	1.1	1	1.2	1.6							
16	10.2	10.9	11.2	11.2	11.0	10.5	9.6	8.0	5.8	2.3	1.3	0.7	0.5	.4	.7	2.0						
17	8.6	9.1	9.2	9.0	9.0	8.6	8.0	6.8	5.1	2.0	1.1	0.4	0	-.2	0	.5	1.5					
18	7.6	8	8.1	8	7.8	7.2	6.8	5.7	4.7	2.2	1.2	0.5	-.1	-.6	-.8	-.7	-.5	.1				
19	7.2	7.5	7.6	7.5	7.1	6.8	6.0	5.2	4.4	3.0	1.8	0.9	0	-.8	-.13	-.16	-.18	-.15	-1.0			
20	7	7.4	7.6	7.5	7.3	6.9	6.2	5.6	4.5	4.0	2.8	1.8	.5	-.6	-.17	-.22	-.25	-.23	-2	-1.6		
	1	2	3	4	5	6	7	8	9	10	11	12	13	14	15	16	17	18	19	20		

TABLE FOR SMOOTHED VALUES OF $d C(h_1, h_2) / dh_1$

h_2	h_1	1	2	3	4	5	6	7	8	9	10	11	12	13	14	15	16	17	18	19	20	
1	3.5																					
2	5.1	3.6																				
3	4.5	3.2	2																			
4	3.9	2.8	1.7	.5																		
5	3.4	2.4	1.5	.4	-.9																	
6	2.9	2	1.1	.3	-.6	-1.4																
7	2.4	1.7	1	.2	-.4	-1	-1.3															
8	2.1	1.4	.7	.1	-.6	-1.1	-1.5	-1.9														
9	1.8	1.2	.6	0	-.7	-1.3	-1.9	-2.4	-2.7													
10	1.7	1	.4	-.2	-.9	-1.6	-2.2	-2.8	-3.3	-3.7												
11	1.7	1.1	.4	-.4	-1.1	-1.9	-2.5	-3.2	-3.6	-3.7	-2.8											
12	2	1.3	.5	-.4	-1.2	-2.1	-2.9	-3.5	-3.7	-3.4	-2.2	-.4										
13	2.2	1.4	.6	-.3	-1.2	-2.1	-2.9	-3.5	-3.6	-3.1	-1.9	-.4	1.1									
14	2.1	1.4	.6	-.2	-1.1	-1.9	-2.5	-3	-2.4	-1.5	-.5	.8	1.6									
15	1.6	1.1	.5	-.1	-.7	-1.3	-1.8	-2.2	-2.4	-2.1	-1.4	-.5	.4	1.3	2.2							
16	1.1	.7	.3	-.2	-.6	-1	-1.4	-1.7	-1.9	-1.7	-1.2	-.6	0	.8	1.4	2.1						
17	.8	.4	.1	-.2	-.5	-.8	-1.1	-1.3	-1.5	-1.5	-1.2	-.7	-.4	.1	.5	.9	1.4					
18	.5	.3	0	-.2	-.4	-.7	-.9	-1.1	-1.2	-1.2	-1	-.8	-.7	-.3	0	.3	.5	.8				
19	.2	.1	0	-.2	-.4	-.6	-.8	-1	-1.1	-1.2	-1.2	-1	-.9	-.6	-.3	0	.2	.5	.8			
20	.2	.1	0	-.2	-.4	-.6	-.8	-1	-1.1	-1.2	-1.2	-1.2	-1.1	-1	-.8	-.5	.2	.1	.5	.9		

TABLE FOR SMOOTHED VALUES OF $\frac{d^2 C(h_1, h_2)}{dh_1^2}$

h₁

112

h₂

1	42	36	46	51	70	76	84	90	98	106	110	110	111	12	13	14	15	16	17	18	19	20
2	36	38	43	49	54	57	61	63	61	57	53	46	39	31	25	20	17	14	11	1		
3	36	46	51	57	63	70	77	83	85	86	81	74	65	54	43	35	30	25	21	18	2	
4	38	51	70	76	84	90	98	106	110	110	105	98	89	75	58	45	38	33	26	23	3	
5	43	57	76	93	113	116	122	129	134	135	130	121	110	92	70	55	47	42	34	30	4	
6	49	63	84	108	134	140	146	154	159	159	154	143	129	107	83	66	55	50	43	37	5	
7	54	70	90	116	140	159	171	178	182	182	176	165	151	126	97	77	64	58	51	45	6	
8	57	77	98	122	146	171	192	201	204	204	197	184	167	142	110	87	73	64	56	50	7	
9	61	83	106	129	154	178	201	223	224	223	216	202	181	153	123	98	82	72	64	56	8	
10	63	85	110	134	158	182	204	224	244	240	232	218	196	165	131	109	91	78	69	61	9	
11	61	86	110	135	159	182	204	223	240	249	243	227	202	168	136	114	95	81	72	65	10	
12	57	81	105	130	154	176	197	216	232	243	245	233	202	167	137	116	98	83	74	67	11	
13	53	74	98	121	143	165	184	202	218	227	233	235	204	165	138	116	99	84	76	69	12	
14	46	65	89	110	129	151	167	181	196	202	202	204	210	163	139	117	99	85	77	70	13	
15	39	54	75	92	107	126	142	153	165	168	167	165	163	159	140	117	99	86	76	70	14	
16	31	43	58	70	83	97	110	123	131	136	137	138	139	140	141	117	99	86	76	69	15	
17	25	35	45	55	66	77	87	98	109	114	116	116	117	117	117	118	100	86	74	67	16	
18	20	30	38	47	55	64	73	82	91	95	98	99	99	99	99	100	101	86	72	64	17	
19	17	25	33	42	50	58	64	72	78	81	83	84	85	86	86	86	86	86	70	60	18	
20	14	21	26	34	43	51	56	64	69	72	74	76	77	76	74	74	72	70	68	54	19	
21	11	18	23	30	37	45	50	56	61	65	67	69	70	70	69	67	64	60	54	44	20	
22	1	2	3	4	5	6	7	8	9	10	11	12	13	14	15	16	17	18	19	20		

TABLE FOR C(h₁, h₂)

$$\left. \frac{d g(h_1, h_2)}{d h_1} \right|_{h_1 = h_{11}} = \frac{1}{2} [-g(h_{10}, h_2) + g(h_{12}, h_2)]$$

$$\left. \frac{d g(h_1, h_2)}{d h_1} \right|_{h_1 = h_{12}} = \frac{1}{2} [g(h_{10}, h_2) - 4g(h_{11}, h_2) + 3g(h_{12}, h_2)]$$

and

$$\left. \frac{d^2 g(h_1, h_2)}{d h_1^2} \right|_{h_1 = h_{10}} = g(h_{10}, h_2) - 2g(h_{11}, h_2) + g(h_{12}, h_2)$$

In terms of three consecutive points the second derivatives are assumed constant. The points are taken close enough together to minimize error.

From the preceding numerical substitutions for the first and second derivatives of $g(h_1, h_2)$ in the differential equation of the shaping filter, the following system of difference equations may be obtained.

$$[a_0(h_{11}) - 2 a_1(h_1)] g(h_{11}, h_2) + a_1(h_{11}) g(h_{12}, h_2) =$$

$$[a_0(h_{10}) - 2 a_1(h_{10}) + a_1(h_{11})] g(h_{10}, h_2)$$

$$[a_0(h_{11}) + 2 a_1(h_{12})] g(h_{11}, h_2) + [a_1(h_{11}) - a_0(h_{12}) - 2 a_1(h_{12})]$$

$$g(h_{12}, h_2) = a_1(h_{11}) g(h_{10}, h_2) .$$

Now, it has been shown that

$$g(h_{10}, h_2) = \sqrt{ \frac{d C(h_{10}, h_2)}{d h_{10}} \Big|_{h_{10}=h_2} - \frac{d C(h_{10}, h_2)}{d h_{10}} \Big|_{h_{10}=h_2}^+ }$$

Thus, the system of two equations and two unknowns can be solved for $g(h_{11}, h_2)$ and $g(h_{12}, h_2)$. Substituting $g(h_{10}, h_2)$, $g(h_{11}, h_2)$, $g(h_{12}, h_2)$ when

$h_2 = h_{10}$ in the formula for $\left. \frac{dg(h_1, h_2)}{dh_1} \right| \begin{array}{l} h_1 = h_{10} \\ h_2 = h_{10} \end{array}$

enables one to compute $b_1(h_{10})$ from the formulas.

$$b_1(h_{10}) = g(h_1, h_2) \left| \begin{array}{l} h_1 = h_{10} \\ h_2 = h_{10} \end{array} \right. \quad \text{and}$$

$$b_0(h_{10}) = \frac{dg(h_1, h_2)}{dh_1} \left| \begin{array}{l} h_1 = h_{10} \\ h_2 = h_{10} \end{array} \right. + a_1(h_{10}) b_1(h_{10}) .$$

Synthesis Techniques

Regression Analysis

The regression analysis utilized in the determination of the wind model coefficients was developed through multivariate regression techniques and applied to the wind model synthesis by the methods described in Section III-4 of this report. This approach proved to be the most adaptable method of determining the coefficients and was later shown to be accurate through analog computer mechanization of the problem. The techniques that were utilized and proved to be only relatively successful or too cumbersome are briefly outlined in this Appendix.

Orthonormal Function Expansion of $R(h, \tau)$

A second approach to the determination of $a_1(h)$ and $a_0(h)$ was the expansion of $R(h, \tau)$ in the form

$$R(h, \tau) = \sum_{i=1}^n \phi_i(h) \psi_i(\tau)$$

where the $\phi_i(h)$ functions were chosen to be solutions of a constant coefficient differential equation. This was done to find the constant coefficient equation which best fits the function $R(h, \tau)$. The $\phi_i(h)$ are defined to be the set of homogeneous solutions which satisfy $D(p, h) R_y(h, \tau) = 0$, $t > \tau$ in the second order form. These ϕ_i 's are also by definition the homogeneous solutions of the weighting filter equation. The ϕ_i 's which best fit the $R(h, \tau)$ data were found to be

$$\begin{aligned} \phi_1(t) &= e^{-\frac{.2t}{19000}} \sin \frac{\pi t}{19000} \\ \phi_2(t) &= e^{-\frac{.2t}{19000}} \left[\cos \frac{\pi}{19000} t - \frac{.2}{\pi} \sin \frac{\pi}{19000} t \right] \end{aligned}$$

These two functions are constructed so as to be orthogonal to each other. The constants which cause them to be orthonormal have been left out.

$\psi_1(\tau)$ and $\psi_2(\tau)$ have been chosen so that the error in the approximation $R(h, \tau) = \psi_1(\tau) \phi_1(h) + \psi_2(\tau) \phi_2(h)$ is minimized. With the ϕ function chosen, the approximation is good to about 10% in the range of h from 4 to 14. The end points of $R(h, \tau)$ are not well-matched by this approximation.

The differential equation coefficients $a_1(h)$ and $a_0(h)$ were found to be

$$a_1(h) = .021$$

$$a_0(h) = .00684$$

and the homogeneous weighting filter differential equation is

$$\frac{d^2 y}{dh^2} + .021 \frac{dy}{dh} + .00684 y = 0$$

The first of the following tables shows the per cent error in the approximation to $R_y(h, \tau)$ and the second shows the values of $\psi_1(\tau)$ and $\psi_2(\tau)$ for the best fit to $R_y(h, \tau)$

Analytical Relations for $b_1(h)$ and $b_0(h)$

Attempts to define $b_1(h)$ and $b_0(h)$ completely in terms of boundary values for $R(h, \tau)$ and its derivatives were not totally successful. An expression for $b_1(h)$ in terms of first derivatives of $R(h, \tau)$ at $h = \tau^+$ and $h = \tau^-$ is easily obtained. The expression for $b_0(h)$ has proven to be very elusive, if there is one. For the second order shaping filter equation all attempts to define $b_0(h)$ in terms of the higher derivatives of $R(h, \tau)$ proved unsuccessful. These derivations are included previously. The advantage of obtaining an

	2	4	6	8	10	12	14	16	18
2	50								
4	8	8							
6	4	2	2						
8	1	3	4	5					
10	2	1	3	5	4				
12	2	3	2	2	1	20			
14	11	1	5	4	5	0	10		
16	14	11	14	3	0	25	7	5	
18	24	100						3.5	2

TABLE

PER CENT ERROR FOR $R(h, \tau) = \psi_1(\tau) \phi_1(h) + \psi_2(\tau) \phi_2(h)$

t	$\phi_1(t) = e^{-\frac{.2 t}{19000}} \sin \frac{\pi t}{19000}$	$\phi_2(t) = e^{-\frac{.2 t}{19000}} \left[\cos \frac{\pi t}{19000} - \frac{.2}{\pi} \sin \frac{\pi t}{19000} \right]$
	$\psi_1(\tau)$	$\psi_2(\tau)$
1000	.160	+ .95
2000	.310	+ .88
3000	.443	+ .79
4000	.558	+ .68
5000	.652	+ .56
6000	.724	+ .43
7000	.773	+ .29
8000	.798	+ .15
9000	.802	+ .01
10000	.783	- .11
11000	.742	- .24
12000	.685	- .35
13000	.611	- .44
14000	.523	- .52
15000	.427	- .58
16000	.323	- .62
17000	.214	- .64
18000	.106	- .64
19000	.0	- .63
20000	-.102	-.60

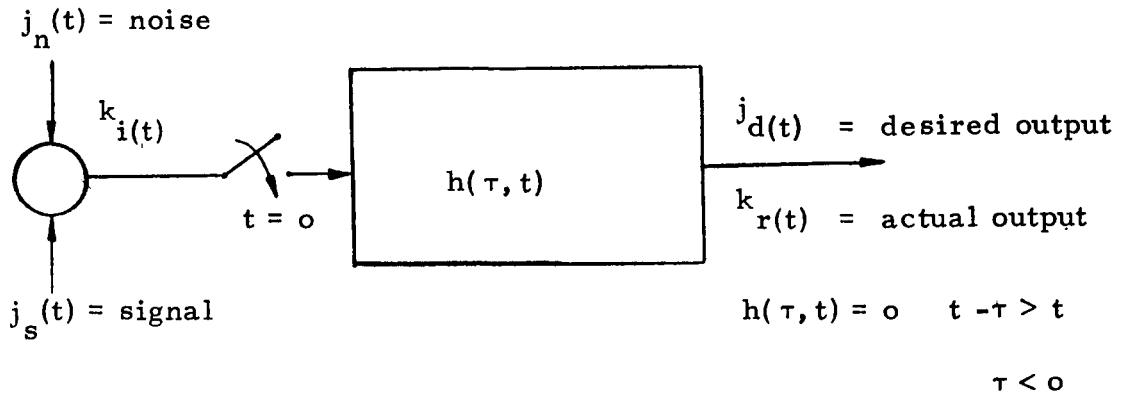
TABLE
VALUES FOR $\psi_1(\tau)$ AND $\psi_2(\tau)$ WHICH GIVE BEST FIT TO $R(h, \tau)$

explicit relation for $b_0(h)$ is obvious and would result in a great simplification of the synthesis procedure.

Analog Computer Synthesis

Several attempts were made to derive $a_1(h)$ and $a_0(h)$ on the analog computer both by hand iteration and by a closed loop iteration procedure. This method is most effective for derivation of $a_1(h)$ and $a_0(h)$, coefficients of the homogeneous equation, by forcing the homogeneous solutions to match $R_y(h, \tau)$ after inserting the proper initial conditions. The initial conditions are found by iteration also. $R_y(h, \tau)$ was set up on a function generator for one value of τ at a time beginning with $\tau = 0$ and a closed loop matching circuit was set up to force either $a_1(h)$ or $a_0(h)$ to the value necessary to zero the error between the shaping filter output and the function $R_y(h, \tau)$. These methods were never really satisfactory and the results were not comparable with those from the regression analysis. It is felt, however, that there is a good possibility that an analog synthesis technique could be implemented if a sizable effort was oriented in that direction. If an accurate matrix method could be formulated to give $g(h, \tau)$, then the analog computer synthesis would be more attractive because $b_1(h)$ and $b_0(h)$ could be obtained directly.

APPENDIX IV
OPTIMAL CONTROL FORMULATION
OF WEIGHTING FILTER SYNTHESIS PROBLEM



- (1) Inputs are zero for negative times.
- (2) Noise process is specified only through the autocorrelation.
- (3) Original problem is formulated to minimize the mean square ensemble difference between actual system output and desired output.

$$k_i(t) = F[k_s(t), k_n(t)] = k_s(t) + k_n(t)$$

$$k_r(t) = \int_0^T h(\tau, t) k_i(t - \tau) d\tau \quad \text{by convolution}$$

- (4) $k_d(t)$ is allowed to be any specified operation on the signal component of $k_i(t)$ which is $k_s(t)$.

- (t) $k_e(t) = \text{system error} \quad k_e(t) = k_r(t) - d(t)$

$$k_e(t) = \int_0^t h(\tau, t) k_i(t - \tau) d\tau - k_d(t)$$

Find $h(\tau, t)$ such that the mean square ensemble average of $\{e^k(t)\}$ is a minimum.

$$\begin{aligned} e^k(t_1) e^k(t_2) &= \left[\int_0^T h(\tau, t_1) k_{i(t_1-\tau)} d\tau - k_{d(t_1)} \right] \left[\int_0^T h(r, t_2) k_{i(t_2-r)} dr - k_{d(t_2)} \right] \\ &= \int_0^T \int_0^T h(r, t_2) h(\tau, t_1) k_{i(t_1-\tau)} k_{i(t_2-r)} d\tau dr \\ &\quad - k_{d(t_2)} \int_0^T h(\tau, t_1) k_{i(t_1-\tau)} d\tau - k_{d(t_1)} \int_0^T h(r, t_2) k_{i(t_2-r)} dr \\ &\quad + k_{d(t_1)} k_{d(t_2)} \end{aligned}$$

$$\begin{aligned} e^k(t_1) e^k(t_2) &= \int_0^T \int_0^T h(r, t_2) h(\tau, t_1) k_{i(t_1-\tau)} k_{i(t_2-r)} d\tau dr \\ &\quad - \int_0^T h(r, t_2) k_{i(t_2-r)} k_{d(t_1)} dr + k_{d(t_1)} k_{d(t_2)} \\ &\quad - \int_0^T h(\tau, t_1) k_{i(t_1-\tau)} k_{d(t_2)} d\tau \end{aligned}$$

by ensemble averaging $e^k(t)$

$$\begin{aligned} \langle e^k(t_1) e^k(t_2) \rangle &= \int_0^T \int_0^T h(r, t_2) h(\tau, t_1) \langle k_{i(t_2-r)} k_{i(t_1-\tau)} \rangle d\tau dr \\ &\quad - \int_0^T h(\tau, t_1) \langle k_{i(t_1-\tau)} k_{d(t_2)} \rangle d\tau - \int_0^T h(r, t_2) \langle k_{i(t_2-r)} k_{d(t_1)} \rangle dr \\ &\quad + \langle k_{d(t_1)} k_{d(t_2)} \rangle \end{aligned}$$

Let $\gamma_{ii}(t_1, t_2) =$ autocorrelation function of input

$$= \langle k_{i(t_2-r)} k_{i(t_1-\tau)} \rangle$$

$\gamma_{dd}(t_1, t_2)$ = autocorrelation function of desired output

$$= \langle k_{d(t_1)} k_{d(t_2)} \rangle$$

t_1 and t_2 show dependence on time of observation.

$\gamma_{id}(t_1, t_2)$ = cross correlation of the input message with the desired output.

$$= \langle k_{i(t_2 - r)} k_{d(t_1)} \rangle$$

$$\gamma_{di}(t_2, t_1) = \langle k_{i(t_1 - \tau)} k_{d(t_2)} \rangle$$

so we have

$$\begin{aligned} \langle k_{e(t_1)} k_{e(t_2)} \rangle = & \int_0^T \int_0^T h(r, t_2) h(\tau, t_1) \gamma_{ii}(t_2 - r, t_1 - \tau) d\tau dr \\ & - \int_0^T h(\tau, t_1) k_{\gamma_{di}}(t_1 - \tau, t_2) d\tau - \int_0^T h(r, t_2) \gamma_{id}(t_2 - r, t_1) dr \\ & + \gamma_{dd}(t_1, t_2) \end{aligned}$$

The input process is stationary, hence

$$\gamma_{ii}(t_2 - r, t_1 - \tau) = \Gamma_{ii}(r - \tau) = \frac{A}{2} \delta(r - \tau)$$

The $h(\tau, t)$ which gives minimum $\langle k_{e(t)} \rangle$ is called the Optimum Weighting Function.

A necessary and sufficient condition that $h(\tau, t)$ be the Optimum Weighting Function is that it satisfy

$$\gamma_{id}(t - r, t) = \int_0^t h(\tau, t) \gamma_{ii}(t - r, t - \tau) d\tau \quad 0 \leq r \leq T$$

Recalling that $\Gamma_{ii}(r - \tau)$ is the stationary correlation function for the input,

$$\gamma_{id}(t - r, t) = \int_0^t h(\tau, t) \Gamma_{ii}(r - \tau) d\tau \quad 0 \leq r \leq T$$

Furthermore, if $\Gamma_{ii}(r - \tau)$ represents white noise,

$$\Gamma_{ii}(r - \tau) = \frac{A}{2} \delta(r - \tau) = \text{white noise autocorrelation function.}$$

Then

$$\gamma_{id}(t - r, t) = \int_0^T h(\tau, t) \gamma_{ii}(t - r, t - \tau) d\tau \quad 0 \leq r \leq T$$

$$\begin{aligned} \gamma_{id}(t_2 - r, t_1) &= \int_0^t h(\tau, t_2) \langle k_i(t_2 - r) k_i(t_1 - \tau) \rangle d\tau \\ &= \frac{A}{2} \int_0^T h(\tau, t_2) \delta(r - \tau) d\tau \end{aligned}$$

$$= \frac{A}{2} h(r, t_2)$$

$$\begin{aligned} \gamma_{di}(t_1 - r, t_2) &= \int_0^T h(\tau, t_1) \langle k_i(t_1 - r) k_i(t_2 - \tau) \rangle d\tau \\ &= \frac{A}{2} \int_0^T h(\tau, t_1) \delta(r - \tau) d\tau \\ &= \frac{A}{2} h(r, t_1) \end{aligned}$$

$$\gamma_{id} = \gamma_{di} = \frac{A}{2} h(r, t_2) = \frac{A}{2} h(r, t_1)$$

$$\text{I. } \Gamma_{ii}(r - \tau) = \gamma_{ii}(t_2 - r, t_1 - \tau) = \frac{A}{2} \delta(r - \tau)$$

$$\text{II. } \gamma_{id}(t - r, t) = \frac{A}{2} h(r, t)$$

$$\begin{aligned} \frac{A}{2} \int_0^T \int_0^T h(r, t_2) h(\tau, t_1) \delta(r - \tau) d\tau dr - \frac{A}{2} \int_0^T h(\tau, t_1) h(\tau, t_1) d\tau \\ - \frac{A}{2} \int_0^T h(r, t_2) h(r, t_2) dr + \gamma_{dd}(t_1, t_2) = 0 \end{aligned}$$

$$\frac{A}{2} \int_0^T h(r, t_2) h(r, t_1) dr - \frac{A}{2} \int_0^T h(\tau, t_1) h(\tau, t_1) d\tau$$

$$- \frac{A}{2} \int_0^T h(r, t_2) h(r, t_2) dr + \gamma_{dd}(t_1, t_2) = 0$$

since $h(r, t_2) = h(\tau, t_1)$

$$\gamma_{dd}(t_1, t_2) = - \frac{A}{2} \int_0^T h(r, t_2) h(r, t_1) dr$$

$$+ A \int_0^T h(r, t_2) h(r, t_2) dr$$

As shown previously

$$\gamma_{id} = \gamma_{di} = \frac{A}{2} h(r, t_2) = \frac{A}{2} h(r, t_1)$$

then

$$\gamma_d(t_1, t_2) = \frac{A}{2} \int_0^T h(r, t_2) h(r, t_1) dr \quad t_1 < T$$

9/18/67

"The aeronautical and space activities of the United States shall be conducted so as to contribute . . . to the expansion of human knowledge of phenomena in the atmosphere and space. The Administration shall provide for the widest practicable and appropriate dissemination of information concerning its activities and the results thereof."

—NATIONAL AERONAUTICS AND SPACE ACT OF 1958

NASA SCIENTIFIC AND TECHNICAL PUBLICATIONS

TECHNICAL REPORTS: Scientific and technical information considered important, complete, and a lasting contribution to existing knowledge.

TECHNICAL NOTES: Information less broad in scope but nevertheless of importance as a contribution to existing knowledge.

TECHNICAL MEMORANDUMS: Information receiving limited distribution because of preliminary data, security classification, or other reasons.

CONTRACTOR REPORTS: Scientific and technical information generated under a NASA contract or grant and considered an important contribution to existing knowledge.

TECHNICAL TRANSLATIONS: Information published in a foreign language considered to merit NASA distribution in English.

SPECIAL PUBLICATIONS: Information derived from or of value to NASA activities. Publications include conference proceedings, monographs, data compilations, handbooks, sourcebooks, and special bibliographies.

TECHNOLOGY UTILIZATION PUBLICATIONS: Information on technology used by NASA that may be of particular interest in commercial and other non-aerospace applications. Publications include Tech Briefs, Technology Utilization Reports and Notes, and Technology Surveys.

Details on the availability of these publications may be obtained from:

SCIENTIFIC AND TECHNICAL INFORMATION DIVISION
NATIONAL AERONAUTICS AND SPACE ADMINISTRATION

Washington, D.C. 20546